RECOMBINANT AAV-MEDIATED GENE TRANSFER FOR THE POTENTIAL THERAPY OF ADENOSINE DEAMINASE DEFICIENT SEVERE COMBINED IMMUNE DEFICIENCY

By

JARED NATHAN SILVER

A DISSERTATION PRESENTED TO THE GRADUATE SCHOOL
OF THE UNIVERSITY OF FLORIDA IN PARTIAL FULFILLMENT
OF THE REQUIREMENTS FOR THE DEGREE OF
DOCTOR OF PHILOSOPHY

UNIVERSITY OF FLORIDA

2008

To all my family, friends, and loved ones, especially Dad, Mom, Amy, and Jake for their thoughts, prayers, inspiration, and love

ACKNOWLEDGMENTS

First and foremost, I thank my primary advisors, Dr. Terry Flotte, Dr. Melissa Elder, and Dr. Arun Srivastava for their mentorship and support throughout my graduate training. I also offer my sincere thanks to my supervisory committee including Dr. David Bloom and Dr. Steve Ghivizzani. Finally, I thank my parents, my girlfriend, Amy, and my most loyal companion, Jake, for their unending love and support throughout graduate school.

TABLE OF CONTENTS

page

LIST OF TABLES

LIST OF FIGURES

Abstract of Dissertation Presented to the Graduate School
of the University of Florida in Partial Fulfillment of the
Requirements for the Degree of Doctor of Philosophy

RECOMBINANT AAV-MEDIATED GENE TRANSFER FOR THE POTENTIAL THERAPY OF ADENOSINE DEAMINASE DEFICIENT SEVERE COMBINED IMMUNE DEFICIENCY

By

Jared N. Silver

December 2008

Chair: Arun Srivastava
Cochair: Melissa Elder
Major: Medical Sciences--Immunology and Microbiology

Adenosine deaminase (ADA) deficiency fosters a rare, but devastating pediatric severe combined immune deficiency (SCID) with a T- B- NK- phenotype, concomitant opportunistic infections including diarrhea, pneumonia, and oral candidiasis, and severe metabolic anomalies. Patients also manifest pathology in a wide array of tissues and organs beyond those of the immune system including significant neurological and musculoskeletal abnormalities. Currently, the standard of care for ADA-SCID consists of enzyme replacement therapy or hematopoietic stem cell transplantation (HSCT). Histocompatible HSCT remains the optimal treatment, but the availability of donors is often limited. Haploidentical HSCT continues to be a therapeutic option, but is associated with decreased engraftment and significantly higher morbidity and mortality. Enzyme replacement therapy does enhance T cell numbers and function while detoxifying tissues of the body. However, the associated expense, need for life-long administration, limited T cell repertoire diversity and the possibility of long term autoimmune and cancer risks necessitates viable, alternative therapies. Gene therapies for ADA-SCID over more than a decade have exclusively involved retroviral vectors coupled with lymphocyte and hematopoietic progenitor target cells. These groundbreaking gene therapies represent an

unprecedented revolution in clinical medicine, but may come with the continued risk of insertional mutagenesis and subsequent tumorigenesis. Moreover, the hematopoietic stem cell transduction and *ex vivo* methodologies employed in these retroviral gene therapies remain complex and inefficient when compared to their *in vivo* counterparts. An alternative gene therapy for ADA-SCID may be to utilize recombinant adeno-associated virus (rAAV) vectors *in vivo* and with a variety of target tissues to foster ectopic expression and secretion of hADA. Recombinant AAV vectors have demonstrated no pathogenicity in humans, minimal immunogenicity, long-term efficacy, ease of administration, and broad tissue tropism. Thus, this dissertation will endeavor to describe not only ADA-SCID with the traditional treatments and past retroviral gene therapies, but primarily focus upon alternative, rAAV-mediated gene therapy strategies to remedy this dynamic and potentially fatal genetic disease.

The first goal of this body of research was to use rAAV type 1 and type 9 vectors to shuttle a secretory version of the human ADA gene to a variety of tissues within a murine model of ADA-SCID in order to foster ectopic expression, secretion, and activity of the enzyme, human adenosine deaminase (hADA). The second goal was to promote a lymphocyte proliferation and potential immune reconstitution within a mouse model of ADA-SCID following enzyme expression, secretion, and activity. This research indicated that single-stranded rAAV type 1 and type 9 vectors containing the plasmid, pTR2-CB-IgK-hADA (or rAAV-hADA) (a) facilitated successful gene delivery to a variety of murine tissues, including heart, skeletal muscle, and kidney, (b) promoted ectopic expression of hADA, and (c) indicated a trend toward enhanced serum-based enzyme activity. Finally, these experiments demonstrated that type 9 vector containing the rAAV-hADA plasmid (d) drove a partial, progressive, prolonged, proliferation of lymphocytes and potential immune reconstitution in a murine model of ADA-SCID.

CHAPTER 1
BACKGROUND

Adenosine Deaminase Deficient Severe Combined Immune Deficiency (ADA-SCID): The Disease and Clinical Phenotype

ADA-SCID may be defined as a rare, severe, pediatric, genetic, metabolic, and immunological disease with unique biochemical features and a broad clinical manifestation centered around chronic infections and failure to thrive. At the heart of this disease is a deficiency of the ADA enzyme, an integral component of the purine salvage pathways of the body. ADA is a protein found ubiquitously throughout most human tissues. Thus, a deficiency of this zinc-dependent 41kDa enzyme affects the human body globally with a predilection for tissues with a high turnover rate, such as those of the immune system. (Aiuti 2004, Aiuti 2003, Hershfield 2003, Huang and Manton 2005, Parkmam 2000, Qasim 2004)

The primary form of the disease represents a pediatric emergency, usually diagnosed in the first year of life, and if left untreated, is often fatal. Approximately 80-85% of patients display primary ADA-SCID. However, ADA-SCID also affects numerous age groups in its delayed onset (at 1-10 years of age) and late-onset (after the first decade of life) forms. The final disease manifestation is a rare partial deficiency in which patients have elevated red cell dATP (up to 30 fold higher than healthy individuals) but remain healthy with normal immune function. (Buckley 2002, Hershfield 2003, Lainka 2005)

Primary ADA-SCID is the most common variety and patients display a profound lymphopenia with a combined T, B, and NK cell deficiency as the typical immunological profile. Laboratory testing of patient blood and urine reveals a unique biochemical profile consisting of elevated adenosine (Ado), deoxyadenosine (dAdo), and dATP, with markedly decreased ADA

enzyme and S-Adenosyl Homocysteine Hydrolase (SAH) activities. (Aiuti 2004, Aiuti 2003, Hershfield 2003, Huang and Manton 2005, Parkmam 2000, Qasim 2004)

Recurrent infections are the hallmark of ADA-SCID and the inevitable result of this combined immune deficiency. Such infections often present as diarrhea, pneumonia, oral candidiasis, otitis media, and/or sinusitis. Opportunistic pathogens such as *Pneumocystis carinii*, *Aspergillus*, and *Cytomegalovirus* are often responsible for recurrent infections in SCID patients. Upon clinical examination, patients have a vestigial thymus, display limited growth in height and weight, and absent lymphoid tissues. In addition, musculoskeletal abnormalities may be revealed on X-ray. Flaring and cupping of the costochondral junctions, pelvic dysplasia, shortened vertebral transverse processes with end-point convexity, and thick growth-arrest lines have been observed. Neurological manifestations of primary ADA-SCID may include neuromotor, cognitive, and behavioral symptoms. Impaired neuropsychological development, sensorineural deafness and nystagmus have also been reported. Moreover, patients may exhibit renal impairment or hepatic symptoms such as a mild to moderate transaminasemia or persistent neonatal hepatitis. Pulmonary insufficiencies have also been documented including poor alveolar development and asthma. Finally, due to the immune dysfunction characteristic of ADA-SCID and the subsequent inability of immune cells to mature, undergo tolerance induction, and perform surveillance of body tissues, autoimmune disease as well as cancer may occur in ADA-SCID patients. (Aiuti 2004, Aiuti 2003, Banerjee, *et al* 2004, Buckley 2002, Fozard 2003, Hershfield 2003, Honig 2007, Huang and Manton 2005, Kaufman 2005, Parkmam 2000, Qasim 2004, Rogers, *et al* 2001)

The Molecular Basis of ADA- SCID

For approximately three-quarters of primary immune deficiencies, the underlying genetic mutations have been well characterized. As of 2003, more than 70 mutations for ADA-SCID

had been identified. Categorized by the nature of the mutation, 41 were missense, 12 splicing, 9 deletion, and 5 nonsense mutations. Hershfield et al. has grouped these mutations according to their corresponding levels of ADA activity in patients: Group 0 mutations, containing deletions and nonsense mutations, correlate with no measurable ADA activity. Group 1, 2, 3, and 4 mutations are composed of missense mutations which correspond to several ranges of activity (expressed as a percent of wild type activity), 0.001 to .07, .06 to .16, .27 to .63, and 1.03 to 28.2, respectively. In the only remaining group, splicing mutations result in varying levels of activity. Described another way, the groupings of mutations may be related to the activity levels characteristic of each ADA-SCID variant. For example, Group 0 and many group 1 mutations correspond to <0.05% activity and thus, primary ADA-SCID. Group 2 and 3 mutations match approximately 0.06 to 0.6% activity and late-onset or delayed-type SCID. Finally, Group 4 mutations correspond to ADA activities 1-1.5% or greater, and thus, partial ADA-deficiency, with effective immune function beyond the second decade of life for affected patients. (Hershfield 2003)

Mutations amounting to amino acid substitutions may be found throughout the ADA protein sequence. Most missense mutations occur in codons composed of CpG dinucleotides. Moreover, half of all mutant ADA alleles occur in single families. In addition, most ADA-SCID patients are heteroallelic, while ADA allele homozygosity correlates with consanguinity or common geographic origin. Following analysis of 100 chromosomes, the most common mutations found by Hershfield et al. were R211H and G216R, which represented 11% and 13% of the samples studied, respectively. Other common mutations included L107P, R156H, A329V, and 955del5. Each of these was associated with 5-7% of the sample chromosomes analyzed. (Hershfield 2003)

The Pathophysiology of ADA-SCID

At its core, ADA SCID is an aberrance of one of the primary purine salvage pathways of the human body. Of all SCID, only purine nucleotide phosphorylase deficiency shares this underlying pathology of impaired purine salvage. Other forms of SCID, such as IL-2 receptor gamma deficiency or Jak3 deficiency, fundamentally impair cytokine/interleukin signaling and suppress lymphocyte development and proliferation. While SCID isoforms that result from Rag1/2 or Artemis mutations adversely affect V,D,J recombination events required for formation of T and B cell receptors. All SCID forms result in immune system malfunction, yet the manner by which these protein/enzyme deficiencies achieve this end is often unique. (Hershfield 2003, Manton 2005), Manton et al. 2005*)

Numerous pathways interact and cooperate in ADA-SCID to promote damage to the immune system as well as the nervous system, musculoskeletal system, liver, kidneys, and lungs. ADA predominantly resides in the cytoplasm of most cell types of the body. Mutations in the ADA gene often result in dramatic reductions of intracellular ADA activity with subsequent accumulations of cellular metabolites such as Ado, dAdo, and dATP. T and B lymphocytes are particularly sensitive to these metabolites. Thus, in the absence of sufficient functional ADA, several intracellular pathways are inhibited. The abundance of toxic metabolites inhibits ribonucleotide reductase activity, an enzyme essential for DNA replication. Also, metabolites, such as dATP, stimulate cellular apoptosis, by stabilizing the apoptosome complex composed of cytosolic cytochrome c, apoptosis activating factor 1, and procaspase 9. Moreover, excess cellular metabolites inhibit the enzyme, S-adenosyl homocysteine hydrolase (SAH hydrolase), which leads to an accumulation of SAH and an inhibition of transmethylation reactions necessary for cell division. Hepatic injury in knockout mice and in some patients may result

Excess metabolites also lead to an inhibition of terminal deoxynucleotidyl transferase (TdT) activity, which facilitates antigen receptor diversity. (Hershfield 2003, Booth et al. 2007)

However, ADA also has extracellular activity as an ectoenzyme in cooperation with CD26, an extracellular dipeptitydl peptidase, in thymocytes and epithelial cells. This ADA-CD26 complex is thought to stimulate G protein coupled receptors in response to extracellular metabolites such as adenosine. In the absence of functional ADA, excessive stimulation of the cell surface with adenosine may mediate cytotoxicity and contribute to immune dysfunction by a mechanism not clearly understood, but observed in lung parenchyma. (Hershfield 2003, Booth et al. 2007)

Screening for ADA-SCID

Just as with early cancer detection, an early diagnosis of SCID remains perhaps the greatest key to patient survival and improved health. While some have advocated screening for primary immunodeficiencies not on the basis of disease frequency, but instead, justified on the basis of disease severity, early treatment efficacy, and potential for low screening costs, currently no screening for ADA-SCID exists. Further, some researchers have argued effectively that the increased morbidity/mortality and associated expense of not-screening justifies screening tests for ADA-SCID with the associated costs, particularly if numerous genetic diseases are screened simultaneously. The old adage, “an ounce of prevention is worth a pound of cure” may apply in this setting. This section will examine some of the arguments for implementation of an ADA-SCID screening program with the relevant methodologies and some of the associated costs. (Manton et al. 2005)

A lack of screening and subsequent late diagnosis, leads to an increased likelihood of immunological deterioration and recurrent infections in ADA-SCID patients. Subsequent HSCT has less likelihood of success with increasing patient age and complicating factors, such as

recurrent infections. The expense of these procedures is tremendous while the associated morbidity/mortality is high. Such observations and clinical outcomes may justify a neonatal screening program for this pediatric immunodeficiency. (Manton et al. 2005). Further, implementation of early screening would facilitate early diagnosis and the potential for earlier, more effective treatment prior to death of lymphocyte progenitors and onset of infections. In other words, early screening, diagnosis, and treatment with PEG-ADA or HSCT, may facilitate growth of endogenous lymphoid progenitors and increase the likelihood of successful engraftment earlier in life. Thus, the benefits of screening are apparent, as are the consequences of not doing so. So, provided the costs of prenatal or newborn screening could be minimized, an ADA-SCID or primary immunodeficiency neonatal screening program should be considered. (Manton et al. 2005)

Moreover, while ADA-SCID is considered a rare, autosomal recessive genetic disease, the population-based data on the frequency of mutations in genes that cause SCIDand the true incidence of the disorder has not been well characterized. It is unknown how many infants dying of pneumonia, measles, serious gastrointestinal infections, etc. yearly worldwide are really succumbing to this “rare” disease, SCID. Further, while genetic in origin, most cases of SCID arise without a family history. ADA-SCID affects infants of both sexes, along with all races, creeds, colors, countries, and cultures. Thus, the probability that SCID may be more common than previously thought, the insidious onset of SCID in families with no medical history of the disease, and the fact that the disease does not discriminate among its available hosts, also provide reason for the adoption of an ADA-SCID screening program. (Manton et al. 2005)

Yet, how would a screening procedure for ADA-SCID be performed? With advances in molecular biology and DNA sequencing, prenatal screening could be performed using mutational

analysis or through measurement of enzyme activity in trophoblasts from chorionic villus sampling or in cultured amniocytes. Early screening in newborns could be achieved in a number of ways. White blood cell counts and differentials may be utilized as a first round of screening for at least primary ADA-SCID. If the patients are lymphopenic, further cellular analysis may include flow cytometry-based profiles of T, B, and NK cells. Additional rounds of screening could come in the form of measurements of erythrocyte ADA activity. And finally, while dAdo could be measured in the urine, S-adenosyl homocysteine hydrolase activity and dATP could be analyzed in red blood cells obtained from blood samples. (Manton et al. 2005, Booth et al. 2007)

And finally, what are the associated costs of ADA-SCID screening? A review by Huang and Manton in 2005 described first-line screening for SCID on the order of $40 for a white cell count and manual differential. While further screening would foster greater expense, additional screening would be justified on the basis of deficient white cell counts or a highly abnormal profile on the differential. Also, with the advent and progression of modern molecular biology techniques, including DNA isolation and sequencing, the cost of such procedures has decreased dramatically in recent decades, affording another powerful tool to screen large populations for ADA-SCID. Moreover, reported costs of HSCT in the first 3 months of life, when an early screening program could be implemented, are less than $50,000. However, the costs of care so increase significantly for seriously ill patients, exclusive of the additional costs of therapy for infections from birth to the time of eventual diagnosis. (Manton et al. 2005)

Current Therapies for ADA-SCID

Histocompatible HSCT remains the best therapy for ADA-SCID. In a recent review by Cavazzana-Calvo and Fischer, it was reported that for children with a primary immunodeficiency such as ADA-SCID, allogeneic HSCT from an HLA-matched sibling donor carries an 80%

chance of cure. The cure rate remains relatively high at approximately 60-70% for HLA-matched unrelated HSCT. Advances in transplantation and engraftment, both in efficiency and duration, have been facilitated by enhanced nutritional care as well as control of infectious complications. (Booth 2007, Cavazzana-Calvo 2007)

Among the disadvantages of histocompatible HSCT is the lack of availability of suitable fully-matched donors, which necessitates the use of haploidentical donors, such as parents. Unfortunately, the cure rate associated with mismatched related donor transplantation compared to that of HLA matched transplantation from a sibling or unrelated donor is significantly lower, on the order of 30%. In addition, immunological complications such as graft versus host disease (GVHD), which results when there is a significant discrepancy between the histocompatibility complexes of the donor and patient, presents another potential disadvantage for any form of allogeneic HSCT. Moreover, as described by Cavazzana-Calvo et al., HSCT is hindered by both the age of the recipient and the presence of infections at the time of HSCT. The success rate is lower with higher morbidity and mortality in older patients and in those with recurrent infections. Allogeneic HSCT may also result in a decline of T cell function over prolonged period of time. Moreover, following HSCT, delayed or partial immune reconstitution may result in the onset of infections and inflammatory/autoimmune conditions. (Booth 2007, Cavazzana-Calvo 2007)

Additional disadvantages of allogeneic HSCT have been reported by Booth et al., Wingard et al., and Honig et al. Booth et al. discussed management options for ADA deficiency, and included a description of long-term HSCT complications in the setting of haploidentical HSCT, such as viral infection and pulmonary hypertension. Wingard et al. offered several categories of long-term immunological and non-immunological complications, all related to

allogeneic HSCT. One category of HSCT complications may be thought of as the result of the transplantation itself, including GVHD, immune deficiency, infections, and autoimmune manifestations. A second category of HSCT complications may be considered the result of the conditioning regimen, particularly myeloablative conditioning, such as sterility, impaired growth, cognitive disturbances, renal insufficiency, alopecia, endocrine conditions, and cardiopulmonary impairment. A third and final category of complications result from a combination of the HSCT and the conditioning regimen. Wingard et al. reported pulmonary insufficiency as a prime example of the third category. This long-term complication results from a confluence of factors including HSCT-mediated GVHD, lung injury from patient preconditioning, and presence of lung infection. Finally, Honig et al. reported significant central nervous system complications, such as mental retardation, sensorineural deafness, and motor dysfunction, for ADA-SCID patients even in the setting of HSCT. While Honig et al. did not correlate disease or transplantion-related factors with the onset of long-term neurological complications, that study did report that HSCT was not able to control manifestation of such complications. Gene therapies, in particular those based on rAAV, may offer a way to bypass a number of these problems associated with HSCT. (Booth 2007, Cavazzana-Calvo 2007, Honig, *et al* 2007, Wingard 2002)

However, ADA-SCID patients who do not have the option of HSCT, do not respond well to HSCT, or are awaiting transplantation, may be treated with polyethylene glycol conjugated bovine ADA (PEG-ADA). This enzyme is administered by intramuscular injection twice weekly. To date, over 150 patients worldwide have received and benefited from PEG-ADA treatment. This form of enzyme replacement therapy facilitates at least a partial correction of the metabolic and immunological defects inherent to ADA-SCID. And, while enzyme replacement

presents a potent therapeutic option with significant benefits, there are also numerous shortcomings worthy of discussion. (Booth 2007, Lainka 2005)

Following administration of enzyme replacement, patients often experience partial recovery of lymphocyte counts, subsets, and function. Clinical improvement may be observed within weeks of the initial administration of PEG-ADA. Clinical benefits manifest as decreased infections and partial recovery of organs and tissues outside of the immune system, such as the liver. Moreover, circulating repeatedly administered PEG-ADA serves to detoxify body tissues at the biochemical level. By removing circulating accumulating metabolites, such as Ado and dAdo, from circulation, PEG-ADA may exert a protective effect on mature lymphocytes. Further, this therapy may be used effectively in patients with numerous forms of ADA-SCID including the delayed-onset form,. Taken together, these observations and clinical results support the assertion that PEG-ADA, at least in the short-term, is effective and life-saving. (Booth 2007, Lainka 2005)

And yet, while PEG-ADA presents a viable therapeutic option, there are numerous disadvantages to enzyme replacement. First, PEG-ADA requires repeated administration over the lifetime of the patient, which makes treatment a lifelong process and may lead to difficulties with patient compliance. Second, PEG-ADA remains incredibly expensive, and thus limits access and availability to patients and clinics worldwide. Third, the long-term benefits of PEG-ADA have yet to be well characterized, and so, remain unclear. A review by Booth et al. in 2006 reported concern that immune function may deteriorate beyond 10-15 years of treatment with PEG-ADA. Fourth, neutralizing anti-ADA antibodies develop in approximately 10% of patients treated with PEG-ADA, mostly in the setting of the delayed or late-onset forms of the disease. Fifth, transient immune dysregulation/autoimmune phenomena may occur in the first

few months of enzyme replacement and may be related to the underlying ADA mutation and the phenotype of the patient. Confounding autoimmune complications include hemolytic anemia, particularly in the setting of catheter-based sepsis (and viral infection) in delayed-onset type patients, the appearance of anti-thyroid antibodies, increase in IgE level, eosinophilia, and highly elevated T cell activation have also been reported. Sixth, for some ADA-SCID patients, despite having received PEG-ADA therapy for 8-15 years and having experienced at least partial immune reconstitution, PEG-ADA and its immunological benefits ultimately may not be protective against the onset of lymphoproliferative disorders which have claimed the lives of at least three patients. However, it must be emphasized that no *direct* link has been demonstrated between PEG-ADA and the onset of lymphoproliferative disorders in ADA-SCID patients. Such disorders are most likely the direct result of compromised immunological surveillance in ADA-SCID patients on PEG-ADA treatment and in the setting of partial immune reconstitution. Please refer to Table 1 for summarized information regarding current therapies for ADA-SCID. (Anderson, *et al* 1990, Booth 2007, Lainka 2005)

Retroviral Gene Therapy for ADA-SCID

Within the field of gene therapy, arguably no other clinical application than that of SCID gene therapy has experienced as many pitfalls and triumphs. Consequently, no other clinical gene therapy has experienced the evolution of technique or undergone the level of scrutiny as has SCID gene therapy. Nearly two decades of work have been dedicated towards achieving correction of SCID defects, particularly those of the X-linked and autosomal varieties, making SCID gene therapy one of the longest running gene therapy endeavors. (Flotte 2007, Parkmam 2000)

The Origins of ADA-SCID Gene Therapy

So, how is it that ADA-SCID gene therapy came to fruition? At least two vital components were necessary for the development of both the initial *in vitro* and *in vivo* ADA-SCID gene therapy studies and subsequent implementation of the first gene therapy-based clinical trials, the gene delivery vehicle and the viral transduction protocol. The gene delivery vehicle which made possible an alternative treatment for ADA-SCID was the retroviral vector, while *ex vivo* stimulation and transduction of dividing target cells, such as lymphocytes and HSCs, provided the second vital step towards viable retroviral gene delivery. (Flotte 2007, Parkmam 2000)

First generation retroviral vectors employed a transgene cassette in which the majority of endogenous elements, such as gag, pol, and env components were deleted and replaced with a therapeutic gene of interest such as human ADA. The gene was flanked on either side by long terminal repeat (LTR) regions consisting of repeated, endogenous nucleotide sequences with promoter/enhancer elements known as U3 and U5 regions, along with adjacent packaging signals. In these initial vectors, upstream of the hADA transgene within the U3 region of the LTR, resided a moloney murine leukemia virus (MoMLV) enhancer. Moreover, given the name of this enhancer element and subsequent leukemogenesis in several X-SCID patients, use of the enhancer may not have been the best approach. Also, downstream of the 3' end of the transgene, resided a poly A sequence in a second LTR region. Later modifications to the vector including deletions of the NCR (negative control region), implementation of a MPSV (myeloid proliferative sarcoma virus) enhancer, incorporation of a demethylating fragment, and the addition of a new PBS (primer binding site) are discussed further in Parkmam et al. Finally, it is also worth noting that because of the nature of retroviral vectors, only cDNAs may be employed

as the transgene of interest, while transgenes containing introns may not be utilized. (Cavazzana-Calvo and Fischer 2007, Cavazzana-Calvo 2007, Flotte 2007, Parkmam 2000)

And, since the cellular targets of these retroviral vectors were lymphocytes and hematopoietic stem cells (HSCs), transduction protocols have evolved as well. Current transduction procedures include a variety of biochemical and cellular components designed to enhance the efficiency of retroviral gene delivery to target cells such as HSCs. *Ex vivo* culture of HSCs has progressed to include the cytokines IL-3 and IL-6, along with stem cell factor (SCF), and most recently, Cdk inhibitors and Flt3 ligand. *Ex vivo* transduction procedures of HSCs were enhanced further with the use of bone marrow stromal cell scaffolds and fibronectin matrices (the latter developed originally by Williams group), which facilitate HSC mobility and adhesion. (Parkmam 2000)

Two recent publications by Di Nunzio et al. in 2007 and Trobridge et al. in 2008 discuss updated protocols for HSC transduction, particularly in the context of lentiviral vectors. Trobridge et al. utilized VSV-G pseudotyped HIV-based lentiviral vectors for transduction of long-term repopulating cells in pigtailed macaques. In several animals, Trobridge et al. reported long-lasting, significant, stable gene-marking at relatively low MOIs (5-10) following a 48 hour *ex vivo* transduction protocol. Interestingly, Trobridge et al. isolates CD34+ primate cells using IgM anti-CD34+ antibody and microbeads. The CD34+ enriched cells were cultured in media with penicillin and streptomycin along with rhSCF, rhuFlt-3 ligand, IL-3, IL-6, thrombopoetin (TPO), and granulocyte colony stimulating factor (G-CSF) for 15-18 hours prior to transduction. For transduction, cells were given the same cytokine mixture in flasks coated with the CH-296 fragment of fibronectin. Protamine sulfate was added to the media as was cyclosporine for some experiments. The cells were cultured for 6.5 to 8 hours with one dose of lentiviral vector, and

then overnight for 17-18 hours with a second dose. Finally, the cells were infused into primate recipients following myeloablative conditioning. In 2007, Di Nunzio et al. reported an updated transduction protocol utilizing lentiviral vectors pseudotyped with the RD114-TR chimeric envelope glycoprotein, made from intracellular and transmembrane domains of feline leukemia virus RD114 and the cytoplasmic tail of murine leukemia virus amphotropic envelope. These pseudotyped vectors were used to transduce cord blood, bone marrow, and peripheral blood-derived HSCs, and then analyzed for transduction efficiency in liquid culture, semisolid culture, and following xenotransplantation into a NOD-SCID mouse model. The results of the Di Nunzio et al. study indicated that pseudotyped vector transduced HSCs at lower multiplicities of infection, with reduced toxicity, and reduced chance of pseudo-transduction at comparable vector copy number per genome, when compared to standard VSV-G based packaging systems. While some variation in the protocol such as incubation times was utilized by Di Nunzio et al. when compared to the Trobridge et al. study, the cytokine cocktail as well as the fibronectin-coated plates utilized were very similar. The Di Nunzio et al. study also centered around studies of human HSC transduction where G-CSF was used to mobilize CD-34+ cells in cord blood, bone marrow, and peripheral blood samples. (Di Nunzio 2007, Trobridge 2008)

A History of ADA-SCID Gene Therapy Using Retroviral Vectors

Gene therapy for ADA-SCID began with pilot trials in the 1990s designed to assess the safety, efficacy, and challenges of retroviral delivery of a good copy of the human adenosine deaminase gene to autologous peripheral blood lymphocytes (PBLs) and/or hematopoietic progenitors (eg HSCs), genetically modified *ex vivo*, and re-infused into patients. The very first legal gene therapy trial for ADA-SCID was conducted in 1990 at the National Institutes of Health (NIH) by Blaese group. To date, 3 clinical trials utilizing PBLs and 7 clinical trials with hematopoietic stem cells have been performed. The tumultuous road undertaken by ADA-SCID

gene therapy researchers has emphasized the need for efficient HSC transduction and the value of selective advantage conferred to transduced cells. The role of simultaneous PEG-ADA administration and the use of a preconditioning regimen have also been elucidated. Some of the most important studies will be described in this section. (Aiuti 2004, Aiuti 2007, Aiuti 2003, Aiuti 2002a, Aiuti 2002b, Blaese 1995, Booth 2007, Bordignon 1995, Engel 2007, Gaspar 2006, Schmidt 2003)

As reported by Aiuti et al. in 2003 and 2004, the initial gene therapy trials for ADA-SCID using PBLs were predicated on the observation that immune reconstitution occurred in patients receiving BMT with sole engraftment of donor T cells. For a time frame of 6 years to more than 12 years, 6 patients received genetically-modified PBLs (or a combination of PBLs and hematopoietic progenitors as with Bordignon et al.) on the order of 3 x 10^11 cells, according to three different retroviral protocols. No adverse events or toxicities were observed. Transduced cells and thus, vector, persisted for years after cessation of cell infusions. Overall, PBL counts were improved as was immune function. However, patients remained on PEG-ADA, which may have significantly impaired the selective advantage conferred to transduced cells, and confounded an analysis of the actual benefit of the administered gene therapy. (Aiuti 2004, Aiuti 2003, Aiuti 2002b, Blaese 1995, Bordignon 1995, Kawamura 1999, Muul 2003)

Justification for the removal of PEG-ADA proved difficult. However, in one patient on PEG-ADA therapy, immune responses became impaired and immune imbalance was apparent clinically. Thus, PEG-ADA was removed gradually as gene therapy was implemented by Aiuti group in Italy. Not surprisingly, once PEG-ADA administration ended entirely, the large majority of PBLs were transduced lymphocytes, testifying to the role of selective advantage in the absence of systemic detoxification by PEG-ADA. For additional information regarding the

cellular and clinical benefits observed in that study, please refer to reviews by Aiuti from 2003 and 2004. Moreover, despite the promise of that study, the underlying metabolic defect was not corrected. Overall, that study emphasized the need for increased T cell infusions, to support greater ADA expression, enzyme activity, and metabolic correction. And, also apparent was the need for hematopoietic progenitor cells, which could not only lead to multi-lineage differentiation of erythroid and myeloid precursors, but also provide sustainable, numerous, transduced lymphoid precursors. (Aiuti 2004, Aiuti 2003, Aiuti 2002b)

So, the way forward in developing a viable, clinical gene therapy for ADA-SCID was relatively clear. Subsequent trials would have to focus, in large part, on HSC transduction. The early results from an umbilical cord blood study by Kohn et al. and an autologous bone marrow study by Bordignon et al. showed that retroviral vectors could successfully deliver the ADA gene to hematopoietic progenitors, as transduced cells achieved engraftment and multi-lineage differentiation but were insufficient in number to promote therapeutic ADA expression. In another study by Schmidt et al., which utilized retroviral transduction of cord blood-derived CD34+ cells for transfer into SCID neonates, it was shown that for one patient, a single progenitor cell yielded a diverse T cell repertoire which persisted from 9 to 94 months. This study also indicated that even a handful of successfully-engrafted, transduced progenitors could provide an immunological benefit to patients. However, future trials would have to yield greater rates of HSC transduction to correct ADA-SCID. Finally, in the early trials utilizing HSCs, PEG-ADA treatment was maintained. Consequently, a lack of selective pressure on the transduced cells may have produced the results inconsistent with full correction of the ADA-SCID defect. (Aiuti 2004, Aiuti 2003, Bordignon 1995, Schmidt 2003)

Then, an improved HSC transduction protocol was adopted by Aiuti group, which was optimized for human CD34+ gene transfer. HSCs were cultured with Flt3 ligand, stem cell factor, thrombopoetin, and IL-3. The vector was loaded onto a surface coated with fibronectin to allow the cells and vector to coalesce. Also, since previous animal and clinical studies indicated that conditioning yielded sustained engraftment with low toxicity, a conditioning regimen was employed. Busulfan had been widely used in pediatric HSC transplantation and thus, was the best candidate for nonmyeloablative preconditioning of the gene therapy recipients. Then, patients were recruited who neither had access to PEG-ADA nor an HLA-identical sibling donor. In the end, two patients were selected for this enhanced gene therapy protocol utilizing HSCs, and infused with bone marrow-derived CD34+ cells. (Aiuti 2004, Aiuti 2007, Aiuti 2003, Aiuti 2002a, Aiuti 2002b, Bordignon 1995, Engel 2007, Gaspar 2006)

The results were impressive. Up to 10% marking was observed in megakaryocytic, erythroid, and CD34+ progenitors, as well as granulocytes. Significant numbers of transduced HSCs remained over time and retained the capacity for multilineage differentiation. And, astoundingly, Aiuti et al. reported that the highest levels of engraftment were observed in T, B, and NK cells (up to a 100% transduced cells). This data once again demonstrated the power of selective advantage in repopulating a deficient immune system. PBL counts improved significantly in both patients, as did immune function and ADA activity levels. Then, this protocol was applied to two additional patients with comparable results. Further details regarding the cellular and biochemical endpoints of that study may be found in reviews by Aiuti group in 2003 and 2004. Overall, that study, with the best results to date, reported correction of the metabolic and immunological defects of ADA-SCID, with no reports of toxicity or leukemogenesis. (Aiuti 2004, Aiuti 2003, Aiuti 2002a, Engel 2007, Gaspar 2006)

Then, in 2007, a review by Booth et al., describing current management options for ADA-deficiency, summarized nicely the more recent information regarding retroviral ADA-SCID gene therapy trials conducted in Milan (by Aiuti et al.) and London (by Gaspar et al.). Both trials operated on similar protocols, using retroviral vectors to deliver the ADA gene to autologous HSCs *ex vivo*, followed by infusion into patients conditioned with Busulphan in Milan and Melphalan in London. (Aiuti 2002a, Booth 2007, Gaspar 2006)

Booth et al. reported that the Milan study, by Aiuti group, had enrolled a total of 8 patients. Patients ranged in age from 0.6 to 5.5 years old, and PEG-ADA was either halted or uninitiated prior to gene therapy. Booth et al. described all patients as healthy and thriving with some follow-up studies ranging up to 64 months. Six of the children, with follow-up periods of 6 months or more, had experienced immunological outcomes consistent with a pronounced selective advantage conferred to transduced cells. Transduced cells accounted for a majority of T, B, and NK cell populations along with 0.1-10% myeloid cells. Other outcome measures such as lymphocyte counts, polyclonal thymopoiesis, and T-cell functions had all increased significantly. In half of the patients, IVIG has been discontinued, with evidence of specific antibody production. Moreover, normalized ADA activity levels have been detected in patient lymphocytes with enhanced activity in patient red blood cells (RBCs) as well. Correction of the metabolic defect underlying ADA-SCID is further evidenced by a reduction in the toxic metabolites (ie dAXP) within RBCs. Finally, vector integrations thus far have been shown to be heterogenous, with no associated clonal expansion. Patient development has been normal with no reported adverse events. (Aiuti 2002a, Booth 2007)

In the London trial, by Gaspar et al. and reviewed by Booth et al., one patient was administered HSCs transduced with a therapeutic retroviral vector, following a mild

preconditioning regimen and a halt to PEG-ADA enzyme replacement 1 month prior to the beginning of gene therapy. Reported outcomes of this trial, two years after initiation, are increased T-cell numbers, normalized proliferative responses, and a resumption of thymopoiesis. Moreover, though the patient has remained well clinically with no prophylactic antibiotics, RBC ADA activity has waned over time in a pattern similar to that observed following HSCT. (Booth 2007, Gaspar 2006)

Finally, a recent study by Engel et al. described a clinical trial adversely affected by the presence of an underlying marrow cytogenetic condition known as Trisomy 8 mosaicism. In this trial, one patient with ADA-SCID was administered autologous, bone marrow-derived CD34+ cells transduced with a therapeutic retroviral vector, following withdrawal of ERT and pre-conditioning with busulfan. In this particular case, myelosuppression persisted, necessitating an infusion of autologous, untransduced bone marrow. Yet, pancytopenia persisted with insignificant levels of gene marking, and a bone marrow biopsy and aspirate were taken. These diagnostic tools, coupled with a retrospective analysis of pretreatment marrow, revealed an underlying cytogenetic condition known as Trisomy 8, which may have inhibited successful CD34+ cell engraftment and subsequent immune reconstitution. (Engel 2007)

Ironically, the greatest strength of retroviral vectors, their ability to facilitate stable integration and confer a selective advantage to the host cells, is also their greatest weakness, as such integration also promotes the type of insertional mutagenesis witnessed in the X-linked SCID trials. Consequently, to date, 5 patients, 4 in Paris and 1 in London, have been diagnosed with leukemia following retroviral gene therapy. In a review by Bushman et al. in 2007, updated retroviral analysis revealed a multi-hit hypothesis to explain the manifestation of T-cell leukemia in the French X-SCID trials. In at least two of the reported adverse events, the first “hit” likely

came in the form of insertion of the therapeutic retroviral vector, and subsequent activation of the LIM domain only 2 (LMO2) protooncogene. The second "hit" appeared to manifest from the IL-2 receptor gamma subunit transgene itself, an activation signal triggering lymphocyte proliferation. A third and final "hit," which may explain the onset of T-cell leukemia, came in the form of a chromosomal rearrangement. Also, following the most recent Aiuti clinical trials for ADA-SCID, an analysis of retroviral vector integration in 2007 demonstrated that while the patients remained free of T cell leukemia, the LMO2 locus (among other loci proximal to protooncogenes or genes controlling cell growth and self-renewal) once again proved to be a "hot spot" for retroviral insertion, just as was the case in the X-SCID trial. In the very least, such a similarity among integration sites in two different trials with two different patient populations for two different forms of the same disorder, SCID, warrants concern and vigilance if retroviral gene therapies are employed in the future. For additional information regarding the phenomenon of insertional mutagenesis, please refer to Baum et al. 2004, Baum et al. 2007, Dave et al. 2004, Hacein-Bey-Abina et al. 2003, Pike-Overzet et al. 2007, Kohn et al. 2003, and Aiuti et al. 2007. Please refer to Table 1 for summarized information regarding retroviral gene therapies for ADA-SCID. (Aiuti 2007, Baum 2007, Baum 2004, Bushman 2007, Dave 2004, Hacein-Bey-Abina S 2003, Kohn 2003b, Pike-Overzet 2007)

In summary, retroviral gene therapy for ADA-SCID, in the US and Europe, has demonstrated the proof of concept for gene-based delivery in the treatment of human monogenetic disease, the efficacy and limitations of this therapeutic modality, and, unfortunately, the risks inherent to retroviral vectors. These limitations and risks highlight the need for alternative vectors, such as rAAV (recombinant adeno-associated virus), capable of versatile, efficient, safe, and long-lasting gene delivery.

Recombinant AAV Gene Therapy for Monogenetic Disease

Viable alternative therapies for ADA-SCID, that may match or surpass the efficacy demonstrated by PEG-ADA, BMT, or retroviral gene therapy, and yet, maintain a solid safety profile while persisting for the long-term, remain elusive. However, of the numerous virus types abundant in nature, only a relative few represent candidates for gene delivery, and at least one, rAAV, may offer a therapeutic avenue for ADA-SCID that remains largely unexplored

Recombinant AAV has been studied in culture, in both large and small animal models, as well as in human clinical trials. Clinical efficacy in humans has proven challenging. Though, such experiments and trials have demonstrated at least two key principles of any prospective gene therapy, feasibility and safety. Moreover, diverse studies have ranged from gene therapy for pulmonary disease such as cystic fibrosis and alpha-1-antitrypsin deficiency, to gene delivery for musculoskeletal or hematopoietic disease such as Duchenne's muscular dystrophy and hemophilia A and B, respectively. Collectively, gene therapies for numerous, debilitating, monogenetic diseases help establish the theoretical and practical basis for a clinical rAAV-based gene therapy for ADA-SCID. This section will begin with a description of adeno-associated virus, particularly in the context of its use as a gene therapy vector, then proceed to an overview of some gene therapy applications relevant to a potential rAAV-based gene therapy for ADA-SCID. (Flotte 2002, Flotte 2004, Flotte 2005, Flotte 2007)

The Nature of AAV and rAAV

Adeno-associated viruses exist in nature as 20 nm, non-enveloped, icosahedral, single-stranded DNA viruses, which are members of the genus Dependovirus, the family, Parvoviridae, and subfamily, Parvovirinae. A highly successful and versatile virus, AAV spans numerous boundaries among species, inhabiting humans, non-human primates, cows, dogs, horses, and birds. AAV currently has 11 established genus members and in excess of a 100 distinct

variants, based on both serotype and DNA sequencing. Since being first identified as a contaminant of adenovirus cultures, AAV was then found to reside in the human gastrointestinal and respiratory tracts. AAV replication is contingent upon the presence of a helper virus, such as herpesvirus, vaccinia, or adenovirus. Without a helper virus, AAV enters a long-term latency period in a variety of mammalian tissues. (Flotte 2002, Flotte 2004, Flotte 2005, Flotte 2007)

AAV manifests many unique properties, and many of these features make the virus suitable for gene delivery: Unlike most viruses, AAV has not been associated with human disease, and is thus, non-pathogenic. Consequently, a low toxicity profile makes AAV a solid candidate as a gene therapy vector. Wild type AAV is also capable of site-specific integration into the AAVS1 site on chromosome 19. This property of wtAAV may be subjected to greater manipulation in the future, though recombinant AAV does still integrate at low frequency. Compared with the genome size and structure of retroviral, lentiviral, adenoviral, and herpesviral vectors, the AAV genome is relatively small and simple, at approximately 4.7 kb, with only 2 genes, *rep* and *cap*, encoding 4 Rep proteins and 3 capsid proteins. This small, simple, and efficient genome facilitates straightforward genetic modification for gene therapy purposes. Moreover, AAV is capable of long-term persistence in host cells, a feature exploited in gene therapy applications. In addition to a lack of pathogenicity, AAV also displays low immunogenicity, with relatively low innate cytokine responses. T cell responses are also typically mild and no clinically-relevant T-cell-related syndromes have been observed. However, neutralizing antibody responses, particularly to AAV2, have been reported. Compared to adenoviral and lentiviral vectors, for example, the low immunogenicity of AAV also proves advantageous in the context of gene therapy. Also, AAV vectors display both a broad tissue tropism and the ability to transduce both dividing and non-dividing cell types. This

innate flexibility of AAV vectors allows gene therapies to target a variety of tissue types with the goal of ameliorating a variety of genetic, metabolic, and infectious diseases. Finally, years of experimentation have yielded reliable recombinant production and purification methods for rAAV, which are essential for any potential gene therapy to be utilized clinically. (Flotte 2002, Flotte 2004, Flotte 2005, Flotte 2007)

In addition, the genetic structure of AAV is worth exploring and relevant to the synthesis of rAAV vectors for gene therapy. With its 4.7 kb genome, AAV relies upon two core genes, *rep* and *cap*, for maintenance of its life cycle. On either side of these two core genes are inverted terminal repeats (ITRs), which are cis-acting elements responsible for viral packaging, integration, genome replication, and to a limited extent, transcription. The *rep* gene produces 4 rep proteins, the longer Rep68 and Rep78, and the shorter, Rep 52 and Rep 40. Two promoters, termed p5 and p19, facilitate transcription of Rep68/78 and Rep52/40, respectively. Collectively, the non-structural Rep proteins perform many functions. The Rep family resolves the termini of the AAV genome during replication by means of the Rep nickase activity, elicits transcription from the AAV genome during active infection while inhibiting gene expression during latency, and promotes viral packaging. Moreover, the second core component of the AAV genome, the *cap* gene, yields three structural proteins, VP1, VP2, and VP3. Most often, AAV capsids contain 60 molecules of capsid protein in a ratio of 3:3:54 of VP1:VP2:VP3. Within the genome, sequences for all three VP proteins are collinear, with VP2 and VP3 as shortened, condensed forms of VP1. Cooperativity among these three VP proteins not only produces the surrounding viral capsid of AAV, but also determines tissue tropism through viral capsid binding to host cell receptors. (Flotte 2002, Flotte 2004, Flotte 2005, Flotte 2007)

Generally, recombinant AAV vectors retain only the ITR regions of the wild-type genome. A therapeutic transgene, specific to the desired application, lies between the two ITRs. A polyadenylation signal is incorporated at the 3' end of the gene and a suitable promoter/enhancer is inserted at the 5' end of the gene. To then package the rAAV plasmid in capsid protein, a number of strategies are available. However, in general, helper plasmids containing *rep*, *cap*, and helper virus genes are co-transfected into permissive cell lines, such as 293 cells, along with the vector plasmid containing the gene of interest. The cells are cultured and lysed. The lysate containing packaged rAAV may then be purified by a number of methods including CsCl density gradient ultracentrifugation and column chromatography. The latter method yields higher vector titers and infectivity. The first decade of rAAV-based gene therapies relied greatly upon rAAV2 vectors, which retained a number of characteristics of the wtAAV vector. And, when utilized *in vivo* and in clinical studies, rAAV remained non-pathogenic, capable of infecting both dividing and non-dividing cells, relatively non-immunogenic, and capable of targeting a variety of host tissues including muscle, brain, retina, liver and lung. Recombinant AAV also persists predominantly in episomal form for extended periods of time, facilitating long-term gene expression. Thus, while the possibility of insertional mutagenesis exists for rAAV, the probability is extremely low when compared to that of retroviruses. And, of numerous clinical trials utilizing AAV, no patient has ever manifested vector-induced oncogenesis. However, it should be noted that while innate as well as T cell responses to AAV are limited, instances of neutralizing antibody formation have been a difficult hurdle to overcome, as such antibodies limit the efficacy of repeated vector administration, particularly for rAAV2. (Flotte 2002, Flotte 2004, Flotte 2005, Flotte 2007)

In addition, recombinant AAV has been packaged into numerous serotypes depending upon the application, route of administration, and target tissue. For example, rAAV1 vectors demonstrate improved transduction of muscle tissue compared to rAAV2, while rAAV6 more efficiently transduces liver than rAAV2. A several hundred fold increase in gene transfer efficiency was observed in one study by Rabinowitz et al., in which rAAV2 plasmids containing the Factor IX and AAT genes were pseudotyped to rAAV1 capsids. In another study by Inagaki et al., later pseudotypes of AAV including type 8 and 9 vectors, cross endothelial barriers upon intravenous administration, or were administered via intraperitoneal injection, to effectively transduce numerous tissues of the body including, liver, pancreas, skeletal muscle, and heart. This tendency of rAAV to transduce specific cell types is dependent upon the given capsid protein and the abundance of receptors on target tissues. Recombinant AAV2 relies upon heparin sulfate proteoglycan as its primary receptor as well as co-receptors such as fibroblast growth factor receptor-1 and $alpha_v$-$beta_5$ integrin. For rAAV4 and rAAV5, the primary receptors have been identified as O-linked sialic acid and N-linked sialic acid, respectively. However, much work remains to elucidate receptors and co-receptors for all serotypes. (Flotte 2002, Flotte 2004, Flotte 2005, Flotte 2007)

Moreover, beyond the discovery and packaging of different pseudotypes of AAV, the virus has also been manipulated in other ways to facilitate tissue targeting and gene transfer. One method by which rAAV vectors have been modified is by the use of receptor-specific ligands. Such ligands are introduced into various sites of AAV capsid genes, such that packaging of rAAV will present these ligands on the viral capsid surface. This form of genetic engineering has been used to target host receptors such as the serpin enzyme complex receptor and the LDL receptor. (Flotte 2002, Flotte 2004, Flotte 2005, Flotte 2007)

Lastly, there are several concerns associated with AAV vectors which are worth describing. One comprehensive review by Tenenbaum et al. described several features of AAV vectors which may present challenges to expanding clinical gene therapy, such as vector integration, biodistribution, immune responses, and vector purity. Unlike wildtype AAV, which integrates into the AAVS1 site on chromosome 19, vector integration for rAAV does not occur in a site-specific manner. As reported in the Tenenbaum et al. review, random vector integration for rAAV has been shown in established cell lines, primary cultures, and *in vivo*, but at low frequency and only in some cases. Moreover, in a recent study by Han et al., where integration of self-complimentary AAV was reported in HSCs, no subsequent hematological abnormalities were observed. However, by contrast, in another recent study by Donsante et al., normal mice and mice with mucopolysaccharidosis VII (MPS VII) were shown to develop hepatocellular carcinoma following neonatal injection of rAAV carrying the b-glucuronidase gene. From four tumors, AAV provirus was isolated, and the site of integrated AAV genomes also corresponded to a locus encoding a number of small nucleolar RNAs (snoRNAs) and microRNAs, which were all upregulated. Though the safety record of rAAV in preclinical and clinical trials has been solid, and mouse studies often do not always equate with clinical studies, this study by Donsante et al. supports continued caution and vigilance with any rAAV gene therapy protocol, particularly when it comes to neonatal administration of rAAV vectors. Overall, as reported by Flotte et al. and Tenenbaum et al., most typically, rAAV vectors remain as episomal concatemers in the nucleus of transduced cells. The predominantly episomal nature of rAAV substantially reduces the risks of insertional mutagenesis and downstream activation of cellular oncogenes when compared to the risks of retroviral vectors. However, the inherent packaging constraints of

rAAV vector capsids present another concern for investigators, by limiting the total capacity to 5 kb. (Donsante 2007, Flotte 2004, Flotte 2005, Han, *et al* 2008, Tenenbaum 2003)

Biodistribution of administered AAV is also a concern described by Tenenbaum et al., especially regarding the potential for vertical or germ-line transmission of vector. Non-human primate models, subjected to numerous methods of administration, have shown that AAV vector genomes may be found in serum, urine, saliva, and semen (following hepatic artery administration), but only transiently and at low levels. Tenenbaum et al. also reported that the risk of germ-line transmission is low, based in part on the observation that motile germ cells have been shown to be non-permissive to even direct exposure to rAAV particles. (Tenenbaum 2003)

Moreover, Flotte et al. and Tenenbaum et al. highlight the need to examine immune responses following rAAV administration to rAAV capsids and the transgene of interest. For rAAV, such immune responses have been limited primarily to the production of neutralizing antibodies, which are most often against serotype 2 capsids and prevent vector re-administration. Yet, at least two recent studies have also demonstrated that cell-mediated immunity against rAAV capsids may also be a concern in some experimental settings. In a study by Wang et al., AAV2 and AAV6 capsid proteins facilitated primary cellular immune responses when injected into the skeletal muscle of random-bred dogs. In another study, Manno et al. demonstrated that rAAV-2 vectors used to transduce human hepatocytes *in vivo* produced therapeutic levels of factor IX. Yet, the therapeutic levels were limited to an 8 week duration, at which point, cell-mediated immunity directed against antigens of the AAV capsid led to the destruction of the transduced hepatocytes. However, it should be noted that even in the latter study, no significant or persistent clinical syndrome was reported and the adverse immune response could potentially

be overcome with short-term immunomodulation. In addition, both humoral and cellular immune responses must be evaluated for the transgene of interest in a gene therapy regimen. The results may vary substantially based on the nature of the gene product and the method of rAAV administration. Finally, though no causal relationship has been demonstrated, an association has been suggested between wildtype AAV, present in the genital tract, and early abortion as well as male infertility. This observation emphasizes the need for rAAV vector purity, free of wildtype AAV contamination, particularly in the clinical setting. Please refer to Table 2 for summarized information regarding rAAV vectors. (Flotte 2004, Flotte 2005, Gao 2002, Hauck 2003, Manno 2006, Tenenbaum 2003, Wang 2007)

Overview of several studies relevant to gene therapy for ADA-SCID

Before considering the strategies one may take towards a recombinant AAV gene therapy for ADA-SCID, the foundations of such work may be found in previous rAAV-based studies. A central running theme among these past studies may be described as a 3-phase process for gene therapy applications. This process begins with the slow, steady step-wise progression from *in vitro* to *in vivo* to clinical studies, then shifts to a broad analysis of the strengths and weaknesses of these studies, and culminates with a description of ways to address the shortcomings of previous studies with implementation of modified protocols. This 3-phased approach has been the hallmark of gene therapy for such diseases as cystic fibrosis, alpha-1 antitrypsin deficiency, Duchenne's muscular dystrophy, and hemophilia. Moreover, a careful progression from *in vitro* to *in vivo* to clinical work, followed by extensive evaluation, and a revised clinical approach, will likely be the general format guiding the development of rAAV gene therapy for ADA-SCID. In this section, just a few of these past studies focused upon gene therapies for monogenetic disease will be described. Attention will be given to overall study strengths and weaknesses, suggested

improvements for future trials, and the relevance of the study to a potential rAAV-based therapy for ADA-SCID.

Recombinant AAV for CF and AAT-Deficiency

For two decades, Flotte lab has endeavored to treat two monogenetic diseases, alpha 1 antitrypsin deficiency (AAT-deficiency) and cystic fibrosis (CF) using rAAV gene therapies. Three primary scientific factors have made this clinical gene therapy work possible, the discovery of the genes responsible for CF and AAT-deficiency, the cloning of those genes into rAAV2, and the development of suitable tissue culture and animal models. Just as with ADA-SCID, which commonly manifests from missense mutations of a single gene, missense mutations of the CFTR gene (encoding the cystic fibrosis transmembrane conductance regulator) and alpha-1 antitrypsin gene (encoding a 52Kd antiprotease secreted from hepatocytes and responsible for the maintenance of lung interstitial elastin) serve as the primary genetic insults manifesting as CF and AAT deficiency, respectively. While first generation vectors incorporated the CFTR and AAT genes within AAV ITRs, along with a poly A region, and type 2 capsids, later vectors utilized such features as a CMV/beta-actin hybrid promoters, pseudotyped capsids, and for CF vectors, a CFTR minigene. (Flotte 2002, Flotte 2005)

Overall, preclinical, phase I, and phase II clinical trial data for CF and AAT-deficiency, demonstrate that rAAV-based gene therapy is viable and safe. These studies were conducted with rAAV2, in almost 150 patients, and in excess of a thousand animals. More specifically, preclinical studies for treatment of CF, in rabbits and non-human primates, showed long-term gene transfer, expression, episomal persistence, and no increase in cellular or cytokine immune response. Subsequently, CF phase I trials demonstrated gene transfer according to a dose-response pattern and some gene expression, while CF phase II trials demonstrated short-term gene transfer. Moreover, results generated from preclinical studies of rAAV2 therapy for AAT-

deficiency proved promising. In such studies, the primary goals were to mimic or surpass the results of alpha-1 antitrypsin enzyme replacement therapy with muscle or liver delivery of the AAT gene and subsequent secretion of viable AAT. Two sets of results from AAT gene therapy studies were collected in both a C57BL6 mouse model and a DNA-PK-deficient mouse model. However, most importantly, data from the C57BL6 model showed that a single intramuscular dose of vector resulted in levels of secreted AAT which would ameliorate the disease in human beings. Clinical trials remain in progress and have incorporated rAAV2-AAT intramuscular injections as well as rAAV1-hAAT vector delivery. As reviewed by Flotte et al., the latter rAAV1 vector is capable of enhancing transduction efficiency in muscle on the order of 500-fold. Thus, gene therapy studies for CF and AAT-deficiency are ongoing, and although a pronounced clinical benefit from such studies has yet to be realized, rAAV-based approaches are ripe with potential. In particular, the advent of rAAV pseudotyping may facilitate clinical efficacy in the near future. Moreover, observed risks of insertional mutagenesis from AAT-deficiency and CF gene therapy studies were found to be lower than those risks observed with retroviruses, given the predominant, DNA-PK-mediated persistence of episomal rAAV genomes. Finally, such studies lay a practical foundation upon which an rAAV based approach for other monogenetic or metabolic disorders, such as ADA-SCID, involving differentiated, slow-replicating target tissues, such as liver and muscle, may be based. (Flotte 2002, Flotte 2005)

Yet, what weaknesses or limitations of these gene therapies for CF and AAT deficiency may be identified? And how do such limitations offer a window into potential improvements for future gene therapy approaches? Initially, animal and clinical work conducted by Flotte lab towards a gene therapy for CF was predicated on the use of rAAV2 vectors. However, the discovery that the luminal surface of recipient airways lacked AAV2 receptors and co-receptors

highlighted the need for an alternative rAAV serotype predisposed to lung transduction. Similarly, the observation that rAAV2 administration promoted the formation neutralizing anti-AAV2 antibodies, which hindered repeated dosing, further supported the need for alternative serotypes. And, while numerous methods of administration including maxillary sinus injection, aerosol inhalation, nasal and endobronchial installation were attempted to enhance gene delivery and expression, the inefficiency of the ITR promoter served as a limiting factor for gene expression, and indicated a need for improved promoter/enhancer elements. Further difficulties such as the rapid turnover of CF airway epithelium suggested a future need for either repeat dosing, enhanced transduction of target tissues, or a need for early administration of vector prior to the full onset of CF lung pathology. Also, inactivation of rAAV2 in the CF airway by glycocalyx, elastase, alpha defensins, and mucus, emphasized the need for simultaneous manipulation of the CF lung milieu along with CFTR gene delivery. (Flotte 2002, Flotte 2005)

But, how is it that CF and AAT-deficiency gene therapies relate to a potential ADA-SCID gene therapy? First, rAAV gene therapy for AAT-deficiency involves delivery of a good copy of the AAT gene to differentiated tissues such as liver and muscle, subsequent gene expression, and AAT secretion at levels meeting or exceeding those of enzyme replacement therapy. Interestingly, rAAV-based gene therapy for SCID may prove remarkably similar to gene delivery for AAT-deficiency, in that a viable copy of the ADA gene could be delivered via intramuscular or intravenous injection, to procure expression and protein secretion from muscle and liver. The hope of this therapy would also be to meet or exceed enzyme replacement therapy that comes in the form of PEG-ADA treatment. Second, the difficulties described in previous CF and AAT gene therapies offer a window into the challenges ahead for ADA-SCID gene therapy. For example, issues such as the most appropriate vector promoter/enhancer,

vector serotype, target tissue turnover rate, and immune response to vector and transgene over time, which proved significant to gene therapies for CF and AAT-deficiency, would also be raised in rAAV gene therapy for ADA-SCID. Third, the gene delivery vehicle for a potential ADA-SCID gene therapy as well as the nature of target disease, a monogenetic illness with complex pathogenesis, parallel those of previously-described CF and AAT-deficiency studies.

Recombinant AAV for Hemophilia

Yet another homologue to rAAV gene therapy for ADA-SCID, may be found in the continuing pursuit of an efficacious, long-lasting gene therapy for hemophilia. The impetus for the development of hemophilia gene therapy may be described as the lack of available treatment for those who suffer with hemophilia as well as the high cost of treatment. Interestingly, these same forces have also driven the development of ADA-SCID gene therapy. Moreover, the identification and cloning of the genes responsible for hemophilia A and B, factor VIII and IX, respectively, combined with the use of rAAV vectors in animal models as well as patients, has yielded mixed results. In a recent review by High et al., the contrast was described between the success that has been reported in a dog model of hemophilia using gene therapeutics, but the lack of long-term success reported in humans. (High 2007)

Thus far, five phase I clinical trials have been conducted to provide gene correction for hemophilia. Methods have included the use of viral vectors combined with *in vivo* gene delivery or *ex vivo* plasmid transfections and reinfusion of gene-modified cells. In some of the trials, both gene transfer and therapeutic benefits were observed, though not sustained. As emphasized by High et al., prolonged expression of factor VIII and IX at therapeutic levels remains the key to the development of a viable hemophilia gene therapy, though this goal still remains elusive, given the challenges with feasibility, efficacy, or safety the clinical trials have encountered. Though other gene therapy vectors such as retroviruses have been used, two

primary AAV trials for hemophilia B have been conducted as well, and met with limited success. In one of those trials, rAAV carrying the factor IX gene was used to transduce skeletal muscle. While factor IX expression occurred only at levels below the therapeutic threshold, expression was maintained long-term. In the second clinical trial, AAV carrying the factor IX gene was delivered to liver tissue. In this case, expression of factor IX was at therapeutic levels, though immune responses limited the duration of factor IX expression. However, hope does remain with rAAV vectors, particularly with the advent of modern serotypes. Of the five original trials, only introduction of AAV into the liver is being actively pursued according to High et al. (High 2007, Pierce 2007, Vandendriessche 2007)

So, what may be learned from past hemophilia gene therapy studies that may be applied to future studies? In this clinical setting yet again, the importance of enhanced transduction efficiency with new serotypes of AAV takes precedence, especially for future trials. For example, recombinant AAV type 8 and 9 offer superior gene delivery to liver compared to rAAV2, while future trials employing rAAV1 could significantly improve targeting of patient skeletal muscle for ectopic expression of factor IX. VandenDriessche et al. reported superior transduction efficiencies, enhanced factor IX expression levels, and reduced immune responses to rAAV type 8 and 9, compared to lentiviral vectors, in hemophilia B and SCID mouse models. (Pierce 2007, Vandendriessche 2007)

Further lessons that may be learned from hemophilia gene therapy studies include the need to reduce or avoid the immune responses observed in the early clinical trials. To this end, transient immunosuppression may prove beneficial. Also, the use of rAAV8 may reduce immunogenicity, because of a more rapid turnover of capsids compared to rAAV2, and reduced uptake by antigen presenting cells. And, particularly in the context of rAAV delivery to the

liver, Pierce et al. also discusses the immunomodulatory potential of protocols which simultaneously promote regulatory T cell activity and rAAV-mediated factor IX delivery. (Pierce 2007, Vandendriessche 2007)

Lastly, does rAAV gene therapy for hemophilia have a bearing upon a potential gene therapy for ADA-SCID? On the positive side, hemophilia gene therapy studies have illustrated the necessity and utility of alternative vector serotypes towards the correction of a single genetic defect. Such alternative approaches may be very useful towards correction of the ADA-SCID defect as well. However, by the same token, numerous studies conducted and reviewed by High et al. and Manno et al. (discussed previously on pg 24), regarding preclinical and clinical hemophilia gene therapy clinical trials, have illustrated the limited predictive value of animal studies. This drawback is important to keep in mind when preclinical trials using rAAV for the treatment of ADA-SCID in animal models are conducted. Yet, gene therapeutics directed at hemophilia continue to evolve to better target multiple, differentiated, target tissues such as liver and muscle using, for example, new rAAV serotypes. Similarly, the success or failure of a rAAV-based remedy for ADA-SCID may depend upon the success or failure of enhanced targeting, transduction, and long-term Factor VIII or IX expression in these same tissues.

Overall, studies such as Manno et al. offer the promise of rAAV gene therapy but reveal the great challenges that lie ahead for future protocols. While therapeutic levels of Factor IX were achieved with no acute or long-lasting toxicity in the recent trial conducted by Manno group, this safety and short-term efficacy was tempered by cell-mediated immune destruction of transduced cells. The goal of long-term, restored (or ectopic) secretion of a therapeutic protein as an alternative to direct clotting factor administration remains feasible but a significant challenge. If successful, potential ADA-SCID gene therapies utilizing rAAV may evolve and be

modeled after these hemophilia studies with ectopic secretion of ADA protein as an alternative to PEG-ADA injections. Moreover, just as with rAAV gene therapy for hemophilia, so to must immune responses to both vector and transgene be monitored carefully for any potential rAAV-based gene therapy for ADA-SCID. (High 2007, Manno 2006)

Recombinant AAV for Duchenne's muscular dystrophy (DMD)

A foundation for rAAV-based gene delivery for ADA-SCID also may be found in gene therapy research to ameliorate DMD. Unlike ADA-SCID, DMD is X-linked, common (1 in 3500 male births), involves mutations of a structural gene (as opposed to an enzymatic gene), and is primarily a disease of the musculoskeletal and cardiopulmonary systems. However, both conditions are progressive, devastating, monogenetic diseases, which affect primarily pediatric patients, and may be treated with rAAV-based gene therapies targeting muscle tissue. In addition, the identification of dystrophin as the massive gene (14 Kb) responsible for DMD served as the first step in the development of rAAV-mediated treatment of DMD. The subsequent development and cloning of mini- or microdystrophins into rAAV, and the use of such vectors to transduce skeletal muscle in several mouse models, have provided the preclinical basis for rAAV-based gene therapy for DMD. (Athanasopoulos et al. 2004, Abmayr 2005)

So, what have preclinical gene therapy studies for DMD and broader gene therapy experiments relevant to the treatment of DMD demonstrated? In a review by Athanasopoulous et al., transgenic mouse and patient data illustrate that myofibers and muscle groups of the limb and diaphragm must accumulate around 20% of wild-type dystrophin expression for substantive correction of the DMD phenotype to occur. However, because the lethality of DMD ultimately rests with cardiopulmonary pathology, an estimated correction of approximately 50% of cardiomyocytes in mdx mice (a model of DMD) may be needed remedy the cardiomyopathy inherent to advanced DMD. (Athanasopoulos et al. 2004, Abmayr 2005)

Meanwhile, broader gene therapy studies, particularly vector studies, have also yielded valuable observations, relevant to a rAAV-based gene therapy for DMD: First, such studies have emphasized the natural tropism of AAV for muscle fibers relative to that of other vectors such retroviruses, adenoviruses, and herpes simplex viruses. Thus, the innate tropism of rAAV makes the vector advantageous in the treatment of DMD (and ADA-SCID). Second, rAAV2 optimally transduces young, regenerating myotubes, like many observed in DMD. These myotubes express high levels of the AAV2 receptor, heparin sulfate proteoglycan, which facilitates efficient rAAV2 transduction. Third, alternative serotypes, such as rAAV1,5,6, and 7 have been shown to significantly enhance the efficiency of murine skeletal muscle transduction compared to rAAV2, with gene expression increasing on the order of two-1000 fold. Fourth, Athanasopoulous et al. also described a study showing that rAAV1 provides a higher transduction efficiency in both liver and muscle than that of rAAV5, 3, 2, and 4. Further, the superior gene transfer characteristics of rAAV1 especially in muscle, may be due to an alternative, unclear entry mechanism, a unique intracellular route of gene delivery, and variations in the amino acid sequence of the VP1 capsid protein of AAV1. It is also worth noting, that AAV7 vectors have demonstrated muscle transduction on par with that of AAV1 while reducing the already low inflammatory response to AAV vectors. This modulation of AAV-induced inflammation is based on the observation that neutralizing antibodies to AAV7 are both rare in human serum and low in activity. (Athanasopoulos et al. 2004, Abmayr 2005)

On the other hand, specific, preclinical gene therapy studies for DMD have shed light on the potential of this therapeutic modality. Athanapoulos et al. described one study in the mdx mouse model, in which rAAV6, carrying a microdystrophin with four-repeats, was delivered by intravenous administration to elicit a number of beneficial effects and advance rAAV gene

therapy for DMD. Such effects include improvements or restoration of force output in an mdx mouse along with widespread gene delivery to skeletal muscle. Other preclinical studies include AAV-mediated minidystrophin delivery via intramuscular (IM) injection the hindlegs and tibialis anterior (TA)muscles of mdx and C57BL6 mice. In this study, improvements in muscle contractile force as well as protection from contraction-induced muscle dysfunction were observed. Another experiment conducted in nude and mdx mice, involved rAAV-mediated microdystrophin delivery by IM to TA muscle, sarcolemmal expression of the microdystrophin, restoration of the dystrophin-associated protein complex, decreases in central nucleation, and an overall inhibition of myofiber degeneration. Further preclinical analysis came in the form of rAAV-mediated microdystrophin delivery by IM to gastrocnemius in an mdx model. In this setting, reversal of the muscular dystrophy was observed with muscle force restoration and improvements of dystrophic muscle contractile function. Finally, recent studies in co-delivery of rAAV6 vectors carrying a microdystrophin or a muscle-specific Igf-1 isoform have demonstrated not only co-expression of both therapeutic elements, but also morphological and functional recovery of dystrophic muscle in mdx mice. Interestingly, a therapeutic synergy occurred, in which dystrophin expression reduced myofiber degeneration and turnover while improving resistance of the muscle fibers to mechanical injury, while co-expression of IgF1 increased muscle mass and strength in mdx mice. An overall correction of the DMD phenotype resulted. (Athanasopoulos et al. 2004, Abmayr 2005)

In conclusion, preclinical studies have demonstrated the efficacy, safety, and feasibility of rAAV-mediated gene delivery towards the treatment of DMD. Preclinical studies have also established the groundwork for potential phase I clinical trials. Such trials would employ rAAV vectors carrying microdystrophin genes, administered by intramuscular injection, with the

primary goal of evaluating treatment safety and/or toxicity. To avoid immune responses to expressed microdystrophins, patients will be chosen with two main criteria in mind, the presence of small, preferably point mutations in the host dystrophin gene, and the presence of 'revertant' dystrophin positive muscle fibers. Either criteria suggests host tolerance to endogenous dystrophin, and thus, an increased likelihood of immunological tolerance to expressed microdystrophins. (Athanasopoulos et al. 2004, Abmayr 2005)

Yet, how does rAAV-mediated gene transfer for DMD compare to a potential rAAV gene therapy for ADA-SCID? Also, while both treatment regimens have their differences, what distinct similarities serve to support an rAAV-mediated approach for the correction of the ADA-SCID defect?

The differences between the two relevant therapies are important to note. Recombinant AAV therapy for DMD involves the replacement of a structural gene in the target host cells, with or without assistance from such co-administered gene therapies as that of IGF1. Ultimately, the hope would be to restore muscle mass and muscle strength, while preventing muscle degeneration and offering protection to myofibers from mechanical injury. By contrast, rAAV therapy for ADA-SCID would involve delivery of an enzymatic gene capable of being expressed and secreted to promote systemic detoxification and immune reconstitution. (Athanasopoulos et al. 2004, Abmayr 2005)

However, both gene therapy applications also share important similarities, by which DMD gene therapy with rAAV vectors provides a basis and model for ADA-SCID gene therapy using the same gene delivery vehicles. Both conditions may be treated with rAAV-based gene therapies targeting muscle tissue. Thus, successful rAAV delivery of microdystrophins to skeletal muscle for the correction of DMD provides a sound model and solid basis for additional

applications, such as rAAV delivery of ADA to skeletal muscle for the correction of ADA-SCID. Likewise, both gene therapy approaches would exploit the ability of muscle tissue to maintain vector genomes episomally and efficiently to express and secrete protein long-term. As such, past success in preclinical gene therapy studies for DMD would justify similar studies for ADA-SCID. Also, both ADA-SCID or DMD gene transfer strategies would be capable of utilizing a broad therapeutic window. In other words, for either DMD or ADA-SCID gene transfer approaches, protein expression levels well above normal, for both adenosine deaminase and dystrophin, are well-tolerated, with no pathological consequences. And so, safe overexpression of microdystophins in DMD gene therapy studies helps justify a strategy to overexpress ADA in ADA-SCID gene therapy experiments. Moreover, both therapeutic regimens are attempting to correct debilitating and potentially lethal monogenetic disorders. Therefore, a sound therapeutic approach, relying upon rAAV, for amelioration of DMD substantiates the application of rAAV towards the correction of another devastating, monogenetic disorder, ADA-SCID. Finally, any viable DMD or ADA-SCID gene therapies will have to address both the underlying genetic defects as well as the functional deficits inherent to each condition. Thus, if DMD gene therapies based on rAAV vectors can potentiate a dual correction of the dystrophin gene and muscle functionality, then ADA-SCID gene therapies utilizing rAAV stand a greater chance of success for correcting multiple defects at genetic, metabolic, and immunological levels. (Athanasopoulos et al. 2004, Abmayr 2005)

Table 1-1. Current Therapies for ADA-SCID & Retroviral Gene Therapy for ADA-SCID

Current Treatment Option for ADA-SCID	Treatment Description	Observed or Potential Advantages of Treatment	Observed or Potential Disadvantages of Treatment	Year of Treatment Implementation
Enzyme Replacement Therapy (PEG-ADA)	Intramuscular injection 1x or 2x weekly of polyethylene-conjugated bovine ADA to provide a serum-based systemic detoxification of accumulating toxic metabolites such as dATP (Booth et al. 2007, Kohn et al. 2005)	*Generally tolerated well at doses that maintain ectopic ADA at activity levels 100 fold above normal *In the short term, immune reconstitution varies, but many cases are reported of full or protective immunity (both in terms of lymphocyte number and function). *In the long term, despite waning immunity, most patients remain clinically well, free of infections, and with normal development trends. *Enzyme acts as a continuously circulating "metabolic sink" (Booth et al. 2007, Kohn et al. 2005)	*In the short-term, ~50% of children remain on IVIG therapy *In the long-term, decline in T cell numbers and function *Significant expense *Repeated administration potentially over the lifetime of the patient (Booth et al. 2007, Kohn et al.2005)	1987 (Hershfield et al.)
Bone marrow or Hematopoietic Stem Cell Transplantation	HLA-typed and matched bone marrow, or CD34+ HSCs, are harvested from siblings, family, or unrelated donors (or, alternatively, haploidentical marrow and HSCs are harvested, for example, from parental donors), cultured, and reinfused into patients to provide immune reconstitution, correction of the metabolic defect, and clinical benefit. (Booth et al. 2007, Honig et al. 2007)	*Standard of care for many years *73% survival for allogeneic matched family donor HSCT *Complications are managed more efficiently than in the past with improved supportive care, improved antibiotic regimens, enhanced conditioning protocols, and better treatment of graft vs. host disease (GVHD) *Substantial improvements in lymphocyte counts and function has been observed in numerous cases of matched HSCT, leading to a correction of the immune deficiency *Substantive improvement in the metabolic defect have been observed followed matched HSCT (Booth et al. 2007, Honig et al. 2007)	*3 year survival is 29% for mismatched or haploidentical transplantation *As of December 2006, no survival outcome data for unrelated or umbilical cord blood transplantation *Often, a matched donor is unavailable. *Mismatched or haploidentical BMT has the poorest outlook with numerous complications due engraftment, infections, and GVHD *The health risks associated with mismatched or haploidentical BMT (or HSCT) have often been associated with poor engraftment, and pre-tranplantation conditioning regimens. (Booth et al. 2007, Honig et al. 2007)	1968 (data stretch back to this year as reviewed by Booth et al.)

Table 1-1. Continued.

Current Treatment Option for ADA-SCID	Treatment Description	Observed or Potential Advantages of Treatment	Observed or Potential Disadvantages of Treatment	Year of Treatment Implementation
Retroviral Gene Therapy	Autologous HSCs or PBLs are harvested from patients, transduced with retroviral vectors carrying the ADA gene, and reinfused into patients to reconstitute patient immunity, correct the underlying metabolic defect, and enhance the clinical prognosis of patients Aiuti et al. 2003 and 2004, Muul et al. 2003)	*Protocols have evolved substantially since the early clinical trials, and provided substantial correction of the underlying metabolic and immunological defects with demonstrable clinical benefits. *No instances of leukemogenesis have been reported for patients treated for ADA-SCID with retroviral gene therapies to date. (Aiuti et al. 2003, 2004, and 2007, Muul et al. 2003, Gaspar et al. 2006)	*Retroviral vectors have been limited to the transduction of dividing target cells, and are thus limited in their capacity to ameliorate the effects of ADA-SCID in post-mitotic or slowly dividing cells, such as those of the central nervous system, liver, lung etc… *The occurrence of 5 total adverse events, associated with the use of similar retroviral vectors for treatment of X-SCID, may present a substantial safety risk regarding the long-term, widespread, or continued use of these vectors for any primary immune deficiency. (Flotte et al. 2007, Bushman et al. 2007)	1990 (Anderson et al.)

CHAPTER 2
INTRODUCTION

Recombinant AAV Gene Therapy for ADA-SCID

General Strategy for a Potential rAAV-Mediated Correction of ADA-SCID

The unique nature of ADA-SCID, its metabolic pathophysiology and its widespread abundance in tissues throughout the body rather than in just those of the immune system, necessitates unique therapeutic approaches. First, ADA SCID allows various metabolites such as adenosine, deoxyadenosine, and ATP to accumulate in tissues throughout the body especially in the immune system. Moreover, the various tissues of the body may possess a variable dependency upon ADA. The implication may be that the greater the tissue dependency upon ADA, the greater the accumulation of toxic metabolites in the absence of ADA, and the more devastating the outcome for that tissue. For example, among tissues of the body, B and T lymphocytes depend heavily upon ADA activity. And, when ADA synthesis and function are impaired, the most glaring feature of the disease is immune system malfunction. Thus, two important conclusions may be drawn: Any *viable therapy* for ADA SCID will have to address first the most severe aspect of the disease, the immune system. In addition, any *potential cure* will have to approach ADA SCID globally, with the intention of remedying numerous tissues of the body including those of the nervous and musculoskeletal systems.

But, how could rAAV be employed to treat or cure a monogenetic disease which primarily affects the rapidly dividing cells of the hematopoietic system and peripherally affects most other body tissues? After all, unlike retroviruses which preferentially integrate into the genome of the target cell and are passed down to multiple lymphoid and myeloid lineages, rAAV integrates much less frequently, and often remains episomal as large molecular weight concatemers in the host cell nucleus. Thus, in cells such as HSCs, though some integration has

been demonstrated for rAAV7 (Han et al.), most episomal rAAV would likely be lost following several rounds of hematopoietic differentiation or renewal. (Han, *et al* 2008)

One possible solution is to target tissues other than hematopoietic stem cells, tissues which are less likely to divide, and thus, more likely to maintain rAAV episomes. Tissues such as skeletal muscle, liver, heart, and even brain, which may also be ADA-deficient, may have the ability to both maintain rAAV for extended periods and utilize an endogenous secretory apparatus to process and release a secretable form of human adenosine deaminase (hADA).

This strategy would exploit the unique properties of rAAV, including low immunogenicity, no known toxicity in humans, relative ease of administration, viral stability, long-term efficacy, and the ability of the vector to target both dividing and non-dividing cell types, to deliver the ADA gene and maintain gene expression with subsequent protein secretion. Please refer to Table 2 for more information regarding rAAV vectors and the serotypes of interest.

Ectopic hADA expression and activity would potentially have two effects which may be thought of as either local or systemic. Local hADA expression could detoxify the parent tissue in which the vector predominantly resides, such as skeletal muscle, liver, or brain. On the other hand, secreted hADA may exert its effects systemically, causing an irreversible, hydrolytic deamination of circulating Ado, dAdo, and dATP. Thus, cell types distant from the site of expression, such as hematopoietic progenitors, may be relieved of their own burden of metabolic detoxification. Ectopic sites of hADA expression would serve a systemic function as a "metabolic sink," a term described by Don Kohn, a pioneer in the field of ADA SCID gene therapy.

Overall, this rAAV gene therapy strategy, modeled after PEG-ADA injections in which the enzyme acts in the serum to detoxify body tissues, would deliver a gene encoding a secretable form of human ADA to detoxify host tissues long-term with as little as a single dose of vector at a fraction of the cost of PEG-ADA. However, it must be noted that the model for this rAAV approach, PEG-ADA therapy, is not without its limitations. Chan et al. found that with PEG-ADA administration, though increases in T, B, and NK cell numbers and protective immune function occur, lymphocyte numbers still remain below normal. In addition, after a few years, lymphocyte proliferation in response to mitogens decreases, and normal responses to antigens are less than expected. Malacarne et al. also found that following a prolonged period of PEG-ADA administration, decreased thymic function, B cell oligoclonality, and increased apoptosis among peripheral T lymphocytes may account for the persistence of immune deficiency even with enzyme replacement. A rAAV-based approach utilizing secretable ADA may parallel both the effects and limitations of PEG-ADA administration, or may surpass the efficacy of enzyme replacement therapy (ERT). Delivery of a secretory hADA gene to a host of diseased target tissues, which would also serve as potential sites of ectopic expression, may provide local and systemic effects not witnessed with ERT. For example, given that ADA-SCID affects numerous tissues throughout the body, gene delivery to liver or even thymus with rAAV9 may ameliorate local tissue deterioration while secreting hADA for systemic detoxification. Finally, depending upon the ADA mutation in any given patient (ie missense or null) and the patient phenotype, and thus the degree of immunological tolerance for ADA, secreted human ADA may be at least as well-tolerated if not more so in the long term than polyethylene-glycol-conjugated bovine ADA. (Chan 2005, Malacarne 2005)

Factors Affecting the Efficacy of A Potential rAAV Gene Therapy for ADA-SCID

A rAAV based approach to ADA-SCID gene therapy would rely heavily upon several experimental and biological factors. As with almost any rAAV gene delivery strategy, the method of administration can be one of the single most important determinants of vector delivery and subsequent gene expression. The experiments proposed for these studies in ADA-SCID gene therapy will focus primarily upon intramuscular delivery of rAAV1 and intravenous administration of rAAV9. Moreover, the timing of vector administration can make a profound difference in rAAV-mediated gene delivery, particularly in the context of a disease which may manifest early in life and progress quickly to lethality, like ADA-SCID. In the case of ADA-SCID, early administration in mice will have to be examined closely, with a time frame of vector delivery from the early neonatal period up to 4 months of age. The correct dosing of vector will also be a key determinant in the efficacy of rAAV-mediated gene delivery. The goal will be to achieve the greatest level of gene delivery and expression with the lowest dose of vector possible.

Additional challenges in the development of a viable rAAV-based therapy for ADA-SCID include the choice of rAAV serotype and promoter/enhancer element, the nature and size of the target tissue of interest, and the potential for an immune response to the administered gene therapy. Often, the serotype and promoter/enhancer may be determined based on the target tissues of interest. In this case, the secretory apparatuses of muscle and liver make these tissues ideal and a hybrid CMV promoter/chicken beta-actin enhancer will be used to elicit ADA gene expression. Moreover, the primary serotypes being employed in this study are a rAAV type 1 vector for direct skeletal muscle targeting, and a rAAV type 9 (or 8) vector for gene delivery to a number of host tissues including liver, skeletal muscle, and cardiac muscle by intravenous administration. An additional factor, which is key to substantive, safe, prolonged gene

delivery/expression with rAAV vectors, is the abundance of target tissue available for transduction and capable of serving as an ectopic site of secretion. Tissues such as skeletal muscle and liver are in large abundance within the body of an animal model, such as a mouse, or within a potential human patient. Also, just as in the case of factor IX /alpha-1 antitrypsin secretion in the setting of rAAV delivery, the immune responses to vector capsid and transgene will have to be carefully analyzed for both ADA and the rAAV vectors which carry the gene.

Yet, one more challenge must be given special attention. Given that adenosine deaminase is normally a cytosolic or membrane-bound ecto-enzyme and not normally a secreted enzyme, how may secretion of rAAV vector-derived and expressed hADA be achieved? One method currently under investigation in Srivastava lab utilizes an Ig (immunoglobulin) K-chain leader sequence to serve as a secretory signal upstream and in-frame with the cloned hADA transgene within a rAAV plasmid backbone. This 5' secretory sequence as well as a c-myc/polyHistidine tag, which lies downstream of the 3' end of the transgene (discussed in the Future Perspectives section), initially were obtained using an expression vector called pSecTag, designed by Invitrogen. The completed gene cassette, containing the 5' secretory signal, the hADA transgene, and the cmyc/polyHis tag, residing within the Invitrogen expression vector, was then cloned into a rAAV plasmid backbone. Once translated, ongoing experiments yet unpublished indicate that the IgK secretory peptide may direct the expressed hADA protein along the secretory pathway of a target cell. Signal peptidase-directed cleavage after the aspartic acid residue 21 of the signal peptide likely follows delivery of translated hADA protein to the cellular secretory pathway. The target cellular secretory pathways normally shuttle protein to internal cellular compartments, the plasma membrane, and to the extracellular space via such organelles as the endoplasmic reticulum and the golgi apparatus. For this approach, the secretory

signal of interest may be utilized to "trick" the target cell of interest into sending the expressed transgene of interest, hADA, along the cellular secretory pathways. (Coloma 1992, Sharoyan, *et al* 2006)

Finally, two choices in animal models exist for ADA-SCID, in which, rAAV carrying the ADA gene may be tested. One mouse model, developed by Blackburn group, has been engineered with a placental gene rescue. In this model, an ADA minigene construct delivered to the embryo is expressed during embryological and fetal development under the control of a trophoblastic response element. The resulting mouse model typically lives for only 3 weeks postnatally, dying of pulmonary insufficiency and a profound pulmonary eosinophilia. Yet, another model, also developed by Blackburn group, utilizes a placental and a foregut ADA rescue. This model displays a partial immune deficiency, which is currently being analyzed. Moreover, the life expectancy of this dual-rescue model, while vastly improved over that of the single-rescue mouse model, is currently being investigated. (Blackburn, *et al* 1998, Blackburn, *et al* 1996)

Endpoints for Evaluating the Efficacy of a Potential rAAV Gene Therapy for ADA-SCID

The clinical trials and animal modeling performed to date for the correction of ADA-SCID underscore the importance of distinct, clear endpoints for the evaluation of each study. Such endpoints not only allow efficacy of any single trial or study to be assessed but also provide a standard by which the outcomes of future clinical trials may be compared as well as clues as to what future protocols may be more successful. Thus, any viable ADA-SCID trial using retroviruses, or potentially, rAAV, would employ a number of cellular, molecular, functional, and clinical endpoints. (Aiuti 2004, Aiuti 2003, Cavazzana-Calvo and Fischer 2007, Cavazzana-Calvo 2007, Parkmam 2000, Qasim 2004)

One of the most important outcomes for any ADA-SCID trial is the cellular response to the administered gene therapy. Prior to rAAV injection as well as post-injection and at numerous time points, a comprehensive evaluation and comparison of both the number and type of immune cells, namely B and T lymphocytes, will serve as a prime indicator of clinical trial efficacy. Depending upon the target tissue, further evaluations may focus upon numbers of transduced versus nontransduced cells, such as lymphocytes, hematopoietic progenitors, or other target cell types like skeletal myocytes. Another valuable approach is to assess the lymphocyte repertoire through the relative numbers of antigen-specific versus antigen non-specific lymphocytes, through TCR and BCR genetic analysis, and indirectly by functional studies involving lymphocyte proliferation to specific antigens and mitogens. Lymphocyte longevity also remains an important indicator of efficacy for ADA-SCID gene therapies. And, although these cellular factors have so far been evaluated following PEG-ADA, BMT, and retroviral gene therapy, cellular indicators will also be vital for a rAAV based approach. Finally, an overall assessment of the correction of the immunological defect will depend upon cellular analysis. (Aiuti 2004, Aiuti 2003, Cavazzana-Calvo and Fischer 2007, Cavazzana-Calvo 2007, Parkmam 2000, Qasim 2004)

Next, any *in vivo* or clinical trial work performed using retroviral, lentiviral, or rAAV based approaches must assess the molecular and biochemical endpoints of SCID gene therapy. Regardless of the particular technique employed, gene delivery to target tissues serves as a hallmark of gene transfer efficiency. However, an analysis of transgene expression at the level of both mRNA and protein is equally as valuable an indicator of transduction efficiency and vector viability. Also, the level of enzyme activity remains an efficient means of evaluating the correction of the metabolic defect characteristic of ADA-SCID. Finally, no biochemical analysis

of an ADA-SCID patient would be complete without a comprehensive profile of dATP, SAH hydrolase, adenosine (Ado) and deoxyadenosine (dAdo)levels found in blood and/or urine. (Aiuti 2004, Aiuti 2003, Cavazzana-Calvo and Fischer 2007, Cavazzana-Calvo 2007, Parkmam 2000, Qasim 2004)

Another method to gauge SCID gene therapy utilizing rAAV, is through studies of immune function. ADA-SCID is a disorder of both immunological differentiation and function. And, while immunological reconstitution would constitute success for rAAV gene therapy, the ability of patient lymphocytes to respond to a variety of antigens and mitogens is essential for the recovery of ADA-SCID patients. Enhanced immune function following rAAV gene therapy, though challenging, may be feasible. And, if improvement in immune function is observed, an rAAV treatment modality may qualify as a standard of care equal or superior to PEG-ADA administration and haploidentical BMT (in the absence of identical BMT from a sibling or matched unrelated donor). (Aiuti 2004, Aiuti 2003, Cavazzana-Calvo and Fischer 2007, Cavazzana-Calvo 2007, Parkmam 2000, Qasim 2004)

Finally, to complete a thorough evaluation of the efficacy of rAAV gene therapy for ADA-SCID, the clinical benefit of treatment must be ascertained. Decreases in recurrent or life-threatening infections are indicative of clinical benefit as is correction of the failure to thrive often observed in ADA-SCID patients. A reversal of failure to thrive may come in the form of improvements in height or weight. Clinical improvement may also manifest as the ability to safely remove IV IG therapy, cease PEG-ADA altogether, or end the search for a compatible bone marrow donor. Finally, improvements in non-immunological symptoms, ranging from neurological and musculoskeletal abnormalities to hepatic, renal, and pulmonary impairments,

would serve as valuable markers of clinical benefit as well. (Aiuti 2004, Aiuti 2003, Cavazzana-Calvo and Fischer 2007, Cavazzana-Calvo 2007, Parkmam 2000, Qasim 2004)

A rAAV1 Strategy for the Amelioration of ADA-SCID

In a review by Flotte et al. in 2007, describing the past and current state of gene therapy, several points discussed help justify the development of a rAAV gene therapy for ADA-SCID: Most importantly, genetic disease which demands expression in the long-term makes a well-suited disease target for lentiviral and rAAV vectors. As in the case of ADA-SCID, this observation may prove useful. Secondly, an understanding of the gene responsible for a given disease must be thorough for applied gene therapy to have a reasonable chance of success. Following over two decades of research related to ADA, one may say the gene has been well-characterized. Third, while it may not be expected that diseases with multifactorial roots, such as cancer, may respond to overexpression of a single gene, monogenetic diseases are more likely to respond to single-gene overexpression. Years of research with retroviruses and PEG-ADA support this conclusion. Thus, ADA-SCID presents a good candidate for treatment by overexpression of ADA from vectors such as rAAV. Fourth, the presence of null mutations in the gene responsible for an illness, increase the likelihood of an adverse immune response, upon introduction of the correct protein to the patient. In the case of ADA-SCID, the majority of mutations in ADA are missense while few are non-sense. Thus, if most ADA-SCID patients were exposed to a correct version of ADA, the chance of an adverse immune response to the protein is reduced compared to the likelihood of an inflammatory reaction in the setting of patient with a null mutation in ADA (or that of a patient with a different condition such as hemophilia, bearing a null mutation in factor VIII or IX). (Flotte 2007)

Finally, one additional justification for the pursuit of a rAAV gene therapy for SCID may be found in additional research studies. Following gene therapy, the amount of target ADA

activity necessary to observe a physiological and clinical benefit is not unattainable, and has been demonstrated in previous retroviral gene therapy trials, such as Aiuti et al. in 2002. According to Aiuti et al., the normal target range of ADA activity in peripheral blood lymphocytes is 1350 +/- 650 nmol (typically of inosine)/hour/mg, while normal ADA activity in RBCs is expressed as 12 +/- 2 umol/hour/ml. Please refer to this study for further information. These values would serve as the target ranges for any rAAV-based gene therapy as well. Alternatively, in a research study by Hershfield et al. in 2003, using a variety of patients with a diverse repetoire of genetic mutations, percent ADA activity values were obtained for immunodeficient patients and partially deficient patients. Immunodeficient patients were reported to have .001% to 0.6% of normal ADA activity levels, while partially deficient patients displayed 1% to 28% of normal ADA activity. A rAAV gene therapy regimen naturally would seek to exceed these values. For example, a minimum boost in ADA activity for immunodeficient patients into the range of enzyme activity for the partially deficient patients, such as 3-10% of normal, may be feasible. Moreover, at this relative level of ADA activity, consistent with a partial deficiency, rather than a pronounced, primary immune deficiency, immunological, metabolic, and clinical benefits may be observed. (Aiuti 2002a, Hershfield 2003)

With these justifications as well as previous rAAV-mediated gene delivery strategies for monogenetic disease previously discussed in mind, one strategy for the treatment of ADA-SCID may be with rAAV serotype 1 carrying a secretory version of the adenosine deaminase gene and a hybrid CMV promoter/chicken beta-actin enhancer (CB). The target tissue of interest is skeletal muscle, while the method of administration would be intramuscular injections. More specifically, current research involves the injection of rAAV1 vectors, with a CB

promoter/enhancer element, shuttling a secretory, cmyc/poly Histidine tagged ADA gene into the quadriceps muscles of ADA-SCID mice bearing a placental/foregut rescue (previously discussed). The tag employed has several purposes. While the cmyc/polyHis tag is currently being utilized in Western Blots, following transfection of 293 cells with rAAV plasmid, to confirm the presence of secretory ADA in tissue culture media, as opposed to the presence of non-secretory ADA in cell culture lysates , and to distinguish between endogenous or vector-derived ADA. Subsequently, in animal studies, the tag may be used to distinguish vector-derived ADA from non-vector derived ADA that is present in varying amounts, depending upon the tissue, in wildtype, heterozygote, and rescued knockout mice. (Flotte 2004, Kapturczak 2005)

Additional aspects of a rAAV1-mediated gene transfer strategy include vector distribution and dosing. To maximize vector distribution in a relatively large muscle like the quadriceps, injections of vector preparations are performed in several sites on the surface of the muscle. Doses of vector for this study range from 1x10^10 to 1x10^12 vector particles. Finally, the goals of this experiment are two-fold: The first goal of this body of research was to use rAAV type 1 vectors to shuttle a secretory version of the human ADA gene to skeletal muscle tissue within a partially immune-deficient murine model of ADA-SCID in order to foster ectopic expression, secretion, and activity of the enzyme, human adenosine deaminase (hADA). Long-term, the first goal would be expanded to express ADA in the same mouse model of ADA-SCID at therapeutic levels. The second goal was to promote an immune reconstitution within this mouse model of ADA-SCID following enzyme expression, secretion, and activity. Long-term, the second goal would be expanded to provide immune reconstitution in the same ADA-SCID knockout mouse model equivalent or superior to that achieved by PEG-ADA injections.

A rAAV9 Approach for the Treatment of ADA-SCID

An alternative rAAV-based strategy to correct the ADA-SCID phenotype rests with two alternative serotypes, type 8 and 9. Recombinant AAV8 and 9 vectors are highly efficient at crossing the endothelial barriers throughout murine vasculature, and transducing numerous tissues, including liver, pancreas, skeletal muscle, and especially, cardiac muscle. Thus, a rAAV type 8 or 9 approach to ADA-SCID gene therapy would seek to achieve the same primary and secondary goals as a rAAV1 approach, though the means and methodology to achieve such ends are different. (Inagaki 2006)

Given the ability of rAAV 8 and 9 to cross endothelium upon injection into the host vasculature, a solid strategy may be to use rAAV9 vectors in the setting of intravascular administration. More specifically, tail vein injections are being utilized currently to deliver rAAV9 carrying the secretory, cmyc/poly Histidine tagged ADA gene to numerous tissues throughout the ADA-SCID mouse model. The greatest advantage of this approach is the potential for global distribution of vector, a quality lacking in previous retroviral methods for delivery of the ADA gene in preclinical and clinical studies. While the dosing range remains the same for this rAAV9 methodology as it is for the rAAV1 strategy, the tissue distribution is potentially much greater. Also, expression of a secretory version of ADA from numerous ectopic sites may enhance the systemic correction of the metabolic and immunological defects inherent to ADA-SCID. And, since secreted ADA may be only a fraction of the total amount of expressed ADA in a given tissue, intracellular ADA may elicit a local correction of the transduced cell types, which could range from neurons to myocytes to hepatocytes.

Similar to the rAAV1 strategy, the goals for a rAAV9 approach toward the potential amelioration of ADA-SCID are two-fold: The first goal of this body of research was to use rAAV type 9 vectors to shuttle a secretory version of the human ADA gene to a variety of

tissues, especially heart, within a partially immune-deficient murine model of ADA-SCID, in order to foster ectopic expression, secretion, and activity of the enzyme, human adenosine deaminase (hADA). Long-term, the first goal would be expanded to express ADA in the same mouse model of ADA-SCID at therapeutic levels. The second goal was to promote an immune reconstitution within this mouse model of ADA-SCID following enzyme expression, secretion, and activity. Long-term, the second goal would be expanded to provide immune reconstitution in the same ADA-SCID knockout mouse model equivalent or superior to that achieved by PEG-ADA injections.

A Secondary Strategy Using rAAV7 for HSC Transduction and Correction of ADA-SCID

Recently published work performed by Srivastava lab (Han et al.) has examined the potential of various rAAV serotypes for HSC transduction. Although much controversy exists surrounding the efficacy of AAV vectors in hematopoietic stem cell (HSC) transduction, the application of this Srivastava lab research to ADA-SCID gene therapy may ultimately prove fruitful. Specifically, this research was performed following a previous study demonstrating significant single-stranded AAV1-mediated murine hematopoietic stem cell transduction. Subsequently, in the most recent Srivastava study (Han et al.), two primary serotypes, namely AAV1 and AAV7 containing self-complementary vector genomes (which bypass the need for viral second-strand DNA synthesis), are reported to facilitate efficient transduction of HSCs in a murine serial bone marrow transplantation model *in vivo*. Self-complementary vectors are discussed further in the next section. (Han, *et al* 2008)

And perhaps most importantly, the analysis of integrated, proviral AAV genomes demonstrates stable integration with no overt hematological abnormalities. This observation may hold the key to overcoming the adverse events of the X-SCID retroviral gene therapy trials. At the outset, retroviral vectors proved promising in animal models and in human clinical trials.

In addition, it must be noted that no patients to date from retroviral gene therapy trials for ADA-SCID have experienced adverse events. However, the occurrence of T cell lymphoma in non-human primates, and the manifestation of T-cell leukemia in 5 pediatric patients following retroviral-based gene therapy for X-SCID (4 from a clinical trial in Paris and 1 from a clinical trial in London), dealt a serious blow to the practice of retroviral gene delivery. Questions as to the risk and safety of retroviral vectors have arisen. Moreover, numerous groups have endeavored to describe the mechanism of insertional mutagenesis underlying these occurrences of T-cell leukemia. Meanwhile, an alternative therapeutic approach to circumvent at least some of the troubles of retroviral gene therapy may be possible. This recent rAAV/HSC transduction study by Srivastava group may offer a new, safe, effective avenue for treatment of hematopoietic disease, including primary immunodeficiencies like ADA-SCID. Further studies are needed. However, of the vectors studied, rAAV7 may be the most useful. Thus, rAAV7 carrying a non-secretory ADA gene, driven potentially by a promoter that is specific to lymphoid progenitors, and targeting HSCs may provide an efficient, safe, and long-term gene delivery alternative for correction of ADA-SCID. (Board of the European Society of Gene and Cell Therapy 2008, Deichmann A 2007, Hacein-Bey-Abina S 2003, Han, *et al* 2008, Kohn 2003a, Kohn 2003b, Pike-Overzet 2007)

Although not part of the body of research described in this thesis, future research based on rAAV7 vectors would also have two primary goals similar to those described for the rAAV1 and rAAV9 strategies: The first goal would be to use rAAV type 7 vectors to shuttle a non-secretory version of the human ADA gene to hematopoietic stem cells or lymphoid progenitors, derived from a partially immune-deficient murine model of ADA-SCID, and subsequently re-infused, in order to foster protein expression and hADA activity in lymphocytes. Long-term, the

first goal would be expanded to express ADA in lymphocytes in the same mouse model of ADA-SCID at therapeutic levels. The second goal would be to promote an immune reconstitution within this mouse model of ADA-SCID following enzyme expression, secretion, and activity. Long-term, the second goal would be expanded to provide immune reconstitution in the same ADA-SCID knockout mouse model equivalent or superior to that achieved by PEG-ADA injections.

Self-Complementary Vectors for the Treatment of ADA-SCID

Self-complementary AAV (scAAV) vectors offer two distinct advantages in the treatment of monogenetic disease over single-stranded rAAV (ssAAV) vectors. First, scAAV vectors possess increased genomic stability over their ssAAV counterparts. Thus, upon delivery to target cells, double-stranded, as opposed to single-stranded DNA, will undergo less degradation and lead to a greater number of persistent genomes. Second, since scAAV utilizes double-stranded DNA, the rate-limiting step of AAV transduction, second-strand synthesis, is unnecessary. Thus, scAAV vectors provide early, stable, high-level gene expression as compared to ssAAV, which foster equivalent gene expression levels only at later time points. (Han, *et al* 2008, Ren 2005)

Particularly in the setting of ADA-SCID, where early treatment may be life-saving, and the time between diagnosis and BMT may be months, an effective, safe, gene therapy with the added advantage of early, high-level gene expression would be a potent tool in the therapeutic arsenal for ADA-SCID. While scAAV vectors are limited by the size of the gene, the tagged, secretory ADA gene for these studies is approximately 1.2 Kb. A scAAV vector is capable of carrying a gene with this relatively small size. Conceivably, scAAV vectors based not only on serotype 7, but also serotypes 1, 8, or 9 could be developed and applied using any of the previously described gene therapy strategies. The two primary goals previously described for

the rAAV1 and rAAV9 strategies are the same for an approach based upon self-complementary vectors. Please refer to Table 3 for more information regarding potential rAAV-based gene therapy strategies. (Han, *et al* 2008, Ren 2005)

Table 2-1. Recombinant AAV Gene Therapy for ADA-SCID

Vectors of interest for this study (General and Specific Classes)	Advantages	Disadvantages (described for general vector classes and may apply in varying degrees to different serotypes)	Origin
Single-stranded rAAV (ssAAV)	*High degree of efficiency *Long-term persistence and expression in host cells *Stable gene transfer into dividing and non-dividing cells *Relatively low immunogenicity (e.g. minimal innate response) *No consistent indication of pathogenicity *Replication-defective (Flotte et al. 2005, Flotte et al. 2007, Kapturczak et al., Inagaki et al.)	*Low packaging capacity *Humoral immune response to capsid *Delayed expression due to the need for second-strand synthesis *Adverse effect upon early embryos suggested from *ex vivo* studies (Flotte et al. 2005, Flotte et al. 2007, Kapturczak et al.)	Humans (e.g. AAV2, AAV3, and AAV5) and non-human primates (e.g. AAV1 and AAV4) (Flotte et al. 2005, Flotte et al. 2007, Hauck et al.)
Self-complimentary rAAV (scAAV)	*All of the above characteristics for ssAAV *Bypasses need for second-strand synthesis and thus, rapid gene expression *Increased stability of vector genomes composed of double-stranded DNA (Ren et al., Han et al.)	*Low packaging capacity (approximately 50-60% of packaging capacity for ssAAV)	Humans and non-human primates
ssAAV1 or scAAV1	*Successful transduction of numerous tissues including skeletal muscle, liver, lung, retina, pancreatic islets,brain, primary vascular endothelial cells, smooth muscle cells, and HSCs (Kapturczak et al., Han et al.)		Non-human primates (antibodies common in non-human primates) (Hauck et al.)
ssAAV7 or scAAV7	*Not neutralized by serum antibodies to other capsids *Sera from humans demonstrates little neutralizing activity *High tropism for skeletal muscle and substantial tropism for HSCs (Gao et al., Han et al.)		Non-human primates (Gao et al.)
ssAAV9 or scAAV9	*Very high transduction of heart tissue (5 to 10x higher than rAAV8) *High transduction of liver *Substantial transduction of skeletal muscle and pancreas (Inagaki et al.)		Human (Inagaki et al.)

Table 2-2. Recombinant AAV-based strategies for the potential treatment of ADA-SCID

Vector	Target Tissue	#Vector Particles Injected	Method of Administration	Outcome Measures
rAAV serotype 1	Skeletal muscle (Kapturczak et al., Flotte et al. 2004)	1x10^10 to 1x10^12	Intramuscular injection	*Serum ADA activity by kinetic assay *Immunological profiling of T, B, and NK cell populations over time by flow cytometry *CBC analysis indicating total lymphocyte counts *Immunohistochemical staining of tissues derived at sacrifice for mice injected with rAAV type 1 and 9 *Analysis of transduction efficiency by quantitative PCR of tissues derived at sacrifice
rAAV serotype 9	Liver, heart, spleen, skeletal muscle, thymus (Inagaki et al.)	1x10^10 to 1x10^12	Tail vein injection	
rAAV serotype 7	Hematopoietic stem cells (Han et al.)	50,000 per cell (Han et al.)	5000 cells via tail vein injection (Han et al.)	
scAAV serotype 1	Skeletal muscle (Ren et al.)	1x10^10 to 1x10^12	Intramuscular injection	
scAAV serotype 9	Liver, heart, spleen, skeletal muscle, thymus	1x10^10 to 1x10^12	Tail vein injection	
scAAV serotype 7	Hematopoietic stem cells (Han et al.)	50,000 per cell (Han et al.)	5000 cells via tail vein injection (Han et al.)	

CHAPTER 3
MATERIALS AND METHODS

Vector Design and Development

The retroviral vector MND-MFG-hADA, provided by Kohn lab at USC, was the template for high-fidelity PCR using the Eppendorf Triplemaster Mix Kit. The resulting PCR product was the human adenosine deaminase (hADA) transgene, which aided in the synthesis of all constructs. The PCR product amplified from the MND vector, hADA, was isolated on a 1.5% Agarose gel, gel-purified using a Qiagen Gel Extraction Kit, TA cloned (using the Invitrogen plasmid pCRTOPO2.1) , and successfully sequenced. Primers for all constructs were generated using Gene Runner software. PCR Primers used in the generation of the TA clone were the forward primer [with a 5' HindIII restriction site] with the sequence, 5'GGAAGCTTAAGTCGAGGCATGGCCCAGACG 3', and the reverse primer [with a 3' EcoRI restriction site] with the sequence, 5'CAGAATTCCGAGGTTCTGCCCTGCAGAGGC3'.

The TA clone was then double-digested with HindIII and EcoRI restriction enzymes (NEBL) to excise the hADA transgene. An expression vector, called pSecTag2 (Invitrogen), was also double-digested with HindIII and EcoRI to facilitate cloning of the hADA transgene. Subsequently, the hADA transgene was cloned into the pSecTag2 vector backbone in-frame with an IgK signal sequence, upstream of the 5' end of the transgene, and a c-myc/poly-Histidine tag, downstream of the 3' end of the trangene. The ligation was performed using T4 DNA Ligase (NEBL). The resulting vector, pSecTag-hADA, was transformed into Sure2 Supercompetent Cells, which were cultivated overnight on ampicillin plates. The next day, colonies were harvested and miniprepped using a Qiagen Spin Miniprep Kit. The resulting pSecTag2-hADA construct was then sequenced. Next, this construct was digested with NheI and PmeI (NEBL) to

excise the IgK-hADA-c-myc/poly-His tag trangene cassette for cloning into a recombinant adeno-associated virus serotype 2 (rAAV2) cloning vector, to produce the plasmid, pTR2-CB-IgK-hADA.

In vitro Experimentation with hADA Constructs

Tissue Culture Using 293 Cells

Studies were performed using 293 human embryonic kidney cells. These cells were obtained from the UF Vector Core and cultured in 6 well plates or T-75 flasks. Cells were cultured in Dulbecco's EMEM or DMEM media (Gibco) at 37 degrees Celsius and 5% CO2. Cell culture media was supplemented with 20% FBS (Sigma), 100 units/ml penicillin, and 100units/ml streptomycin. Finally, the complete media was run through 0.2 micron filters to remove most potential contaminants. For T-75 flasks, approximately 10-12 ml of complete media was used per flask. For 6 well plates, each well was supplied with approximately 2-3 ml of complete media. Every 24 hours, plated 293 cells were evaluated for confluency. At 72 hours, typically the 293 cells were split using trypsin, which aids in the detachment of cells adhered to the bottom of the flask or well. All media was prepared fresh at approximately 30 day intervals.

Transfections

293T cells (a human embryonic kidney cell line expressing SV40 large T antigen) were transfected using a lipofectamine 2000 (Invitrogen) strategy. Approximately 1-2 x 10^5 cells were plated into each well of a six-well (10cm^2) tissue culture dish 24 hours before transfection. For transfection the next day, when the cells were approximately 90-95% confluent, 2ml of Opti-Mem I reduced serum media (Gibco) was added to each well. Then, 250ul of Opti-Mem I culture media (Gibco) was added to 4ug of each experimental vector (pSecTag-hADA or pTR2-CB-IgK-hADA), 4ug of positive control vector (pTR2-CB-UF11 containing the cDNA for green

fluorescence protein-GFP), or no vector (negative control), in a 15ml conical tube, and incubated for 5 minutes at room temperature. The hADA transgene cDNA which was cloned into a rAAV backbone had expression driven by a hybrid chicken beta-actin enhancer/CMV promoter (CB), while the pSecTag-hADA construct, which is derived from an Invitrogen expression vector, had expression driven by a CMV promoter. Then, in separate 15ml conical tubes (one for each corresponding tube of vector/Opti-Mem mixture), 250ul of Opti-Mem I was added to 10ul of lipofectamine 2000, and incubated at room temperature for 5 minutes. Subsequently, the lipofectamine/Opti-Mem I solutions were each added to their corresponding vector/Opti-Mem I solutions, mixed gently, and incubated at room temperature for 20 minutes. These newly-combined solutions containing complexes of vector (and no vector) with lipofectamine 2000 in Opti-Mem were added to individual wells of the 6-well tissue culture plate to initiate transfection. The plate was then incubated at 37 degrees Celsius in a CO2 incubator for 4-6 hours, at which time the media was replaced with 2ml of fresh Opti-Mem solution per well. Finally, at time points ranging from 24 to 48 to 72 hours from the initiation of transfection, media samples were collected for subsequent Western blot analyses. Moreover, at 72 hours post transfection initiation, the 293 cells in each well of the tissue culture plate were lysed to provide further samples for Western blot analyses.

Western Blotting

Western Blotting, or immunoblotting, allowed a determination of the relative amounts of hADA protein present in different tissue culture media and cell lysate samples. Samples were taken from tissue culture serum and cell lysates following 24 to 72 hour transfections of 293 cells with two experimental vectors, pSecTag-hADA and pTR2-CB-IgK-hADA, one positive control vector, pTR2-CB-UF11, and no vector. A BioRad Western Blotting kit, containing gel electrophoresis and transfer apparatuses, anti-c-myc antibody bound to horseradish peroxidase

(HRP) (Invitrogen), and Amersham Biosciences ECL Western Blotting Detection Kit were utilized. The molecular weight ladder used was the Bio-Rad kaleidoscope (Catalog # 161-0324).

Samples were harvested from tissue culture media and cell lysates following lipofectamine 2000-mediated transfection of 293 cells. First, a pre-cast 12-15% percent Tris-HCl polyacrylamide gel from Bio-Rad was inserted into a Bio-Rad gel electorphoresis apparatus (add cat number). Running buffer was prepared using Bio-Rad 10X Tris-HCl SDS stock solution, diluted to 2 liters using ddH2O. The running buffer was then added to the gel electrophoresis apparatus covering the gel. Laemmli sample buffer from BioRad was then prepared using 950ul of stock solution added to 50ul of beta-mercaptoethanol in a 1.5 ml microcentrifuge tube. Then, approximately 25-35ul of each media or cell lysate sample was added to an equal volume of Laemmli sample buffer in individual 1.5 ml microcentrifuge tubes. The tubes were wrapped in parafilm and immersed in boiling water for 5 minutes. The samples from each tube were then added to the individual wells of the pre-cast polyacrylamide gels immersed in gel running buffer within the gel electrophoresis apparatus. A protein molecular weight marker was also added to two wells on either side of the sample wells. The electrophoresis was run at 200 volts for approximately 90 minutes or until the blue bands, created by the Laemmli sample buffer and corresponding to each sample, had proceeded visibly through the stacking gel and achieved substantial migration through the running gel. The distance the visible bands were run through the running gel corresponded to the separation of the molecular weight bands of the visible molecular weight marker. Then, the gel was removed from the gel electrophoresis apparatus and sandwiched between a nitrocellulose membrane and absorption pads above and additional absorption pads below, all contained within a plastic

matrix. The membrane and absorption pads had previously been immersed in transfer buffer (recipe described below). The plastic matrix, containing the gel, nitrocellulose membrane, and absorption pads, was inserted into a gel transfer apparatus (BioRad). Next, chilled transfer buffer, prepared from 10X Tris HCl (BioRad) combined with 10% methanol and ddH2O in a total volume of 2 liters, was added to the gel transfer apparatus. A cold pack was added to the transfer apparatus to help maintain a low temperature during the gel transfer process and a magnetic stir bar was added to the base of the apparatus to facilitate stirring of the solution throughout the transfer process. For 60 minutes, 100 volts were applied to the apparatus to facilitate transfer of proteins present within the gel to the nitrocellulose membrane. The membrane was then removed from the plastic matrix and incubated with milk proteins to bind to any remaining, exposed adherent sites on the membrane overnight.

The next day, PBS-Tween was prepared using a stock solution of 10X phosphate buffered saline (Gibco) and .1% Tween 20 (Sigma-Aldrich) diluted in ddH2O to 2 liters total volume. Next, primary antibody, anti-cmyc-HRP (Invitrogen) was diluted 1:800 in PBS-Tween to a total volume of 20ml in a 50ml conical tube. The nitrocellulose membrane was removed from the milk protein solution, immersed in PBS-Tween, and washed manually in approximately 20 ml of PBS-Tween. The manual washes were repeated two more times to remove any excess milk protein solution. Then, the diluted anti-cmyc-HRP antibody solution was added to the membrane for a one-hour incubation period at room temperature, on the orbital shaker, and at low speed. The membrane was removed from the antibody solution, immersed in 400-600ml of PBS-Tween, and placed on an orbital shaker at low speed at room temperature for 15 minutes for further washing. Subsequently, three additional 5 minute washes were performed on the orbital shaker at low speed with fresh PBS-Tween added for each wash. Then, using an Amersham

Biosciences ECL detection kit, 2.5ml of each of two provided, proprietary detection solutions was added to the nitrocellulose membrane and incubated for one minute to promote an HRP-mediated fluorescence signal from any bound anti-cmyc antibody. The membrane was removed from the solution, placed in saran wrap, and subjected to autoradiography using Amersham Biosciences film. (http://www.protocol-online.org/prot/Molecular_Biology/Protein/Western_Blotting/ http://www1.gelifesciences.com/aptrix/upp00919.nsf/Content/5E2EC600736AC010C12572C0008120D6/$file/RPN2135_Rev_E_2006_web.pdf)

Production and Purification of rAAV Vectors

The University of Florida Gene Therapy Center and Vector Core produce rAAV serotypes for these studies. Virus production included the use of helper/packaging plasmid like pDG that supplied all necessary helper functions as well as *cap* and *rep* in *trans*. For example, the primary ADA vector construct of interest was co-transfected , by calcium phosphate precipitation with pDG, into individual cell factories of 70-95% confluent 293 cells. Recombinant AAV then was prepared by iodixanol precipitation and hand-packed heparin column purification. Physical titer (genome number) was determined by dot-blot. The infectious titer and extent of wild type AAV2 contamination was determined by infectious center assay (ICA). Spin concentrators were used to de-salt.

In vivo Based Experimentation

Mouse Model

While there are no known naturally occurring animal models of ADA deficiency because the ADA mutation in mice is lethal to an embryo, two types of hADA knockout mice exist. Although the original type of hADA knockout mouse demonstrates a profound immune deficiency along with bone and kidney defects, it is rescued from embryonic lethality by

transgenic ADA expression in the placenta. However, these mice die of severe respiratory distress at only 3 weeks of age, which both increases the discomfort experienced by these animals and inhibits the quality of research which may be performed.

As a more viable alternative, a more recent strain of ADA knockout mice, which expressed hADA in not only the placenta, but also in the forestomach, was utilized for these experiments and often lived a normal lifespan. These knockout mice displayed only a partial immune deficiency and less severe pulmonary inflammation. This more recent mouse model limited the distress and discomfort experienced by the animal as, in many cases, the mice remained relatively healthy. Further, this model minimized the number of animals required to obtain viable data because the animals often lived a normal lifespan, and thus, provided long-term data as opposed to that of only 3 weeks in duration.

Maintenance of the Mouse Colony

Animals were checked daily. Some of the mice were partially immunocompromised, so they were prone to infection. However, under SPF conditions and given that these mice lack the severe immune deficiency of alternative SCID mouse models, we expected these mice to do better than the alternative model. If infection or the following conditions (see below) were observed in the mice, consultation with the ACS was sought. If necessary, antibiotic treatment or mouse sacrifice was utilized.

ACS guidelines (relevant to rodents) for monitoring distress were followed, including (a) loss of 15% of body weight from baseline weight and age when assigned to the protocol or based on a comparison to a control group of animals of the same age (a growth nomogram would have been used to adjust the basal weight for growing animals), (b) major organ failure or medical conditions unresponsive to treatment, such as respiratory distress, icterus, uremia, intractable diarrhea, self-mutilation or persistent vomiting, (c) clinical or behavioral signs in

rodents unresponsive to appropriate intervention (in the case of rodents, abnormalities that persisted for 24 hours) including inactivity, labored breathing, sunken eyes, hunched posture, piloerection/matted fur, one or more unresolving skin ulcers, abnormal vocalization when handled, tumors that affected normal function [or that became ulcerated], and anorexia.

Mouse Colony Experimental Procedures

Muscle injection

For muscle administration of the virus, mice were anesthetized with 1.5 -2.5% isoflurane inhalation. Approximately 25-100µL of a sterile solution containing the rAAV vectors was administered percutaneously by intramuscular injection into the right or left quadriceps muscle (or right or left gastrocnemius muscle), using primarily a 31g needle (or insulin syringe), but not using any needle greater than 27g. This injection took place primarily in mice at typically 6-8 weeks of age. While the number of rAAV particles injected in early experiments ranged from approximately 1x10^10 to 1x10^11 particles, later experiments utilized approximately 3x10^11 vector particles.

Localized mouse fur removal

In order to facilitate accurate and efficient intramuscular injection of SCID mice, hair/fur removal in the immediate area of the injection site using Nair was necessary. Removal of the mouse hair/fur with Nair allowed the investigator to better visualize and mark the injection site to ensure efficient injection and, subsequently, upon sacrifice, fostered efficient removal of that site for analysis. Further, the mice were anesthetized with isoflurane, induced at 5% and maintained at 1.5%-2.5%, when using Nair, to avoid ingestion of the Nair. Also, the Nair was cleaned from the skin before the mice were awake to groom themselves. The entire procedure for localized fur removal took no longer than five minutes per mouse.

Intravenous injection

For intravenous administration of the virus, mice were anesthetized with 1.5- 2.5% isoflurane inhalation. Approximately 50-100ul of a sterile solution containing the vectors was administered by intravenous injection into the tail vein using an insulin syringe. This injection took place in the mice at typically 6-8 weeks of age. The number of rAAV particles injected was approximately 3x10^11 vector particles.

Collection of blood samples

Blood samples were obtained by facial vein or retro-orbital bleeding under 1.5-2.5% isoflurane anesthesia. Blood was obtained at intervals of no less than 14 days and typically at intervals of 30 days. Peripheral blood gathered from the mice was added to the serum separator tubes which were then centrifuged for 5 minutes at 6000rpm to prepare mouse serum. This serum was utilized for an analysis of hADA enzyme activity. Alternatively, harvested peripheral blood also was added to EDTA coated anti-coagulation collection tubes. This blood was subjected to flow cytometry and CBC analyses. At any given time point, typically blood was collected either for the purpose of enzyme analysis or CBC/Flow cytometry analyses. For any given blood draw, no more than 10% of total volume was collected. For example, for the average mouse at 8-10 weeks of age and weighing approximately 25g, approximately 50 ul of serum was obtained from approximately 100 ul of blood.

Saline injections

Following each blood collection, in order to facilitate recovery and provide for the continued health and well-being of the animals, 50-100ul of sterile lactated ringers was injected subcutaneously under the skin and fur, which was scruffed just above the neck, using a sterile insulin syringe.

Anesthesia and Euthanasia

The investigators utilized Isoflurane (with an Omnicon f/air scavenge) for anesthetic purposes. Isoflurane allows for rapid induction and stable maintenance during anesthesia, and rapid recovery from procedures such as injections, skin tests, and bleeds. Additionally it allows for precise control of drug duration avoiding problems associated with under- and overdosing of parenterally administered anesthetic agents. Usage of Isoflurane for anesthesia of mice followed the UFL Animal Care and Use Committee's recommendations http://nersp.nerdc.ufl.edu/ ~iacuc/ principl.htm and http://nersp.nerdc.ufl.edu/~iacuc/mousedose.htm). For euthanasia of mice, isoflurane was administered by inhalation using a precision vaporizer at 5% for induction (a sealed box to reduce stress secondary to restraint) and at 1.5 - 2.5% for maintenance (a small face mask), followed by exsanguination.

Genotyping

DNA extraction

To facilitate genotyping, the first step was to purify genomic DNA for subsequent PCR analysis. Purification was performed using the Qiagen DNeasy Blood and Tissue Kit. Briefly, tail tips were taken from mice bred in the University of Florida Cancer Genetics Research Center Breeding Suite. These mice were the offspring of several breeding pairs, purchased directly from Jackson Laboratories, which carry the null ADA allele.

Briefly, the tail tips were subjected to Proteinase K treatment in the presence of Buffer ATL. The mixtures were then placed in a thermal mixer or heating block to facilitate tissue lysis overnight. Then, the samples were vortexed. Next, Buffer AL and ethanol were added to each sample with subsequent vortexing. The entire mixture was then added to DNeasy Mini spin columns followed by centrifugation. The columns were washed with Buffer AW1 and, in turn,

Buffer AW2. In the latter step, the column membrane was dried with additional centrifugation. Finally, Buffer AE was used to elute the purified genomic DNA into a microcentrifuge tube.

More specifically, for each mouse of interest, 0.4-0.6 cm of tail clipping was added to a 1.5 ml microcentrifuge tube. Then, 180ul of Buffer ATL and 20ul of Proteinase K was added to each tube, mixed by vortexing, and incubated at 56 degrees Celsius in a thermal mixer or water bath.

The samples were then vortexed for 15 seconds. Next, 200ul of Buffer AL were added to each tube, followed by vortexing. Then, 200ul of 96%-100% ethanol were added to each tube, followed by vortexing. The mixture was then pipetted into DNeasy mini spin columns and centrifuged at 8000 rpm for 1 min. The flow through and collection tubes were discarded, as was the case for each subsequent wash step. In the first wash, 500ul of Buffer AW1 was added to each column, followed by centrifugation at 8000 rpm for 1 minute. In the second wash, 500ul of Buffer AW2 was added to each column, followed by centrifugation at 13000 rpm for 3 minutes to dry the spin column membrane. Next, the spin column was placed in a 1.5 ml microcentrifuge tube and 150ul of Buffer AE was added directly onto the spin column membrane.

The column was allowed to incubate for 1-3 minutes at room temperature, followed by centrifugation at 8000 rpm to elute genomic DNA. The preceding elution step was repeated to elute additional genomic DNA. The samples were then stored at -20 degrees Celsius until PCR analysis was performed.

PCR (polymerase chain reaction)

Following DNA extraction, successful genotyping depended upon 3 separate PCR protocols. The results from each reaction, taken together, elucidated the genotype of colony

mice. And, all of the following PCR reactions were graciously provided by Blackburn Lab at the University of Texas in Houston.

The first PCR amplified a 700bp section of the ADA knockout allele. The presence of this 700bp band on a 2.5% Agarose gel indicated that the animal is either a heterozygote or homozygous knockout. The absence of this band indicated the animal is wildtype. This reaction relied upon two primers. The forward primer has the sequence, 5'AGAGCAGCCGATTGTCTGTT, with a Tm of 64.0 degrees Celsius. The reverse primer has the sequence, 5'AGAATGGACCGGACCTTGAT, with a Tm of 64.5 degrees Celsius. Mixed in a 0.5ml microfuge tube are the following components under the following reaction conditions described in Table 3-1.

The second PCR amplified a 274 bp region of the wildtype ADA allele. The presence of a 274 bp band on a 2.5% agarose gel indicated the mouse was a heterozygote or wildtype animal. The absence of this band indicated that the animal is a homozygous knockout. For this reaction, the forward primer has the sequence 5'CCTCTGAGCCATGATTCTGA, with a Tm of 63.0 degrees Celsius. The reverse primer has the sequence, 5'AGAATGGACCGGACCTTGAT, with a Tm of 64.5 degrees Celsius. Mixed in a 0.5ml microfuge tube are the following reaction components under the following reaction conditions described in Table 3-2.

The third and final PCR amplified a 470 bp region of the ADA transgene (Tg). The presence of this 470 bp band on a 2.5% Agarose gel indicated the presence of the ADA transgene, which was expressed in both the placenta and foregut tissues, and necessary to rescue the mouse from prenatal lethality. For this reaction, the forward primer had the sequence, 5'AGCCAACGCAGACCCAGAGA, with a Tm of 69.5 degrees Celsius. The reverse primer had the sequence, 5'GCAGGCCCTGGTTCACAAGA, with a Tm of 70.0 degrees Celsius.

Mixed in a 0.5ml microfuge tube were the following reaction components under the following reaction conditions described in Table 3-3.

Immunohistochemistry

At approximately 30 and 60 days post-injection [and in some cases at 90 and 120 days] of rAAV1 and rAAV9 vectors, mice were euthanized and brachial artery blood samples were taken for serum protein analysis. Liver, kidney, pancreas, spleen, heart, thymus, and quadriceps muscle from both legs were harvested. Tissues were trimmed and either snap-frozen in liquid nitrogen for subsequent genomic DNA isolation or fixed in 10% neutral-buffered formalin (NBF) for immunohistochemical analysis.

Tissues were fixed in NBF between 12-24 hours and then rinsed twice in 1X PBS for five minutes each. Fixed tissues were processed and embedded in paraffin wax and sectioned at 4 μm thickness. Tissue sections were deparaffinized, rehydrated, and blocked for endogenous peroxidase with 3% hydrogen peroxide in methanol for 10 minutes. All primary antibodies were incubated at room temperature for one hour.

To detect vector-mediated hADA expression, antigen retrieval was performed in Antigen Retrieval Citra Solution (Biogenex, San Ramon, CA, USA) for 30 minutes in the steamer then rinsed in Dako Wash Buffer (1X TBS with 0.05% Tween) (Dako-Cytomation, Glostrup, Denmark). Tissues were blocked with Background Sniper (Biocare Medical, Concord, CA, USA) for 15 minutes and rinsed in wash buffer. Rabbit anti-ADA (1:800; Atlas Antibodies, Stockholm, Sweden) and normal rabbit immunoglobulin (Vector Laboratories, Burlingame, CA, USA), used as a negative control, were diluted in Antibody Diluent (Zymed®, Invitrogen, Carlsbad, CA, USA) and incubated on tissues followed by rinses in wash buffer. Secondary antibody, Mach 2 Rabbit-HRP Polymer (Biocare Medical), was incubated on tissues at room

temperature for 30 minutes followed by rinses in wash buffer. Bound antibody was detected by developing with Cardassian DAB chromagen (Biocare Medical). Tissues were counterstained with hematoxylin (Vector Laboratories) then dehydrated and coverslipped. Slides were scanned by Aperio ScanScope CS Digital System (Aperio, Vista, CA, USA).

To detect vector-mediated, c-myc tagged hADA, antigen retrieval was performed as for anti-ADA staining. Tissues were blocked with Rodent Block M (Biocare Medical) for 30 minutes and rinsed as previously mentioned. Mouse anti-c-myc (1:50; Invitrogen) was diluted in the aforementioned diluent and incubated on tissues then rinsed with wash buffer. Straight diluent (no primary) was used as the negative control. MM Polymer-HRP (Biocare Medical) was incubated on tissues at room temperature for 20 minutes with subsequent rinses with wash buffer. Antibody detection was performed using Cardassian DAB. Tissues were counterstained and scanned as previously detailed.

No antigen retrieval was required to detect GFP in tissues with UF11 vector. Tissues were blocked as with hADA detection and rabbit anti-GFP (1:40,000; Abcam, Inc., Cambridge, MA, USA) was bound to tissues then rinsed with wash buffer. Straight diluent was used as the negative control. The remaining steps for the assay were the same as with ADA detection.

Flow Cytometry

Background

Flow cytometry is a technique for identifying, counting, and separating cells (or molecules) suspended in a stream of fluid. More specifically, this technique allows for a determination of the percentage of specific cell populations as well as an assessment of cellular features, such as size, shape, and the presence or absence of tumor markers. Flow cytometry allows for a quantitative and qualitative analysis of cell populations. As a laser-based technology, a beam of light is directed onto a stream of fluid carrying cells moving single-file

past the laser. A number of detectors are aimed at the point where the stream passes through the light beam; one in line with the light beam (Forward Scatter or FSC) and several perpendicular to it (Side Scatter (SSC) and one or more fluorescent detectors). Each suspended cell, passing through the laser, scatters the light and, with the aid of monoclonal antibodies bound to fluorochromes, also leads to an emission of light at a higher wavelength than that of the light source. This resulting scattered light reveals information about cellular size, shape, and structure. The fluorescent light is picked up by a series of detectors, which analyze fluctuations in brightness related directly to fluorescent emission peaks. The amount of fluorescence detected is proportional to the amount of fluorescent antibody bound to a given cell. If the level of fluorescence significantly exceeds the background fluorescence (associated with non-specific binding of antibodies), then a given fluorescence signal approximately corresponds to the presence of a cell of interest. A collection of fluorescence signals may then be used to approximate percentages of cell populations.

Modern flow cytometers can analyze several thousand particles every second by the emission and scattering of light. These machines can also sort cells and particles having specified properties. The technology has applications in a number of clinical and research fields. The data coming from flow-cytometers is typically plotted as one-parameter histograms (e.g. cell numbers plotted against side or forward scatter) or as two-parameter dot plots (e.g. cell populations which are plotted against 2-axes, one axis representing a marker, such as CD3, and another axis representing a different marker, such as CD4). Specific regions of two dimensional dot plots containing specific cell populations can be identified and separated using a process called gating. The plots are often made on logarithmic scales.

(http://en.wikipedia.org/wiki/Flow_cytometry, http://www.cancer.gov/Templates/db_alpha.aspx?CdrID=335066, (Jaroszeski and Radcliff 1999))

Procedure

Fresh mouse peripheral blood was collected monthly by facial vein bleeds. The blood was deposited in lavender-top EDTA tubes to prevent coagulation, which were then inverted and agitated to mix the blood with the EDTA coating the tube. The tubes were set on a towel over a bed of ice to maintain a low temperature but not freeze the samples. The samples were then taken to the Flow Cytometry Core at the UF Cancer Genetics Research Staining. For each sample, 50ul of blood was pipetted into BD Falcon 5ml polystyrene round-bottom tubes in preparation for staining. Next, a mastermix of stained antibodies was created to facilitate efficient delivery to the blood samples. The flow antibodies targeted five immunological markers, CD19, CD3, CD4, CD8, and NK1.1 (eBioscience). The stains of interest bound to each antibody and used to target each immunological marker were APC, FITC, PacificBlue, PE, and PE-Cy7. More specifically, the stained antibodies were. Each antibody had a concentration of 0.2 mg/ml except which was 0.5 mg/ml. And, for each 50ul of blood, 0.5 ug of each antibody was used. Thus, 2.5 ul of each antibody was used per blood sample, except for , which necessitated only 1 ul per blood sample. The volume of each antibody per blood sample was then multiplied by the total number of samples (which varied from experiment to experiment) to arrive at the total volume of each antibody required for all blood samples. The total volumes of each antibody could then be added together in one microcentrifuge tube to create a master mix. Then, to calculate the volume of mastermix to distribute to each sample tube, the respective volumes of each antibody needed per blood sample were added together. For example, for 4 of the antibodies, 2.5 ul were needed per blood sample, while for , 1 ul was

needed per sample. Added together, 11ul of all the antibodies combined were needed per sample. Thus, 11ul of master mix was pipetted into each blood sample and mixed with further pipetting. Following a brief vortex, the sample tubes were then allowed to incubate at room temperature in a dark cabinet for 15 minutes. Next, 3 ml of red blood cell lysis buffer was added to each tube. The tubes were then spun in a centrifuge for 10 minutes at 1200 rpm to pellet the lymphocytes and red cell debris. The supernatant was aspirated off and 500ul of 1X PBS and 2% FBS was added to the cell pellet. The sample tubes were vortexed to resuspend the pellet. Then, vacuum-mediated laminar flow was used to remove the sample from the sample tubes for analysis in the flow cytometer (BD SLR from BD Biosciences), followed by analysis using FACS Diva software.

Real-Time Quantitative PCR

Background

Real-time PCR is a technique which facilitates both a qualitative and quantitative analysis of a DNA of interest, such as vector DNA, with high specificity and sensitivity. Thus, Real-time PCR allows not only a determination of the presence or absence of rAAV vector DNA, but also an accurate calculation of the amount of vector DNA, or starting template copy number, present in a sample. By contrast, standard PCR methods allow for qualitative or, at most, semi-quantitative DNA analysis. Moreover, standard PCR relies upon a reaction followed by agarose gel electrophoresis and ethidium bromide staining in search of a band or bands with a size consistent with the desired PCR product. The presence of a desired band indicates the presence of the DNA of interest. Real-time PCR or qPCR, when used quantitatively, relies upon a reaction in which a fluorescent reporter molecule provides substantial fluorescence only when bound to double-stranded DNA. In other words, the amount of fluorescence correlates directly with the amount of dsDNA present in a sample. And, as the amount of dsDNA increases, so to

does the amount of fluorescence. This relationship forms the basis for a determination of starting template copy number, or the amount of DNA of interest present in a given sample.

The two most common fluorescent approaches to real-time PCR analysis are DNA-binding dyes such as SYBR Green 1 and oligonucleotide primers or probes which are dye-labeled and sequence-specific such as TaqMan.

Procedure

Genomic DNA (gDNA) isolation was performed on flash frozen liver, stomach, spleen, kidney, pancreas, skeletal muscle, lung, and heart samples with the QIAGEN DNeasy Tissue Kit (Qiagen) and DNA concentrations determined by UV spectrophotometry (Eppendorf, Biophotometer). The procedure for genomic DNA extraction was described previously under the section for genotyping. Then, vector sequences were detected using Taqman real-time PCR. One microgram (1 ug) of DNA was used in all quantitative PCR reactions according to a previously described protocol (Poirier et al. and Song et al.). Primer pairs and the Taqman probe were designed to bind to the CMV enhancer/chicken ß-actin promoter, and were vector-specific. The standard curve was established by spike in concentrations of the CBAT plasmid (Figure). All samples were done in triplicate. The technique has as sensitivity of 100 copies per microgram on input DNA. Reaction conditions followed those recommended by Perkin-Elmer/Applied Biosystems. Also, qPCR was performed using the ABI Taqman 7900HT. (Poirier, *et al* 2004, Song, *et al* 2002).

ADA Enzyme Activity Assay

Background

The Adenosine Deaminase Assay Kit (DZ117A), provided by Diazyme Laboratories, represented one avenue for determining ADA enzyme activity in serum from mice given PBS, a control vector, or the experimental rAAV-hADA vectors. Originally, this assay was designed for

the clinical setting, to determine ADA activity in human serum samples. For the purposes of this study, the goal was to detect human ADA activity in mouse serum samples. The following assay description was adapted from the Diazyme protocol.

The guiding principle of the ADA activity assay was the enzyme-mediated deamination of adenosine to inosine, which was then converted to hypoxanthine by purine nucleoside phosphorylase. An additional enzyme, xanthine oxidase, then catalyzed the formation of uric acid and hydrogen peroxide from hypoxanthine. The resulting hydrogen peroxide was combined with 4-aminoantipyrine and N-Ethyl-N-(2-hydroxy-3-sulfopropyl)-3-methylaniline in the presence of peroxidase. This chemical reaction generated quinone dye, the absorbance of which was monitored kinetically. The change in absorbance over time was then used to determine ADA activity.

Procedure

The following protocol and control information was kindly provided by Diazyme regarding the adenosine deaminase assay kit. Refer to Table 3-4 for information regarding instrumentation and instrument settings.

For the assay, reagents R1 and R2 were pre-equilibrated to room temperature prior to the assay. Then, 180 uL of reagent R1 and 5 uL of plasma sample were added to a 1.5ml microcentrifuge tube and mixed. The solution was incubated in a water bath maintained at 37 degrees Celsius for 2 minutes. Next, 90 uL of reagent R2 was added to the tube and mixed. The solution was then incubated for 5 min at 37 degrees Celsius, transferred to the cuvette, and subsequently monitored for absorbance at 556 nm for 3 min with 1 min intervals to obtain $\Delta A/min$ values. Then, the average rate of the absorbance change ($\Delta A/min$) was calculated using the following formula:

$$\Delta A/min = \frac{(\Delta A_1/min + \Delta A_2/min + \Delta A_3/min)}{3}$$

Using the average rate of the change in absorbance (ΔA/min), ADA activity (U/L) in the plasma sample was determined by using the formula:

$$ADA\ (U/L) = \frac{\Delta A/min. \times Tv}{\varepsilon \times Sv \times L} = \Delta A/min \times 1050$$

One unit of adenosine deaminase is defined as the amount of adenosine deaminase that generates one micromole of inosine from adenosine per minute at 37 degres Celsius.

The Diazyme ADA activity assay also included an ADA calibrator at approximately 50 U/L and an ADA control at approximately 30 U/L, though there was some variability in the U/L activity values from vial to vial. The activities of the adenosine deaminase calibrator and control were determined by a UV spectrophotometer measuring a change in absorbance at 550 nm resulting from the deamination of adenosine. For the calibrator and control, as for any samples, one unit of adenosine deaminase is defined as the amount of adenosine deaminase that generates one micromole of inosine from adenosine per minute at 37 degrees Celsius. The adenosine deaminase calibrator and control were prepared in a bovine serum base, and provided in lyophilized powder and stored at –20^{o}C. The vials of adenosine deaminase calibrator and control were opened very carefully, avoiding any loss of material, and reconstituted with exactly 1 ml of diH_2O. The vials were then closed and allowed to stand for 30 minutes at room temperature, to dissolve the contents completely by gentle swirling or rotating. Once reconstituted, the components of each vial were stable for 1 to 2 weeks at 2-8°C. Then, 5ul of the calibrator and the control were run, in the same fashion as any sample, with the previously described kinetic assay protocol. This reaction was used to confirm that the expected ADA activity for the ADA

calibrator (approximately 50 U/L) and the expected ADA activity for the ADA control (approximately 33 U/L) plus or minus a 20 percent range of error were indeed observed, and thus, the given experimental conditions and assay kit were satisfactory. The adenosine deaminase calibrator and control were used for quality control procedures to examine and to verify the accuracy and precision of this quantitative adenosine deaminase assay.

Table 3-1 Amplification of the Knockout (KO) Allele for Genotyping (Courtesy of Michael R. Blackburn)

	PCR Reagents	PCR protocol
5 ul	5X Buffer	5 min at 94 degrees Celsius
1.5 ul	25mM MgCl2	1 min at 94 degrees Celsius
0.5 ul	10mM dNTP Mix	1 min at 60 degrees Celsius
1.0 ul	100pMol/ul ADA KO allele forward primer	2 min at 72 degrees Celsius for 30 cycles 10 min at 72 degrees Celsius
1.0 ul	100pMol/ul ADA KO allele reverse primer	Then, samples maintained at 4 degrees Celsius
5.0 ul	gDNA	
0.5 ul	Taq polymerase	
10.5ul	dH20	
25.00 ul	Total volume per reaction tube	

Table 3-2 Amplification of the Wildtype (WT) Allele for Genotyping (Courtesy of Michael R. Blackburn)

	PCR Reagents	PCR Protocol
5 ul	5X Buffer	5 min at 94 degrees Celsius
1.5 ul	25mM MgCl2	1 min at 94 degrees Celsius
0.5 ul	10mM dNTP Mix	1 min at 60 degrees Celsius
1.0 ul	100pMol/ul ADA WT allele forward primer	2 min at 72 degrees Celsius for 30 cycles 10 min at 72 degrees Celsius
1.0 ul	100pMol/ul ADA WT allele reverse primer	Then, samples were maintained at 4 degrees Celsius
5.0 ul	DNA	
0.5 ul	Taq polymerase	
10.5 ul	dH20	
25.00 ul	Total volume per reaction tube	

Table 3-3 Amplification of the ADA minigene or transgene (Tg) necessary to rescue the mouse from prenatal lethality (Courtesy of Michael R. Blackburn)

	PCR Reagents	PCR Protocol
5 ul	5X Buffer	5 min at 94 degrees Celsius
1.5 ul	25mM MgCl2	1 min at 94 degrees Celsius
0.5 ul	10mM dNTP Mix	1 min at 66 degrees Celsius
1 ul	100 pMol/ul ADA Tg allele forward primer	2 min at 72 degrees Celsius for 30 cycles 10 min at 72 degrees Celsius Then, samples were maintained at
1 ul	100pMol/ul ADA Tg allele reverse primer	4 degrees Celsius
5.0 ul	gDNA	
0.5 ul	Taq polymerase	
10.5 ul	dH20	
25.00 ul	Total volume per reaction tube	

Table 3-4 Settings and Instrumentation for ADA Enzyme Activity Assay (Information provided by Diazyme Laboratories)

Instrument:	Parameter settings:
Beckman Coulter DU 800 UV-spectrophotometer with kinetic function using a 0.1ml cuvette	Used water to blank (autozero) cuvette at 556nm Reaction Temperature: 37°C Reaction time: 10 min Wavelength: 556 nm Reference wavelength: 800 nm Sample/Reagent: 1: 54

CHAPTER 4
RESULTS

Specific Aims for this Research

This research is intended to address a total of five specific aims: Aim 1 is to clone a secretory version of the hADA gene into a single-stranded rAAV backbone. Aim 2 is to test this construct for protein expression and secretion in 293 cell tissue culture. Aim 3 is to characterize the general nature of the immune deficiency in a mouse model of ADA-SCID. Aim 4 is to achieve successful gene delivery and protein expression *in vivo* following administration of rAAV vectors. Lastly, Aim 5 is to promote enhanced serum ADA activity and subsequent immune reconstitution in the ADA-SCID mouse model of interest. In the following sections, each of the above aims will be addressed.

Successful Cloning of a rAAV-hADA Construct

Critical to the success of this gene therapy endeavor was Aim 1, the cloning of a secretory tagged version of the human ADA gene into a single-stranded rAAV vector. To that end, as described in Chapter 3 under Vector Design and Development, several intermediate constructs were generated to facilitate cloning of the final vector of interest, rAAV-hADA (or by the alternative identification-pTR2-CB-IgKsshADAcmycpolyHistag). In the following section, figures of all relevant constructs produced or utilized in the synthesis of the final product, rAAV-hADA, are included and described. As described previously in Chapter 3, traditional cloning methods were employed to PCR amplify the human ADA gene (hADA) from a retroviral plasmid supplied by Dr. Donald Kohn, MND-MFG-hADA, shown in Figure 4-1. In this retroviral plasmid, the M stands for murine leukemia virus LTR-deleted (replaced with myeloproliferative sarcoma virus LTR), N for negative control region deleted, and D for d-primer binding site replaced. Finally, this is the retroviral human ADA plasmid used as the

master template for PCR of all hADA inserts to be TA cloned and subsequently inserted into pSecTag2 expression vectors as well as rAAV vectors.

TA cloning into pCRTopo2.1 vector backbone (Invitrogen) was done and confirmed by DNA sequencing. The resulting TA clone, known as hADAtagTAright or pCRTopo2.1-hADA, is shown Figure 4-2. Next, the hADA gene was cloned into the expression vector pSecTag2 (Invitrogen) containing an IgK secretory signal sequence flanking the 5' end of the hADA transgene and a c-myc-poly-His tag flanking the 3' end of hADA transgene- Figures 4-3a and 4-3b. The resulting construct, pSecTag2-hADA, was used to transfect 293 human embryonic kidney cells and to confirm expression of hADA via immunoblot. Finally, the entire transgene cassette, containing sequences for hADA, the IgK secretory tag, and the c-myc-poly-His tag, was cloned into a rAAV backbone. This final construct, rAAV-hADA (or pTR2-CB-IgKsshADAcmycpolyhistag), shown in Figure 4-4, contained the hADA transgene cassette cloned into a recombinant adeno-associated virus type 2 plasmid backbone. Flanking the transgene cassette were AAV inverted terminal repeats (ITRs) upstream of the 5' end of the cassette and downstream of the 3' end. Additional elements found upstream of the transgene cassette were a CMV promoter and a chicken beta-actin enhancer. Downstream of the transgene cassette also resided a polyadenylation signal sequence.

In conclusion, the rAAV-hADA plasmid was sequenced to confirm that the synthesized construct matched the desired construct. Upon confirmation of the sequencing data, Aim 1, to successfully clone a secretory version of the hADA gene into a single-stranded rAAV vector was achieved. The focus of Aim 2 was testing of the newly-synthesized rAAV construct for protein expression and secretion in 293 cell tissue culture.

In vitro Analysis of hADA Constructs Reveals Protein Expression and Protein Secretion

Following cloning of both pSecTag2-hADA and rAAV-hADA constructs, the ability of each construct to express and secrete hADA protein in tissue culture was evaluated and confirmed to satisfy Aim 2 of this research. While expression of hADA protein was a critical step in evaluating the viability of the hADA constructs of interest for any attempt at *in vivo* preclinical gene therapy, equally as important was the need to confirm secretion of hADA. The process of lipofectamine 2000 (Invitrogen)-mediated transfection of 293 cells was utilized, followed by immunoblot of both tissue culture media and cell lysate samples, to achieve the goals of confirming both protein expression and secretion *in vitro*. For both Western Blots, a HRP-bound, monoclonal, anti-cmyc antibody (Invitrogen) was utilized to identify the presence of vector-derived protein from either the control or the experimental vectors, pSecTag2-hADA or rAAV-hADA.

In Figure 4-5, this Western Blot demonstrated both expression and secretion of hADA protein from the pSecTag2-hADA Invitrogen-based expression vector. Lane 0 contains the protein standard with marks corresponding to relevant molecular weights in kilodaltons (Kd). Moving from left to right across the blot, lane 4 demonstrates c-myc-tagged hADA protein from harvested tissue culture media at 72 hours post lipofectamine 2000-mediated transfection of 293 cells with pSecTag2-hADA (Figure 4-3). Interestingly, Lane 4 shows a triple band at the expected molecular weight of 48 Kd for secreted vector-derived hADA. This triple band may represent several secreted isoforms of c-myc-tagged hADA.

Lanes 7 and 8 highlight cmyc-based western blotting of 293 cell lysates samples. Lanes 7 and 8 contain non-secreted c-myc-tagged hADA designated by triple bands at approximately 48 Kd. A negative control was utilized in Lane 9 in a media sample, which manifested no secreted hADA protein. The media in this lane was from 293 cells not transfected with plasmid.

In Lane 10 is a negative control cell lysate sample in which non-secreted hADA protein is undetected. The cell lysate in Lane 10 was derived from 293 cells transfected only with rAAV plasmid containing the gene for green fluorescent protein (GFP), as opposed to the hADA transgene. This control plasmid or pTR2-CB-GFP(UF11) not only provided a negative control for expression of hADA protein in cell media, but also provided a positive control for transfection by facilitating expression of intracellular GFP and thus, confirming successful transfection. GFP was clearly visible by light microscopy as early as 24 hours post-transfection. Finally, Lane 11 represents a repeat of Lane 4, and contains hADA bands from tissue culture media taken at 72 hours from 293 cells transfected with twice the amount of c-myc tagged ADA plasmid as that utilized for the Lane 4 media sample (8 micrograms of pSecTag2-hADA plasmid as opposed to 4 micrograms).

The second Western Blot image (Figure 4-6) has a photograph overlayed on the nitrocellulose sheet used for protein transfer to align the molecular weight ladders on either side of 12 sample lanes. Lanes 1-6 and Lane 12 contain media samples harvested at 72 hours post 293 cell transfection. Lanes 7-11 contain cell lysate samples harvested at 72 hours post transfection. The antibody used for detection is once again a HRP-labeled monoclonal anti-c-myc antibody.

On this Western Blot (Figure 4-6), there are 2 lanes with the protein molecular weight ladder on either side of the 12 sample lanes. The media sample in Lane 2 contained a single band (designated by brackets) which served as a positive control for secretion of c-myc-tagged secretory protein. This single band represented c-myc-tagged angiostatin protein. This protein was derived from the construct pTR2-CB-K1K3 (Courtesy of Flotte Lab and Pedro Cruz), which was transfected into one well of a 6-well plate in parallel with transfection of pSecTag2-hADA

and rAAV-hADA. The angiostatin protein has 316 amino acids and was found at the expected 36 Kd molecular weight in the tissue culture media in Lane 2 following 72 hours post-transfection. Moreover, in Lane 8, the loaded cell lysate sample also contained a single band (designated by brackets) at 36Kd. In this case, the angiostatin band served as a positive control for non-secreted c-myc-tagged protein. In cell media samples in Lanes 3 and 4, bands representing secretory hADA from the pSecTag2-hADA construct were found at approximately 48kD (significantly above the 40kD ladder mark). Most importantly, in cell media samples in Lanes 5 and 6, bands representing secretory hADA from the rAAV-hADA vector were also found at 48kD. Non-secreted hADA expressed from the pSecTag2-hADA plasmid in 293 cell lysates were seen as multiple dark bands in Lanes 9 and 10. Similarly, non-secreted hADA protein expressed from the rAAV plasmid and harvested from 293 cell lysates, was observed as multiple dark bands in Lanes 11 and 12. Lanes 1 and 7 contained samples which served as negative controls for both secreted and non-secreted c-myc-tagged protein. In Lane 1 was a negative control media sample and in Lane 7, a negative control cell lysate sample, both harvested from 293 cells at 72 hours post-transfection with the pTR2-CB-UF11 control vector. In both Lanes 1 and 7, the negative control was validated with absence of a band representing c-myc-tagged hADA protein.

Immunoblot data for both the preliminary pSecTag2-hADA construct and the final rAAV-hADA constructs demonstrated abundant cellular expression and substantial secretion of hADA. The presence of molecular weight isoforms of hADA, which are approximately 47-49kD in size and in both the 293 cell lysate and media samples, support a conclusion of *in vitro* protein expression and moderate protein secretion. This data supports the conclusion that Aim 2 was achieved.

Genotyping and Immunological Profiling of the ADA-SCID Mouse Model

Prior to characterization and use of the mouse model of interest (as described in Chapter 3 Materials And Methods and utilized for Preliminary Experiments 1 & 2) for rAAV injections, identification of the genotype of the ADA-SCID mice helped distinguish the knockout animals, which manifest a partial immune deficiency, from their wildtype and heterozygote littermates, which display no immune deficiency. The development of reliable genotyping laid the foundation for addressing Aim 3, general characterization of the immune deficiency in the mouse model of ADA deficiency. A description of the immunological phenotype of the ADA-SCID mouse model was necessary to help define the nature and severity of the knockout mouse immune deficiency and to distinguish between the immune deficient knockout mice and the healthy, immune competent wildtype mice. If the immune deficiency was not substantial, the likelihood of facilitating a vector-induced immune reconstitution was low. (Blackburn, *et al* 1998, Blackburn, *et al* 1996)

Genotyping by PCR Facilitates Identification of Knockout, Heterozygote, and Wildtype Mice

Mice of the strain, FVB;129-Ada<tm1Mw> Tg(PLFSADA)2465Rkmb/J (JAX® Mice and Services Stock# - 003297), were obtained from the Jackson Laboratory. These mice were rescued from embyonic lethality by transgenic expression of ADA in the placenta, and were further rescued from lethality at 3 weeks of age [from severe respiratory distress due most likely to profound pulmonary inflammation, including eosinophilia] with transgenic expression of ADA in the forestomach. From various generations as well as the original mice, tail clippings were obtained, genomic DNA was extracted, and PCR of genomic DNA was performed to amplify the null ADA allele, the wildtype allele, and the ADA rescue minigene. A number of the original mice manifested both the null ADA allele and the wildtype allele alongside the ADA

minigene rescue. Consequently, these mice were characterized as heterozygotes and bred to generate offspring which, following PCR, displayed only the null ADA allele alongside the ADA minigene rescue. These offspring, which represented homozygous ADA deficient mice, were then interbred to generate knockout mice for subsequent gene therapy experimentation. The genotyping data for the null knockout and wildype alleles, as well as the minigene rescue, for several of the ADA-SCID knockouts utilized for rAAV injections, are shown in Figure 4-7, 4-8, and 4-9. All PCR-based genotyping was made possible by protocols provided by Michael R. Blackburn in the Department of Biochemistry and Molecular Biology at the University of Texas Health Science Center at Houston.

The image captured for Figure 4-7 is of a 1.5% agarose gel stained with ethidium bromide, which shows the presence of the PCR-amplified null or knockout allele. This knockout allele is a band at molecular weight of 700 bp and is characteristic of the ADA-SCID knockout mice. Along the top of Figure 4-7 are mouse identification numbers for positive control mice, numbered 1377 and 214, and experimental mice to be used for rAAV injections, numbered 27, 28, 29, and 30. Along the left side of the gel is a molecular weight marker with the designated band sizes labeled on the image. Also, although not shown in this image, a negative control sample was run to examine the possibility of background DNA template contamination. A PCR tube was loaded with all reagents necessary for the PCR reaction to proceed except for template DNA. When this sample was run on a lane of the 1.5% agarose gel (data not shown), no band was visible, suggesting that DNA contamination was not present for this set of PCR reactions. The gel represented in Figure 4-7 confirms the presence of the knockout allele for the designated mice. However, only taken together with the data from Figure 4-8 could the full genotype of the animals be ascertained.

Figure 4-8 contains an image of another 1.5% agarose gel stained with ethidium bromide, which shows the presence of the PCR-amplified wildype allele for positive control mice, designated by mouse identification numbers across the top of the figure, and numbered 1394 and 1389. This wildtype allele is represented by a band at molecular weight of 274bp. A molecular weight marker is present in the center of the figure with the designated molecular weights. Finally, the lanes corresponding to mice numbered 27, 28, 29, and 30 are missing the 274bp wildype allele. This observation, taken together with the presence of the knockout allele for each mouse in Figure 4-7, indicates that the genotype for each mouse is homozygous null in nature. Also, although not shown in this image, a negative control sample was run to examine the possibility of background DNA template contamination. A PCR tube was loaded with all reagents necessary for the PCR reaction to proceed except for template DNA. When this sample was run on a lane of the 1.5% agarose gel (data not shown), no band was visible, suggesting that DNA contamination was not present for this set of PCR reactions.

Finally, Figure 4-9 represents a third 1.5% agarose gel stained with ethidium bromide, which confirms the presence of the ADA minigene rescue, expressed in both placenta and foregut tissues of the ADA-SCID knockout mouse model utilized for these studies. The amplified ADA minigene PCR product is designated by a band at a size of 470bp for positive control mice numbered 1375, 1377, and 214, as well as experimental mice 27,28, 29, and 30. Just as with the PCR experiments conducted for amplification of the null and wildtype alleles, a negative control PCR reaction, described previously, was run alongside the PCR reactions conducted for amplification of the minigene PCR product. Although the data is not shown, the gel lane containing the negative control sample was clear.

The preceding results describe the overall PCR-based genotyping procedure used to identify the presence of absence of the wildtype, null, and minigene ADA alleles. This procedure thus allowed for an identification of null, heterozygote, or wildtype mice. Only with genotyping, could subsequent analysis of the immune system of the ADA-SCID mouse model, Aim 3, be achieved.

Flow Cytometry and CBC Analysis Facilitate a Characterization of the Immune Deficiency of ADA-SCID Knockouts

Prior to *in vivo* testing of rAAV vectors packaged in serotype 1 and 9 capsids, one question in addition to genotyping of the mice necessitated an answer: What is the nature of the immune deficiency in this mouse model of ADA-SCID? This question directly reflects the goal of Aim 3. If indeed significant immune deficiency was present, then the likelihood that an applied rAAV gene therapy strategy could demonstrate immunological benefit was substantial. However, if the immune deficiency of these knockout mice [with placental and a foregut ADA minigene rescue] was minimal compared to the immune system of wildtype or heterozygous mice, and given that the knockout immune system is not likely to be enhanced [following gene therapy] beyond that of wildtype mice, then the likelihood of observing substantial improvement in immunocompetence was low. On the other hand, if the immune system of these ADA-SCID knockout mice was severely deficient compared to that of wildtype or heterozygous littermates, and more closely aligned with that of the alternative ADA-SCID mouse model [which is characterized by only a placental ADA minigene rescue and death at 3 weeks of age], then a single-stranded rAAV-based gene therapy even administered much earlier than the planned 6-8 weeks of age, may not have been able to progress in time to provide secreted hADA enzyme, a significant immunological response, and rescue or clinical benefit for the knockout mice. With this set of considerations in mind, the goal was to develop a general immunological profile for

ADA-SCID knockout mice compared to that of their wildtype/heterozygous littermates. To that end, two primary tools, flow cytometry and CBC analysis, were utilized to help define the nature of the partial immune deficiency described by Jackson Laboratories for this ADA-SCID mouse model. To create a general immunological profile for this ADA-SCID mouse model, the focus of this experiment was to calculate the numbers of B (CD19+), CD3+, CD4+, CD8+, and NK (CD16+) cells in peripheral mouse blood over time.

Figure 4-10 represents the compilation of both flow cytometry data and CBC analyses collected over a 5-month period from a group of ADA-SCID knockout mice (n=4) and wildtype/heterozygous littermates (n=3), from ages of 4 months to 8 months old. More specifically, while flow cytometry provided percentages of each individual immune cell subset for each mouse, complete blood counts (CBC) analysis provided a count of total lymphocytes. Both components, immune cell subset percentages and total lymphocyte counts, were utilized to enumerate B cell, CD3+ cell, CD4+ cell, CD8+ cell, and NK cells numbers in mouse blood at monthly time points. The calculation to determine the numbers of each cell type of interest was according to the following formula: *% cell subset* (%B cells, %CD4+ cells, %CD8+ cells, etc…) *x total lymphocyte count (K/ul) = the number (#) of cells/subset* (# B cells, #CD4+ cells, #CD8+ cells, etc). After cell enumeration for knockout and wildtype controls, averages of these cell counts, as well as standard deviations, were calculated and plotted as a bar graph for each monthly time point as shown in Figure 4-10.

Along the Y-axis are total lymphocyte counts and along the X-axis are the various time points at which the lymphocyte counts were determined for each of two experimental groups, knockout mice and wildtype control mice. Overall, even with substantial standard deviations, the data suggest that the total lymphocyte, B cell, CD3+ cell, CD4+ cell, and CD8+ cell counts

of the knockout mice are substantially lower than those of the wildtype controls. Figure 4-10 indicates that while average lymphocyte counts of wildtype controls are 2-3 fold more than knockout animals, while B cell, CD3+ cell, CD4+ cell, and CD8+ cell counts of wildtype mice are 2-4 fold higher than equivalent immune cell subset counts from knockout mice. Statistically, when all counts of immune cells derived from knockout mice over all time points are compared with those of wildtype mice over all time points, significant differences with p values less than 0.05 were observed for total lymphocytes and all cell subsets with the exception of natural killer (NK) cells (total lymphocytes $p<.0001$, B cells $p<.0001$, CD3+ cells $p<.0001$, CD4+ cells $p=.0003$, CD8+ $p<.0001$, NK cells $p=.8875$).

Overall, the goal of Aim 3 to characterize the general nature of the immune deficiency in a mouse model of ADA-SCID was accomplished using flow cytometry combined with CBC analyses. An immunological profile of the knockout versus the wildtype ADA-SCID mice was performed by determining absolute lymphocyte counts as well as of lymphocyte subset populations over the course of 120 days in the ADA-SCID mouse model.

In vivo Analyses of rAAV-hADA Vectors Packaged in Serotype 1 and Serotype 9 Capsids through Experiments 1 and 2

In previously described studies, confirmation of hADA protein expression and secretion in tissue culture, along with characterization of the substantial immune deficiency of the ADA-SCID mouse model of interest, presented an opportunity to investigate viability of the rAAV-hADA vector *in vivo*. A total of four *in vivo* studies, identified as Experiment 1, 2, 3, and 4, contributed to this body of research and are discussed in the remaining sections of Chapter 4. The following sections will first entail an analysis of Experiments 1 and 2, and then proceed to analyses of Experiments 3 and 4. There are two primary aims relevant to the four *in vivo* studies which will be addressed in the following sections, Aim 4 and Aim 5. The goal of Aim 4 is to

achieve successful gene delivery and protein expression *in vivo* following administration of rAAV vectors. In addition, the goal of Aim 5 to promote enhanced serum ADA activity and subsequent immune reconstitution, will be evaluated.

Initially, in what will be referred to as Experiment 1, the serotype 1 vector was administered intramuscularly to 10 wildtype mice of an ADA-SCID mouse model [described in Chapter 3 Materials and Methods]. These wildtype mice, unlike knockout mice of the same strain, do not display an immune deficiency. However, given the difficulty of initially breeding knockout animals, the approach adopted for this experiment was to focus primarily upon Aim 4, to test the ability of the rAAV1-hADA vector to foster gene delivery as well as expression and secretion of hADA in the mouse model of interest, without a focus on immune reconstitution.

With the primary goal of Experiment 1 being hADA expression/secretion secondary to gene delivery, 6 wildtype mice were administered a high dose of 1x10^11 vector particles, while 4 wildtype mice were administered a low dose of 1x10^10 vector particles. An additional 4 wildtype mice were injected with the control vector rAAV1-hAAT, which contains the gene for human alpha-1 antitrypsin. This gene codes for a serine protease inhibitor, which under normal physiological conditions, is produced in the liver and acts in the lungs to neutralize neutrophil elastase and, in turn, exert a protective effect on lung architecture. This vector was meant to provide a positive control for protein expression in the skeletal muscle of the mouse model of interest. Finally, 4 wildtype mice were administered PBS (one or the other) to serve as negative control for vector transduction, protein expression, and serum enzyme activity. The dosage of vector was 1x10^11 vector particles for all animals and the mice were all 10-12 weeks of age in Experiment 1.

In addition, in what will be referred to as Experiment 2, the rAAV9-hADA vector was analyzed *in vivo* in the same mouse model as used for Experiment 1. However, at the time Experiment 2 was conducted, few knockout mice rescued with the ADA minigene were successfully bred. While most knockout mice were maintained as breeders, a total of four could be used for experimentation. Thus, rAAV9-hADA vector was administered by intravenous injection to two knockout and two wildtype mice. In this experiment, the positive control vector, rAAV9-GFP(UF11), was injected intravenously into one knockout and one wildtype mouse. The control vector was meant to demonstrate efficient viral transduction and protein expression, in this case GFP, in the ADA-SCID mouse model. PBS was administered intravenously to one knockout and one wildtype mouse to serve as the negative control for injection and provide untreated negative control mice. The dosage of vector was 1x10^11 vector particles for all animals, and the mice were all 6-8 weeks of age in Experiment 2.

In Experiment 2, for the two PBS-injected control animals, any background levels of vector transduction, protein expression, and enzyme activity were evaluated. Similarly, identical endpoints were assessed for control mice administered rAAV9-GFP(UF11) and for mice administered rAAV9-hADA. For the knockout mice administered rAAV9-hADA, as well as all PBS and rAAV9-GFP(UF11)-injected knockout mice, an immunological endpoint assessing any proliferation (?what) of lymphocytes was determined. In keeping with the described endpoints, the ultimate goals of this experiment were to address Aim 4 and Aim 5. It must also be noted that the aforementioned immunological endpoint for Experiment 2, 3, and 4 is limited to calculation of total lymphocyte counts and enumeration of lymphocyte subset populations, which are used in this thesis as surrogate markers for immunocompetence. However, true immune function studies have not yet been performed for the experiments described in this thesis and

none of the aforementioned descriptions should be interpreted to mean restoration of immune function.

The rAAV-hADA Vector Provides Modest Gene Delivery in Experiment 1, but Substantial Gene Delivery in Experiment 2

On day 60 post-injection of rAAV1-hADA, the experimental wildtype mice utilized for Experiment 1 were sacrificed, and partial necropsies to harvest quadriceps, spleen, and liver were performed. Subsequent quantitative PCR analysis to assess overall vector transduction efficiency revealed mixed results for the low dose and high dose animals. Table 4-1 shows the qPCR data obstained for vector-injected and control mice following intramuscular injection of rAAV1-hADA into wildtype animals of the ADA-SCID strain. While the numbers of vector genomes in the negative control mouse tissues (derived from mice #1583 and #1587) were relatively low, only two of the high dose experimental mice had substantial levels of vector genomes above background levels (#1352 and 1356). Of the low dose group, one sample was contaminated and could not be used, while the other two clean muscle samples did not show significant levels of vector. Moreover, of the three animals administered the positive control vector, rAAV1-hAAT, two showed substantial levels of transduction in skeletal muscle. The latter observation demonstrated, at least in principle, that significant vector transduction by rAAV was possible in this particular mouse model. However, no substantial quantities of vector were observed in liver or spleen for any animals, despite the potential for some blood-borne vector transport following intramuscular injection.

Yet, Table 4-2 reveals a different story of vector transduction following intravenous injections of rAAV9-hADA in both knockout and wildtype mice of the ADA-SCID strain of interest. In Experiment 2, the mice numbered 1382 and 1369 were negative control animals administered PBS intravenously. The analyzed tissues described in the table were all free of

vector, testifying to low background levels of vector in this experiment. Two experimental animals, 1377 (knockout) and 206 (knockout), were sacrificed at 40 days post injection of vector and revealed substantial vector transduction in kidney, pancreas, spleen, liver, heart, thymus, and skeletal muscle tissues. For knockout animal 1377, the highest levels of transduction were in spleen, heart, and thymus tissues. For wildtype animal 206, the highest degree of transduction efficiency was found in spleen, heart, and liver tissues. Interestingly, while kidney, thymus, and skeletal muscle transduction was greater for knockout animal 1377 than for wildtype animal 206, every other wildtype tissue displayed much greater vector transduction in wildtype rather than knockout animals.

For the remaining knockout animals sacrificed at day 60 post-vector injection, all tissues for both mice #1379 and #1368 showed abundant vector transduction, with the exception of thymus for mouse #1368 for which sample was not obtained. Similarly, kidney, spleen, pancreas, liver, and skeletal muscle tissues, successfully derived from wildtype control mouse #1365 (given rAAV9-GFP(UF11)), all showed a high degree of vector transduction. Heart and thymus tissues for mouse #1365, were lost during cryopreservation. Also, experimental, wildtype mouse #1383 (which received the rAAV9-hADA vector) had high levels of vector transduction in kidney, spleen, liver, and heart tissues; thymus from this mouse was not harvested.

Overall for Experiment 2, but not without exception, vector transduction of wildtype mouse tissues was superior to that of knockout mouse tissues. For example, control wildtype mouse #1365, compared to its knockout counterpart, #1368, both given rAAV9-GFP(UF11), had superior vector transduction in kidney, spleen, pancreas, and liver tissues. Similarly, experimental wildtype mouse #1383, compared to its knockout counterpart, #1379, both given

rAAV9-hADA, had substantially greater levels of vector transduction in spleen, liver, and heart tissues. Although, this latter comparison between knockout mouse #1379 and wildtype mouse #1383, both given rAAV9-hADA, is not as apparent as it is for mice given rAAV9-GFP(UF11). For example, both kidney and skeletal muscle tissues of knockout animal #1379 displayed greater numbers of vector genomes than for wildtype animal #1383.

In summary, Experiment 1 yielded modest gene delivery results for skeletal muscle tissues of rAAV1-hADA-injected animals, while Experiment 2 utilizing intravenous injections of rAAV9-hADA to both knockout and wildtype mice, produced abundant gene delivery to a host of tissues including murine heart. This data supported Aim 4, which was predicated on the goal of accomplishing gene delivery using rAAV-hADA vectors.

Preliminary Immunohistochemical Analyses Reveal hADA Expression at Modest Levels Following rAAV1-hADA Injections and at Substantial Levels Following rAAV9-hADA Administration

Consistent with modest gene delivery from rAAV1-hADA was modest protein expression identified by histological analysis for Experiment 1. Figure 4-11 shows representative images of immunohistochemical staining for hADA in murine skeletal muscle at day 30 and day 60 post-intramuscular injection of rAAV1-hADA. Panel A of Figure 4-11 shows some alternating stained muscle fibers consistent with hADA expression in mouse #1354, which was sacrificed at day 30 post-vector injection. Panel B shows lighter hADA staining in murine skeletal muscle fibers in an alternating pattern from mouse #1356 at day 60 post-vector injection. Panel C illustrates hADA staining in a negative control muscle sample derived from mouse #1587 on day 60 post-vector administration. The degree of background staining observed is consistent with a light, diffuse brown color, though no substantially dark bands are observed. Lastly, Panel D demonstrates staining for hAAT in positive oontrol muscle tissue derived from

mouse #1363 on day 60 following administration of the control vector, rAAV1-hAAT. All images were captured using Aperio Imagescope software at a magnification of 4.0 X.

Figures 4-12, 13, and 14 display images gathered from staining of cardiac muscle and splenic tissues derived from both knockout and wildtype mice of the ADA-SCID strain from Experiment 2. Figure 4-12 shows in Panel A and B, hADA staining of cardiac muscle tissue derived from knockout mice #1377 and #1379, respectively, on days 40 and 60, respectively, following rAAV9-hADA administration. In both panels and for both mice, abundant hADA staining is observed among numerous cardiomyocytes. Panel C shows image of negative control cardiac muscle tissue derived from PBS-injected knockout mouse #1369. Little to no background staining is observed. All images were captured using Aperio Imagescope software at magnification of 4.0 X. Similar to Figure 4-12, Figure 4-13 shows hADA stained cardiac muscle tissue for wildtype mouse #206 (Panel A) on day 40 post-vector injection and for negative control wildtype mouse #1382 (Panel B) on day 60 post-PBS injection, which were both utilized in Experiment 2. Lastly, Figure 4-14 displays images of hADA staining in the spleen of vector-injected wildtype mouse #1383 (Panel A) as well as the spleen of PBS-injected wildtype mouse #1382 (Panel B) on day 60 of Experiment 2. While a degree of diffuse brown background staining was observed in spleen of control animal #1382 along with some scattered brown cells, substantially more relative cellular staining for hADA was observed in mouse #1383 on day 60 following administration of rAAV9-hADA. All images were captured using Aperio Imagescope software at magnification of 4.0 X for cardiac tissue and 15.0 X for splenic tissue.

In summary, the modest degree of protein expression in murine skeletal muscle following injection of rAAV1-hADA in wildtype animals was consistent with the modest degree of gene

delivery achieved for mice in Experiment 1. Similarly, for Experiment 2, abundant hADA expression was detected in cardiac muscle tissue of rAAV9-injected wildtype and knockout mice in which gene delivery was substantial. Expression of hADA was also observed in spleens of wildtype animals injected with type 9 vector. These results suggest that Aim 4, which is focused upon successful gene delivery and protein expression *in vivo*, was achieved modestly for Experiment 1 and substantially for Experiment 2.

Preliminary Analyses of Serum-Based Enzyme Activity, Following Vector Administration, Remain Inconclusive for both Serotypes of Interest for Experiment 1 and Experiment 2

At this point in this narrative of ADA-SCID gene therapy, preliminary studies revealed two sets of results for two endpoints of interest, gene delivery and protein expression. Partial success was observed for gene delivery in Experiment 1, involving intramuscular injection of rAAV1-hADA into healthy wildtype animals of the ADA-SCID strain, while substantial gene delivery was demonstrated for Experiment 2 following intravenous administration of rAAV9-hADA into both knockout and wildtype mice of the ADA-SCID strain. Second, modest immunohistochemical staining for hADA in Experiment 1 was observed, while abundant staining for hADA in Experiment 2 was shown. The next goal was to focus upon Aim 5, to determine the presence or absence of enhanced serum enzyme activity to support Experiments 1 and 2.

While Figure 4-15 (parts A, C, and D) shows graphical representations of enzyme activity over time for Experiment 1, Figure 4-16 and Table 4-3 show enzyme activity at varying time points for each experimental and control mouse utilized for Experiment 2. All activity levels are reported as averages and in terms of Units of ADA activity. One Unit of ADA activity was described by the manufacturers of the clinical assay (Diazyme) as the amount of ADA enzyme necessary to produce one micromole of inosine from adenosine in one minute at 37 degrees

Celsius. It is also worth noting that the average activity values are based upon group sizes which vary typically by 1 to 2 animals from time point to time point based on sample availability.

Beginning with enzyme activity data collected over time for Experiment 1, Figure 4-15 part A shows a high degree of background ADA activity on day 9 in both control groups, wildtype mice administered PBS instead of vector, and wildtype mice administered rAAV1-hAAT vector (vector map produced with Clone Manager software included as Figure 4-15 part B) instead of rAAV1-hADA vector. These control groups have serum ADA activity levels registering on the order of 6.4 Units and 5 Units, respectively. However, wildtype mice belonging to the ADA high and low dose groups, all administered rAAV1-hADA, showed only 4 Units and 3.2 Units of ADA activity, respectively. By day 25 (Figure 4-15 part C) post-injection of vector or PBS, ADA activity for PBS and AAT control groups increased to 7.5 Units and 6.0 Units, respectively. Moreover, ADA activity for the experimental groups (ADA high dose and ADA low dose) increased to 6.9 Units for the ADA high dose group and to 7.7 Units for the ADA low dose group. An increase of nearly 3 Units for the high dose group and nearly 3.5 Units for the low dose group could not be validated though given the high level of background ADA activity. Finally, Figure 4-15 part D illustrates measured serum ADA activity on day 32 post-intramuscular injection of vector or PBS. In this case, enzyme activity of PBS and AAT control groups was 6 Units and 4.3 Units, respectively, showing respective decreases of 1.5 and 1.7 Units of enzyme activity. Simultaneously, the ADA high dose group had an average of 6 Units of ADA activity while the ADA low dose group had an average of 9.5 Units. While the high dose group lost 1 Unit of activity, the low dose group gained nearly 2 Units. As Figure 4-15 part D shows, ADA activity in the low dose group is substantially above that of both control groups, yet the previously high levels of background activity relative to ADA activities of the

experimental groups cast doubt on the veracity of the enzyme activities observed on day 32 for the ADA low dose group.

The enzyme activities for Experiment 2 is shown in Figure 4-16. Supplemental information on the exact ADA activity levels measured and plotted in Figure 4-16 may also be found in Table 4-3. Figure 4-16 displays ADA activity in Units for each experimental and control, knockout and wildtype mouse of interest at varying time points, including days 22, 40, and 60, post-IV injection of vector or PBS. Proceeding from left to right across Figure 4-16, control knockout mice numbered 1369 (given PBS) and 1368 (given rAAV9-GFP(UF11)) showed enzyme activity levels on the order of 4-6 Units for day 22, while experimental knockout mice (#1377 and #1379) had enzyme activity levels in the same range. Also, for day 22, wildtype control animals numbered 1382 (given PBS) and 1365 (given rAAV9-GFP(UF11)) had enzyme activity levels between 6-8 Units, while the wildtype animals administered rAAV9-hADA (#206 and #1383) showed enzyme activity levels on the order of 8-15 Units. This observed increase in serum ADA activity in vector-injected wildtype mice was consistent with enhanced gene delivery generally observed for the same experimental animals.

Next, day 40 results in Figure 4-16 were limited to two experimental animals sacrificed soon thereafter, knockout mouse #1377 (administered rAAV9-hADA) and wildtype mouse #206 (also administered rAAV9-hADA). While #1377 mouse demonstrated moderately increased ADA activity from 6 Units (day 22) to nearly 8 Units (day 40), here again, the vector-injected wildtype mouse, #206, demonstrated much more increased activity from 9 Units to nearly 25 Units.

Finally, day 60 data in Figure 4-16 indicated only a small increase from 4 to 5 Units of enzyme activity for knockout mouse #1379 while control knockout animals (#1368 and #1369)

had decreased ADA activity from 4 to 6 Units on day 22 to range of 1 to 3.5 Units by day 60. Also on day 60, wildtype control mice identified as #1365 and #1382 had ADA activities of 9.8 and 12.3 Units, respectively, representing increase of nearly 2 Units and 6 Units, respectively. Wildtype mouse #1383 administered rAAV9-hADA, had measured ADA activity of 12.9 Units. Overall, Figure 4-16 shows that background ADA activity in widltype control animals may present a significant problem in evaluation of vector-induced ADA activity, as is the case with day 60 data, though background was less of a problem on, for example, day 22. That being said, serum ADA activity in the wildtype animals administered rAAV9-hADA appears substantially greater than that observed for knockout animals administered identical vector at identical doses. While knockout animals administered rAAV9-hADA showed only modest increases in ADA activity, the control knockout animals showed decreases in ADA activity over time.

Overall, no conclusive evidence or trend could be gathered from the serum enzyme activity data collected for Experiment 1, while only slight increases in enzyme activity for treated knockout animals in Experiment 2 with parallel decreases in untreated knockout animals, suggested, but by no means clearly identified, a trend or significant increase in serum ADA activity. Thus, this data had limited merit towards substantiating Aim 5.

Immunological Profiling of ADA-SCID Mice Administered rAAV9-hADA in Experiment 2 Suggests a Positive Trend toward Potential Immunological Benefit but Provides no Conclusive Evidence

The final endpoint for the initial studies was analyses of restoration of lymphocyte numbers to in ADA-SCID knockout mice receiving experimental vector in Experiment 2. While serum ADA activity levels improved only modestly for rAAV9-hADA-injected knockout animals and substantially, at some time points, for wildtype animals also injected with rAAV9-hADA, the limited enzyme activity analysis done thus far also revealed slight decreases in enzyme activity in control mice over time. Given these observations, one question that

remained for Experiment 2 was whether or not an immunological benefit could be shown in vector-injected knockout mice.

Figure 4-17 shows a graph of immunological responses, followed over time, to the administration of rAAV9-hADA, rAAV9-GFP(UF11), or lactated ringer PBS, for Experiment 2. The time points along the X-axis are at day 0 (the day of injections), day 30 post-injection, and day 60 post-injection. Also, the X-axis lists the individual knockout mice utilized for intravenous injections along with the corresponding vector, control vector, or PBS treatment. The Y-axis illustrates absolute counts of immune cells derived from both flow cytometry and CBC analyses. The derivation of lymphocyte counts is described further in previous subsections on immunological profiling in this chapter. The different colored bars for each animal at a given time point refer to the levels of each individual immunological subset or total lymphocytes. It is also worth noting that while most blood samples were harvested from the knockout mice of interest for this study, 2 samples (day 0 #1379 and day 30 #1369) were not viable and could not be used for flow or CBC analyses.

Interestingly, Figure 4-17 shows decreasing trends for control knockout mouse #1368 (administered the control vector, rAAV9-UF11) from day 0 to day 60. For control mouse #1368, total lymphocytes, along with B, CD3+, CD4+, and CD8+ cells all show steady decreases with time. Similarly, decreasing trends for total lymphocytes, B cells, and CD4+ T cells were also observed for the control knockout mouse #1369 (administered PBS). On the other hand, knockout mouse #1377, which was administered the rAAV9-hADA vector, showed increasing trends for total lymphocytes, along with B, CD3, CD4, and CD8 cells by day 30 post-injection. Similarly, knockout mouse #1379, also given the rAAV9-hADA vector, showed modest

increases in B, CD3, CD4, and CD8 cell populations over time, though the overall lymphocyte count modestly decreased over time.

Overall, Figure 4-17 reveals that the control knockout mice showed decreasing trends in total lymphocyte and immune cell subset counts, while the knockout mice, administered the rAAV9-hADA vector, showed a modest immunological benefit over time. However, with the limited number of animals utilized for Experiment 2, no definitive conclusions could be drawn. As such, no concrete evidence to substantiate Aim 5 was yet available. These preclinical gene therapy studies would have to be expanded to greater numbers of knockouts to witness any potential immunological benefit to the gene therapy. Moreover, variation in dose to produce a more pronounced enzymatic and immunological benefit would be implemented. Finally, the background enzyme activity levels observed for the wildtype mice of the ADA-SCID strain would exclude these animals from continued, expanded studies.

Expanded *In vivo* Analyses of rAAV-hADA Vectors Demonstrate Long-Term Gene Delivery and Protein Expression, while Indicating Protein Secretion, Enzyme Activity, and a Potential Immunological Benefit in Experiments 3 and 4

With the identification of secreted hADA protein derived from rAAV-hADA in culture, a general assessment of the immunological profile of the ADA-SCID mouse model, and initial *in vivo* data from Experiments 1 and 2, which indicated substantial gene delivery and protein expression, but inconclusive enzyme activity and immunological data, the next step was to expand testing of the rAAV-hADA vector *in vivo* at higher vector doses and exclusively in knockout mice. Thus, the next two studies of this project, referred to as Experiment 3 and Experiment 4, were conducted and have been described in the following sections. These two studies are predicated on the lessons learned from the mixed results of earlier experiments (Experiment 1 and 2) and were intended to further support Aims 4 and 5 of this research endeavor. These earlier studies indicated a need to use a higher dosage of vector (3x10^11 to

1x10^12 vector particles) potentially to elicit a greater degree of gene delivery, protein expression, serum enzyme activity, and immunological response. Earlier studies also emphasized the need to focus upon the generation of substantial numbers of knockout mice. With these two lessons learned, an exploration of the viability of this vector *in vivo*, at an increased dose, and exclusively in young, knockout mice of consistent age, proved to be the challenge for Experiment 3 and 4.

In Experiment 3, the rAAV-hADA plasmid was packaged in serotype 1 and 9 capsids to be administered to ADA-SCID knockout mice by intramuscular or intravenous injection, respectively. The dose was increased from 1x10^10 or 1x10^11 vector particles to 3x10^11 vector particles per mouse, based on preliminary studies. The age of the knockout mice utilized for the following experiments was 6-8 weeks. The use of a young animal model may have served to mimic the pediatric patients afflicted with ADA-SCID. For Experiment 3, 5 knockout animals (n=5) were administered, via tail vein injection, 3x10^11 particles of rAAV9-hADA, while 4 knockout animals (n=4) were administered, via intramuscular injection into the right quadriceps, 3 x 10^11 particles of rAAV1-hADA. In addition, 3 knockout mice were used as negative controls. Finally, one mouse was injected with a rAAV9-GFP(UF11) (GFP-green fluorescent protein) control vector. Then, at several time points post injection, blood was withdrawn for analyses of serum ADA activity and for flow cytometry of stained lymphocytes. Also, on day 120 post-injection, the mice were sacrificed so that tissue could be harvested to analyze additional endpoints, including the degree of gene delivery/transduction efficiency by qPCR and protein expression by immunohistochemical staining for hADA. Collectively, these endpoints would allow for a further assessment of Aims 4 and 5.

Lastly, in Experiment 4, following the successful breeding of larger groups of mice, a total of 31 knockouts were used to test the single-stranded vector, rAAV9-hADA, at two different doses, 3x10^11 and 1x10^12 vector particles, alongside *in vivo* testing of a self-complementary version of the same vector, called sc-rAAV9-hADA. A total of 10 knockout mice were administered rAAV9-hADA at the low dose (3x10^11 vector particles), while 10 knockout mice were administered the high dose (1x10^12 vector particles). A total of 5 knockout animals were given the self-complementary vector at a dose of 3x10^11 vector particles, while 6 knockouts were administered lactated ringer PBS. All vectors and PBS were administered by tail vein injection into 6-8 week old ADA-SCID mice. Several endpoints were also assessed. Blood was taken at day 0, 30, and 45 post-injection of vector or PBS for CBC and flow analyses. On day 55 post-vector administration, 10 animals, including 4 high dose, 3 low dose, and 2 PBS-injected mice were sacrificed. Tissues were harvested from the sacrificed mice for quantitative PCR and immunohistochemical analyses. The data collected proved beneficial towards an evaluation of Aim 4 and 5.

Experiment 4 is ongoing and will be continued out to days 100 and 150 post-vector administration using the remaining 20 mice. The latter time points, along with the remaining gene delivery, protein expression, serum enzyme activity, and immunological data will not be covered in this thesis, but will be collected in the near future. Serum activity analyses for all relevant time points will be conducted at the end of Experiment 4 on the same day, using the same reagents, and under the same experimental conditions, to limit experimental variability which may occur when performing the assay at different dates and times. Thus far, no mice administered the self-complementary vector have been sacrificed. These mice will remain until the end of the experiment to maximize data collection.

Injections of rAAV-hADA Vectors, Including Serotypes 1 and 9, Foster Successful Gene Delivery in ADA-SCID Knockout Mice in Experiments 3 and 4

As described in greater detail previously, Experiment 3 was designed to administer rAAV1-hADA and rAAV9-hADA vectors to ADA-SCID knockout mice, to facilitate gene delivery, protein expression, enhanced serum enzyme activity, and immunological responses. At day 120 post-injection, animals were sacrificed and necropsies were performed to harvest tissues for two purposes, immunohistochemical staining of hADA and for quantitative PCR, the latter as an indicator of gene delivery and transduction efficiency. In this section, the data gathered from quantitative PCR (qPCR) will be described.

In Table 4-4, qPCR data from Experiment 3 has been listed. In the far left column entitled "Mouse ID," the identification numbers for each animal are listed. In the next column entitled "Vector or PBS," the use of rAAV or alternatively, PBS, is noted. Then, the column entitled "Day of Sacrifice" designates the day post-IV or IM injection on which the mice were sacrificed, necropsied, and tissues harvested for qPCR analyses. Continuing along Table 4-4 is the column named "Vector copy number/tissue/ug of DNA," meaning that for each of the subsequent tissues [and columns] of interest (ie. heart, kidney, lungs, stomach, liver, spleen, skeletal muscle, pancreas, and thymus), the values listed represent the vector copy number per microgram (ug) of extracted DNA.

For Experiment 3, the mice were 8 weeks old at the time of injection and the degree of gene delivery did vary from tissue to tissue and mouse to mouse in the experimental groups. In each tissue [with the exception of pancreas], the control samples for mice numbered 27, 36, 41, and 1375 did not show significant levels of vectors. Thus, these control tissues provided an adequate basis of comparison and negative control copy number values for the sample tissues from rAAV injected animals. Also, mouse #31 and mouse #33 died prior to day 120 due to

rapid, excessive hemorrhaging under isoflurane anesthesia during facial vein bleeding. At necropsy, several tissues were still viable for qPCR analysis and the vector copy number values of only the viable tissues have been included in Table 4-4.

For rAAV9-hADA injected animals, numbered 29, 30, 40, 28, heart tissue samples revealed substantial vector transduction long-term for each animal. The vector copy numbers range from 1x10^3 to 7x10^3 for each heart tissue sample. In kidney tissue, copy number varied from 5.8x10^2 to 1x10^4 suggesting significant levels of vector transduction in this tissue for at least three mice of the experimental group, identification numbers 28, 29, and 31. While liver transduction levels varied from 2x10^2 to 2x10^3, mouse #28 and mouse #29 appeared to have the highest levels of transduction. For lung tissue, substantial long-term transduction was indicated for all mouse samples, with copy numbers ranging from 1.1x10^3 to 8.5x10^3. Skeletal muscle transduction had greater variability compared to heart or lung, with copy numbers ranging from as low as 2x10^2 to as high as 1.1x10^4. Three mice, #29, 30, and 31, indicated the highest levels of transduction. Pancreatic tissue samples as well had a high degree of variability in terms of the vector copy number, with samples from mouse #29 and mouse #30 indicating copy numbers at approximately 2x10^3. In spleen, copy numbers were relatively low except for one animal, mouse #30, with 2.2x10^3 vector genomes per ug total DNA. All animals showed little vector transduction of the stomach. Similarly, all animals except #29 (1.2x10^4 vector genomes/ug total DNA), showed little transduction of the thymus.

For the 4 animals injected intramuscularly with rAAV1-hADA, little transduction was expected or observed for either heart or kidney tissue. Vector transduction in the liver ranged from a low copy number of 3x10^2 to a high of 1.6x10^3. For both lung and pancreatic tissue, only animal #39 had substantial levels of vector at copy numbers in each tissue of 2.8x10^3 and

3.6x10^3, respectively. Tissue samples from murine spleen, stomach, and thymus revealed little vector transduction. However, the primary target tissue, skeletal muscle, for which two quadriceps samples were taken at necropsy, revealed substantive levels of rAAV transduction with vector copy numbers ranging from 6x10^3 to 1.6x10^5. While the majority of type 1 vector administered intramuscularly was expected and observed in muscle tissue, vector which migrated through the circulation to other tissues such as liver and lung was also observed in some cases.

In the final study, Experiment 4, the degree of gene delivery was assessed at day 55 post-vector injection of single-stranded rAAV9-hADA vector. Table 4-5 contains the quantitative PCR data obtained for all murine tissues derived from the sacrifice of 10 mice. Four mice were administered a high dose (HD) of vector (1x10^12 vector particles), four were injected with a low dose (LD) of vector (3x10^11 vector particles), and two were given lactated ringer PBS. The tissues harvested at necropsy for HD, LD, and PBS groups, included heart, liver, pancreas, kidney, thymus, and skeletal muscle. While nearly all negative control tissues for mouse #145 and mouse #156 displayed no background AAV vector, abundant gene delivery was detected for nearly all tissues with considerable variability between the vector copy numbers calculated for each mouse and for any given tissue. For the LD group of animals, heart, liver, kidney, and skeletal muscle tissues had the highest average copy numbers and the most consistently copy number values. Interestingly, Table 4-5 also shows the high degree of gene delivery for the HD group of ADA-SCID knockout mice. In a clear dose response relationship, over 3 times as much vector administered to the HD group yielded vector copy numbers, for the identical tissues as those studied for the LD group, on the order of 2-23 times greater. Overall, the degree of gene delivery and vector transduction efficiency observed for Experiment 4, by day 55 post-vector injection, was substantial.

In summary, gene delivery data from Experiments 3 and 4 corroborated an assessment of substantial gene delivery to target tissues, including skeletal muscle for type 1 vector and heart for type 9 vector. In addition to heart, a substantial degree of transduction efficiency was indicated for the type 9 vector by consistent, persistent, and abundant vector copy numbers in numerous murine tissues such as kidney, liver, and skeletal muscle. This data supports Aim 4 of this research.

Recombinant AAV-hADA Vectors, Including Serotypes 1 and 9, Mediate Substantial Protein Expression *In vivo* in Murine Heart, Kidney, Liver, and Skeletal Muscle Tissues in Experiments 3 and 4

Upon confirmation of substantial, long-term, *in vivo* gene delivery to a variety of murine tissues, the next goal for Experiment 3 and 4 was to qualitatively assess protein expression in the same murine tissues. One method by which this goal could be accomplished was by immunohistological staining for human ADA (hADA) protein.

In Experiment 3, both rAAV1-hADA and rAAV9-hADA vectors were used. In Experiment 4, only rAAV9-hADA vectors were used and analyzed. For the mice injected with rAAV1-hADA, the primary tissue of interest was skeletal muscle, and two samples of quadriceps muscle tissue were harvested from each mouse for staining purposes. Additional tissues including heart, liver, spleen, thymus, lung, stomach, and pancreas were harvested for staining from animals injected with type1 vector, though the presence of staining was not highly anticipated even with the likelihood of some vector particles entering the circulation following intramuscular injection. For rAAV9-hADA vector, the primary tissues of interest for immunohistochemical staining were heart, liver, kidney, and skeletal muscle, though pancreas, spleen, lung, and stomach were also harvested and stained. Identical tissues were also stained for hADA in negative control (PBS-injected) mice. For Experiment 3 only, in positive control mice administered rAAV9-GFP(UF11), identical tissues were stained for green fluorescent

protein. Finally, for both Experiment 3 and 4, hematoxylin and eosin staining was also performed for each mouse tissue to assess qualitatively the presence or absence of an immune response which could have been targeted to either transgene or vector capsid. In the following section, representative images of immunohistochemical staining of murine tissues, derived from control mice and experimental mice [administered either type 1 or type 9 vector] from both Experiment 3 and 4, have been included and described. All images were captured using Aperio Imagescope software. Immunohistochemical staining for Experiment 3 may be found in Figures 4-18, 19, and 20. Immunohistochemical staining for Experiment 4 may be found in Figures 4-21 and 4-22.

Figure 4-18A provides an example of the hADA staining observed in murine skeletal muscle tissue, derived from the quadriceps of an ADA-SCID knockout mouse, and obtained at sacrifice on day 120 following intramuscular injection of rAAV1-hADA. Throughout the section of muscle illustrated on the left of Figure 4-18A, intermittent hADA staining is shown. The banding pattern of numerous brown staining muscle fibers throughout this tissue section, with unstained fibers in between stained fibers, is characteristic of rAAV vector-based protein expression. The observed staining on the left of Figure 4-18A is shown relative to the absence of hADA staining in negative control murine skeletal muscle tissue shown on the right of Figure 4-18. The latter skeletal muscle tissue was derived from knockout mice administered lactated-ringer PBS instead of vector. In Figure 4-18B, the identical skeletal muscle shown on the left of Figure 4-18A, was stained using hematoxylin and eosin (H&E). This staining revealed no clear inflammatory infiltrates in the vector-injected muscle tissue.

Figure 4-19A illustrates one example of hADA staining within cardiac muscle tissue of knockout mice sacrificed at day 120 post-intravenous injection of rAAV9-hADA. Figure 4-19A

has images of murine ventricle at low and high magnification. The lower magnification was meant to show that vector-driven hADA expression may be observed throughout the tissue section. The higher magnification shows more clearly the variable levels of hADA staining of murine cardiomyocytes which would likely correlate with substantial, but variable levels of hADA expression in individual cardiomyocytes. By comparison, Figure 4-19B shows the level of background hADA staining in the murine heart, at low and high magnifications, of an ADA-SCID knockout mouse administered lactated ringer PBS instead of vector. The images show relatively little, if any, background hADA. Figure 4-19C displays the identical cardiac muscle tissue used for hADA staining in Figure 4-19A, though, in this instance, H&E staining was performed and showed no apparent cardiac inflammation. Figure 4-19D shows a high magnification image of GFP-stained murine cardiac muscle tissue, derived from an ADA-SCID knockout mouse administered rAAV9-GFP (vector map illustrated in Figure 4-19E), and sacrificed on day 120 post-IV injection of vector. In this case, the cardiac muscle tissue serves as a positive control for protein expression in the heart of the ADA-SCID knockout model. The image shows a number of positively-stained cardiomyocytes with varying levels of GFP expression.

Figure 4-20A illustrates the hADA staining of kidney tissue derived from an ADA-SCID knockout mouse which was sacrificed on day 120 following intravenous injection of rAAV9-hADA. Low and high magnification images are shown. The low magnification image displays the abundance of hADA staining throughout the region of the kidney which may be described as the renal medulla/pelvis. The darkly-stained cells are also shown at high magnification and are likely epithelial cells of the collecting ducts and Loops of Henle. Background hADA staining in the renal medulla/pelvis region of murine kidney tissue, harvested from ADA-SCID knockout

mice administered lactated ringer PBS instead of vector, is also displayed in Figure 4-20B at low and high magnification. While some patches of background hADA staining may be viewed on negative control tissue sections, such background is easily surpassed by the abundant, widespread, dark staining of the kidney tissue derived from the vector-injected knockout mouse shown in Figure 4-20A. Figure 4-20C shows H&E staining of the identical kidney tissue used for hADA staining in Figure 4-20A. No inflammatory infiltrate was visible.

In Experiment 4, following rAAV9-hADA administration in both low and high doses, cardiac muscle once again demonstrated abundant protein expression. Figure 4-21 contains three images, labeled A, B, and C. In image 4-21A, immunohistochemical staining for hADA in murine heart reveals, abundant, darkly-stained, cardiomyocytes in tissue harvested from mouse #186, on day 55 following administration of single-stranded type 9 vector at the high dose of 1x10^12 vector particles. Consistent staining for hADA in the murine heart was observed for both the low dose and high dose animals. Figure 4-21A is a representative image of the results gathered for the vector-injected knockout mice. Figure 4-21B captures an image, at the magnification utilized for Figure 4-21A (5.0x using the Aperio Imagescope), which demonstrates the hADA staining of cardiac muscle tissue obtained from PBS-injected negative control mouse #145. The degree of background staining for hADA is minimal. Lastly, Figure 4-21C shows the same cardiac muscle tissue as that shown in Figure 4-21A, derived from mouse #186, though the staining in this instance is with H&E. No inflammatory infiltrates responding to vector or transgene are visible.

Also revealed in Experiment 4 was a substantial degree of hADA staining in murine liver tissue following administration of a high dose of vector to an ADA-SCID mouse. Although not seen in all animals, the abundant staining of hADA in the liver tissue of mouse #186, provided

the first evidence of rAAV-mediated hADA protein expression in hepatocytes. Figure 4-22A shows the dark staining of numerous hepatocytes, relative to the negative control liver tissue displayed in Figure 4-22B (from PBS-injected mouse #145). Although not shown, a broader image of the liver section displayed in Figure 4-22A revealed the same degree of hADA staining abundant throughout large cross-sections of this murine liver sample. Lastly, Figure 4-22C displays an H&E stain of the identical murine liver section used for Figure 4-22A. No inflammatory infiltrates are visible in response to vector or transgene.

Overall, Experiment 3 demonstrated substantial hADA staining in murine skeletal muscle, following administration of rAAV1-hADA and abundant, consistent staining of cardiac muscle tissue derived from rAAV9-hADA. This data suggests skeletal muscle and heart as the primary sites of ectopic hADA expression, and potentially, secretion. Also, the detection of hADA protein in kidney tissue of at least one type 9 vector-injected mouse suggested kidney as a possible secondary site of hADA expression and potential secretion. Experiment 4 confirmed the cardiac-based hADA expression propagated by the type 9 vector. Also, the detection of abundant hADA expression in at least one mouse, treated with a high dose of type 9 vector in Experiment 4, suggested liver as another site of hADA expression and potential secretion. This qualitative protein expression data further supports Aim 4 of this research.

Recombinant AAV-hADA Administration, Followed by an Analysis of Serum ADA Activity over Time, Suggest hADA Secretion and Enhanced Enzyme Activity in Vector-Treated Versus Control ADA-SCID Knockout Mice

Following an analysis of rAAV vector gene delivery, and having observed, in select tissues of vector-injected mice, substantial hADA expression over that of tissues from negative control mice, the next question in this narrative of a potential rAAV-based gene therapy for ADA-SCID was whether or not hADA was secreted and capable of serum-based enzyme activity? In this section, the goal is to provide the serum enzyme activity data for Experiment 3,

obtained at several time points post-injection of type 1 and type 9 vectors, in knockout mice, and compared to that of negative control animals administered lactated ringer PBS. Overall, while the data from Experiment 3, involving rAAV9-hADA administration to 5 knockout mice and rAAV1-hADA administration to 4 knockout mice, was not statistically significant, the data was suggestive of moderately-increased, serum-based, enzyme activity and thus, a moderate level of hADA protein secretion. Figure 4-23, parts A, B, and C, presents bar graphs of serum ADA activity over the first 45 days of Experiment 3 for ADA-SCID knockout mice administered rAAV1-hADA by intramuscular injection, compared to the background ADA activity levels of saline-injected ADA-SCID knockouts. Figure 4-24, parts A, B, and C, presents equivalent bar graphs of serum ADA activity for vector-injected versus saline-injected knockout mice over the same time period, following intravenous administration of rAAV9-hADA. Moreover, as described previously, serum enzyme activity data for Experiment 4 will be assessed upon conclusion of Experiment 4 to either confirm or deny the trend observed in Experiment 3. Given the current, ongoing status of Experiment 4, serum enzyme data is not yet available at present. Yet, what has the serum enzyme data from Experiment 3 shown?

The Experiment 3 data begins with Figure 4-23 part A, which shows serum ADA activity for knockout mice on day 9 following administration of rAAV1-hADA vector. The ADA activity levels are presented along the Y-axis in terms of "Units" of ADA activity with identification of the experimental versus control knockout groups along the X-axis. One unit of ADA activity, according the manufacturers of the enzyme assay (Diazyme Laboratories), is defined as the amount of ADA enzyme needed to convert 1umol of adenosine to inosine in one minute at 37 degrees Celsius. On day 9, the level of ADA activity is low (an average of 2.1 Units), even relative to the background ADA activity level in the serum derived from saline-

injected knockout mice (an average of 5.1 Units.). However, by day 30 post-IM injection of rAAV1-hADA (Figure 4-23 part B), the measured ADA activity for the vector-injected mice was on average 6.4 Units, compared to the background level of, on average 3.9 Units. The increase on average for the experimental mice administered vector was 4.5 Units of ADA Activity. However, by day 45 post-vector injection, ADA activity levels between both experimental and control groups were approximately equal (Figure 4-23 part C). The experimental group had an average of 4.4 Units of activity, while the negative control serum had an average of 3.8 Units of activity.

Experiment 3 also revealed serum ADA activity for knockout mice following intravenous injection of rAAV9-hADA vector, and beginning with Figure 4-24 part A. The latter figure describes serum enzyme activity on day 9 post-vector injection. On average, vector-injected knockout mouse serum had 7.5 Units of ADA activity compared to 5.l Units in the serum harvested from PBS-injected knockout mice. By day 30 post-administration of vector, shown in Figure 4-24 part B, a decrease in average ADA activity was observed for the experimental mice, which was then determined to be 4.8 Units, compared to the average level of ADA activity for the control mice, 3.9 Units. Finally, Figure 4-24 part C illustrates average ADA activity levels at day 45 post-IV injection of rAAV9-hADA. For the vector-injected knockout mice, average serum ADA activity increased to 7.8 Units, compared to 3.8 Units in the serum harvested from saline-injected knockout mice.

Overall, the enzyme activity data currently available from Experiment 3 suggest a trend towards enhanced serum-based enzyme activity following administration of rAAV-hADA vectors, though the evidence is not conclusive or significant. Ongoing enzyme assays for Experiment 4 may confirm or deny the observed trends. However, this serum ADA activity data

does provide the first supporting evidence toward one goal described in Aim 5 of this project, to promote enhanced serum ADA activity.

Recombinant AAV9-hADA Vector Elicits a Substantial Proliferation of Lymphocytes in Treated Knockout Mice Compared to Untreated Knockout Mice in Experiment 3

Having observed substantial gene delivery and protein expression in Experiment 3 and 4, as well as a trend toward enhanced enzyme activity in Experiment 3, and thus, an indication of moderate levels of secreted hADA following injection of rAAV-hADA, one final question remained: Is rAAV-hADA capable of stimulating a proliferation of lymphocytes (ie an immune response to vector-based delivery and expression of hADA) in the ADA-SCID knockout mouse model?

The goal of this section is to present the immunological data following rAAV-hADA administration, derived from flow cytometry and CBC analyses, and gathered over the course of 4 months for Experiment 3 and 45 days for Experiment 4. Just as with the earlier analyses of ADA-SCID knockouts compared to their wildtype littermates, the immunological endpoints of interest included a determination of B, CD3+, CD4+, CD8+, and NK cell counts along with total lymphocyte counts. Overall, the immunological data gathered, following rAAV1-hADA injections, did not indicate a proliferation of lymphocytes in vector-injected knockout mice compared to control knockout mice for Experiment 3. However, following rAAV9-hADA administration, a substantial, progressive, and prolonged proliferation of lymphocytes was indicated in the vector-injected knockout mice compared to the control knockout mice for Experiment 3. Lastly, though current immunological analyses for Experiment 4 have only been conducted out to day 45 post-vector administration, an early, positive trend toward increases in lymphocyte populations of treated versus untreated mice, holds potential for this study.

Figure 4-25 and Table 4-6 describe graphically and numerically the response of lymphocyte populations to rAAV1-hADA vector injections for the knockout animals of Experiment 3. In Figure 4-25, the left-half of the diagram contains an immunological profile over a 90-day time period for knockout animals which received an intramuscular injection of rAAV1-hADA. The equivalent immunological profile for the negative control knockout animals is found on the right-half of the diagram. Examination of both Figure 4-25 and Table 4-6 reveal that the immunological profile for the experimental animals (n=4), including total lymphocytes along with B, CD3+, CD4+, CD8+, and NK cells, is unremarkable, when compared to the immunological profile of the control group. Total lymphocyte counts as well as counts of the individual subsets are very similar at each time point to the total lymphocyte and subset counts of the negative control group.

Figure 4-26 and Table 4-7 describe graphically and numerically the increases in lymphocyte populations in response to rAAV9-hADA vector injections in the knockout animals of Experiment 3. In Figure 4-26, the left-half of the diagram contains an immunological profile over a 90-day time period for knockout animals which received an intravenous injection of rAAV9-hADA. The equivalent immunological profile for the negative control knockout animals is found on the right-half of the diagram. The NK cell counts remain relatively equal between the vector-injected knockout mice and the control mice over the 90-day time course study. However, the total lymphocyte counts as well as B, CD3+, CD4+, and CD8+ cell populations all generally show a steady, step-wise increase in numbers over time, and exceed the levels of identical cell populations derived from the negative control mice. Statistically, when the day 90 lymphocyte and immune cell subset counts of the type 9 vector-injected mice are compared to the counts of the negative control mice, no p value less than or equal to .05 was observed. Yet,

when the lymphocyte and cell subset counts of the type 9 vector-injected mice on day 90 of Experiment 3 are compared to the values observed on day 0, p values of less than .05 were observed for each cell group (Lymphocytes p=.0038, B cells p=.0120, CD3+ cells p=.0027, CD4+ cells p=.0025, CD8+ cells p=.0064, NK cells p=.0004).

Finally, the early data gathered for Experiment 4, detailing the appearance of any trends in the various lymphocyte populations of interest has been displayed in Figure 4-27. Along the x-axis of this figure are the experimental groups of interest, the PBS-injected knockout mice (N=6), the low-dose (LD), type 9, vector-treated ADA-SCID knockout mice administered 3x10^11 vector particles, the high dose (HD), type 9, vector-treated knockout mice given 1x10^12 vector particles, and the type 9 self-complementary vector-treated knockout mice also given 3x10^11 vector particles. Along the y-axis are total lymphocyte counts derived from both CBC and flow cytometry data. In Figure 4-27, just as with similar, previous figures, the colored bars each correspond to either the total lymphocyte population or to the lymphocyte subset populations as shown. Interestingly, while the observed trend for the lymphocyte populations of the PBS-injected group appear to be decreasing or stabilizing over time, the observed trend for the lymphocyte populations of the treated animal groups appears to be increasing, especially in the animals of the low-dose (LD) group. Since Experiment 4 will be continued to day 100 and day 150 post-vector injection, only with the combined flow and CBC analyses provided at these later time points, can the presence of absence of a lasting, positive trend be ascertained.

In summary, the immunological data gathered from Experiment 3 and 4 and based upon rAAV9-hADA administration, support a positive trend toward lymphocyte proliferation in treated versus untreated ADA-SCID knockout mice. Thus, the immunological data help achieve Aim 5. However, further studies, including the remaining work of Experiment 4, must be

pursued to confirm or deny the significance of the observed trends and assess any benefit to immune function that may or may not accompany the observed trends.

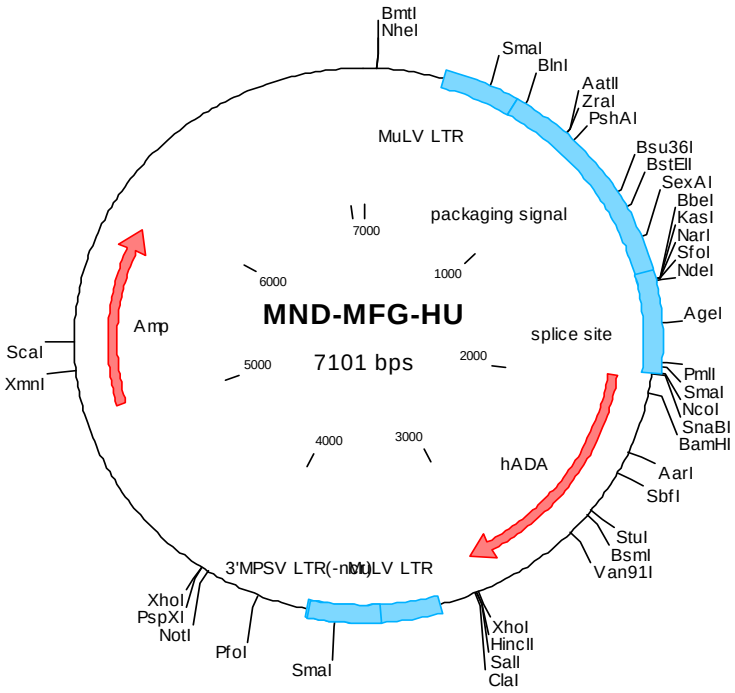

Figure 4-1. Map of the Retroviral Vector, MND-MFG-hADA (produced using Clone Manager software), obtained from Donald B. Kohn, MD at the USC Keck School of Medicine, and used as the template for high fidelity PCR amplification of the hADA transgene, with subsequent cloning into a recombinant AAV vector

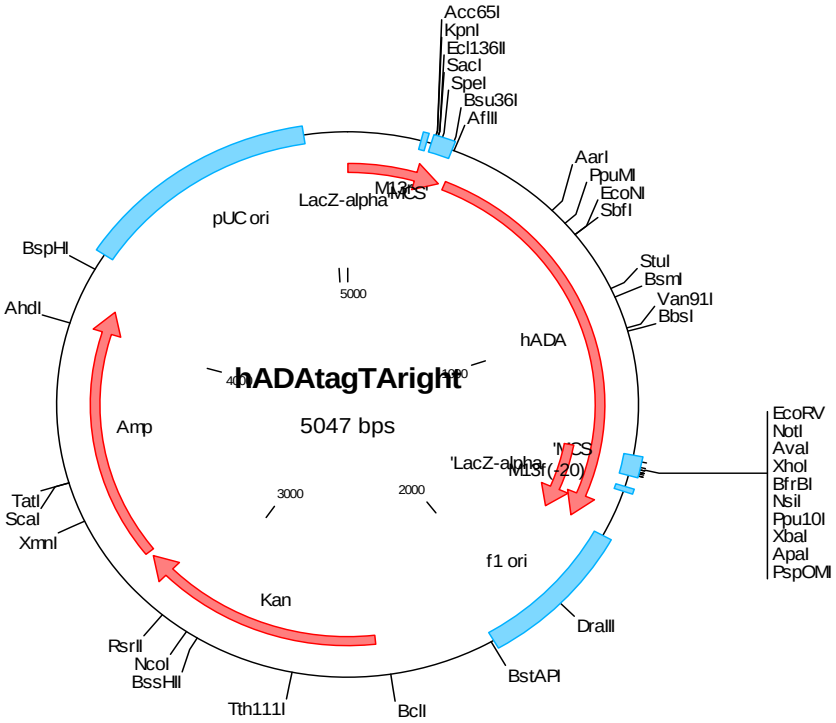

Figure 4-2. Map of the hADA TA Cloning Vector, entitled “hADAtagTAright” (or pCRTopo2.1-hADA) This construct was used as an intermediate cloning step, to facilitate cloning of the hADA gene into a rAAV vector This vector was produced when the hADA PCR product amplified from the retroviral vector, MND-MFG-hADA, was cloned into a pCRTopo2.1 plasmid from a Topo TA Cloning kit (Invitrogen)

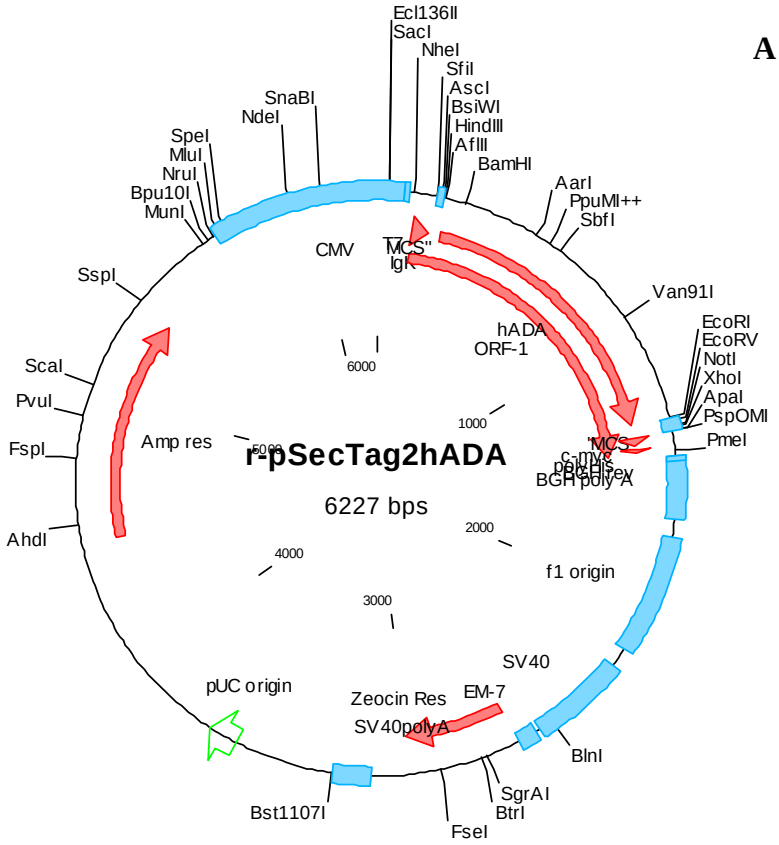

Figure 4-3. Map of the expression vector, pSecTag2-hADA, and sequence of the secretory, tagged hADA transgene cassette A.) Clone Manager software was used to produce this vector map of pSecTag2-hADA, which contains the hADA transgene linked to a 5' IgK secretory signal and a 3'c-myc/polyHistidine tag. This construct was formed by cloning the hADA gene, obtained through restriction digest of pCRTopo2.1-hADA (Figure 4-2), into the pSecTag expression vector (Invitrogen) B.) The DNA sequencing of the 5'IgK-hADA-cmyc/polyHis 3' transgene cassette within pSecTag2-hADA and cloned directly into rAAV-hADA

B

```
     NheI    NcoI
           -------  ------
  1  agcctggcta gccaccatgg agacagacac actcctgcta tgggtactgc tgctctgggt
                    >>.....ORF-1.....>
                    >>.....IgK ss.....>

                                Cfr10I
                                -------
                                NgoMIV
                                -------
                                 NaeI     BssHII BsiWI     AflII
                                -------   -------------    ------
                               SfiI        AscI        HindIII
                          -------------- ---------     -------
 61  tccaggttcc actggtgacg cggcccagcc ggccaggcgc gccgtacgaa gcttaagtcg
     >........ORF-1........>
     >..IgK ss..>>

                 BsaHI
                 ------
121  aggcatggcc cagacgcccg ccttcgacaa gcccaaagta gaactgcatg tccacctaga
     >........ORF-1........>
         >>.......hADA.......>

      BamHI
      ------
181  cggatccatc aagcctgaaa ccatcttata ctatggcagg aggagaggga tcgccctccc
     >........ORF-1........>
     >........hADA........>

                                       MslI
                                     ----------
241  ggctaacaca gcagaggggc tgctgaacgt cattggcatg gacaagccgc tcacccttcc
     >........ORF-1........>
     >........hADA........>


301  agacttcctg gccaaatttg actactacat gcctgctatc gcgggctgcc gggaggctat
     >........ORF-1........>
     >........hADA........>


361  caaaaggatc gcctatgagt ttgtagagat gaaggctaaa gagggcgtgg tgtatgtgga
     >........ORF-1........>
     >........hADA........>

                       AarI
                     --------
421  ggtgcggtac agtccgcacc tgctggccaa ctccaaagtg gagccaatcc cctggaacca
     >........ORF-1........>
     >........hADA........>

                                                                SbfI
                                                              --------
              PpuMI                                             EcoNI
```

Figure 4-3. Continued

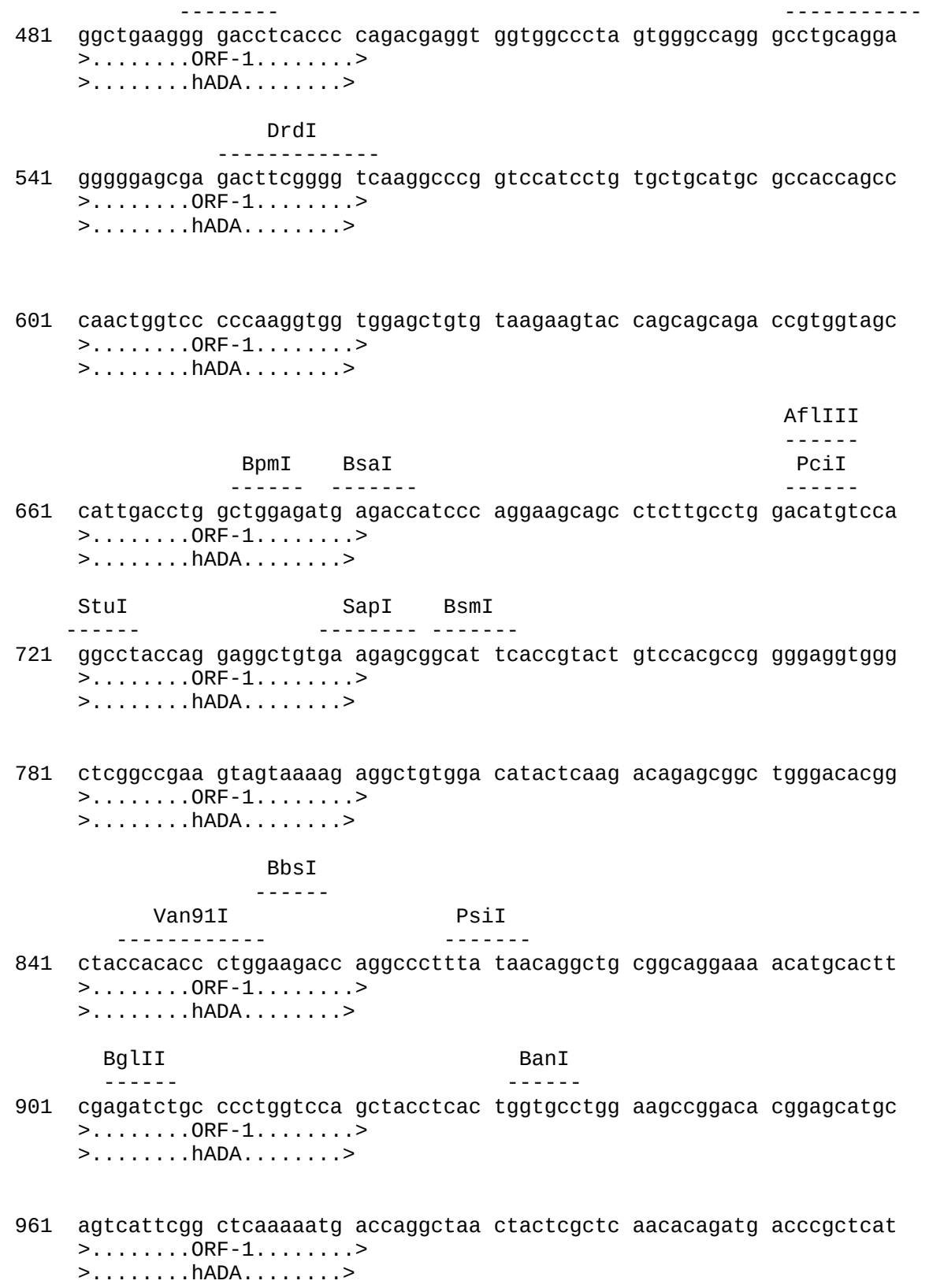

Figure 4-3. Continued

```
1021  cttcaagtcc accctggaca ctgattacca gatgaccaaa cgggacatgg gctttactga
      >........ORF-1........>
      >........hADA........>



1081  agaggagttt aaaaggctga acatcaatgc ggccaaatct agtttcctcc cagaagatga
      >........ORF-1........>
      >........hADA........>



1141  aaagagggag cttctcgacc tgctctataa agcctatggg atgccacctt cagcctctgc
      >........ORF-1........>
      >........hADA........>

                                                          AvaI     ApaI
                                                         -------  ------
                                                          XhoI    BseSI
                                                         -------  ------
                    EcoRI      EcoRV                 NotI          PspOMI
                    ------     ------              --------        ------
1201  agggcagaac ctcggaattc tgcagatatc cagcacagtg gcggccgctc gaggagggcc
      >........ORF-1........>
      >.hADA.>>

                                                 AccI
                                                ------
                                                HincII
                                                ------
                                         HaeII   SalI
                                         ------ ------
1261  cgaacaaaaa ctcatctcag aagaggatct gaatagcgcc gtcgaccatc atcatcatca
      >........ORF-1........>
       >>....c-myc....>>
                                                      >>.poly-His.>

              PmeI   MspA1I
             ----------------
1321  tcattgagtt taaacccgct ga
      >.>>
      >.>>
```

Figure 4-3. Continued

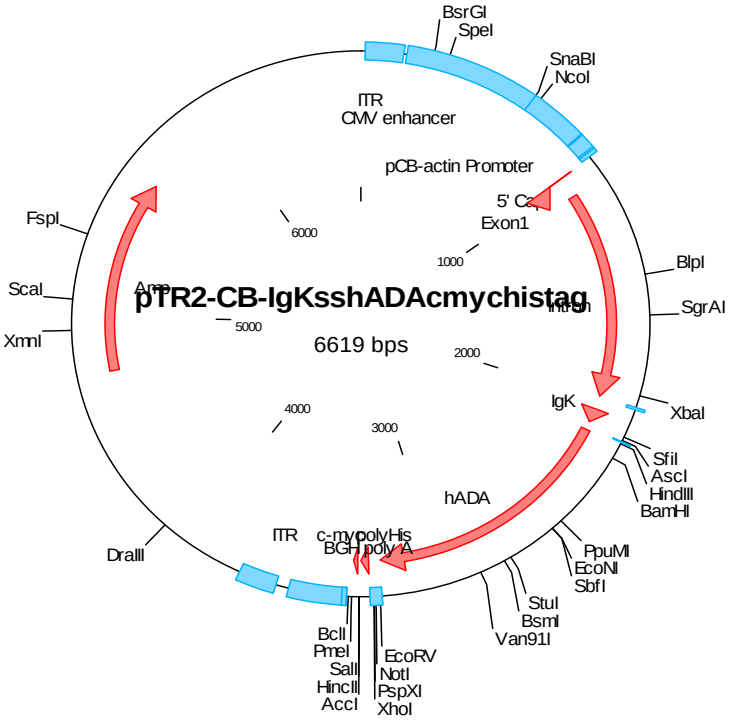

Figure 4-4. Map of the primary rAAV vector of interest, known as pTR2-CB-IgKsshADAcmychistag or rAAV-hADA. This construct was produced by cloning the hADA transgene cassette identified in Figure 4-3 into a rAAV serotype 2 cloning vector.

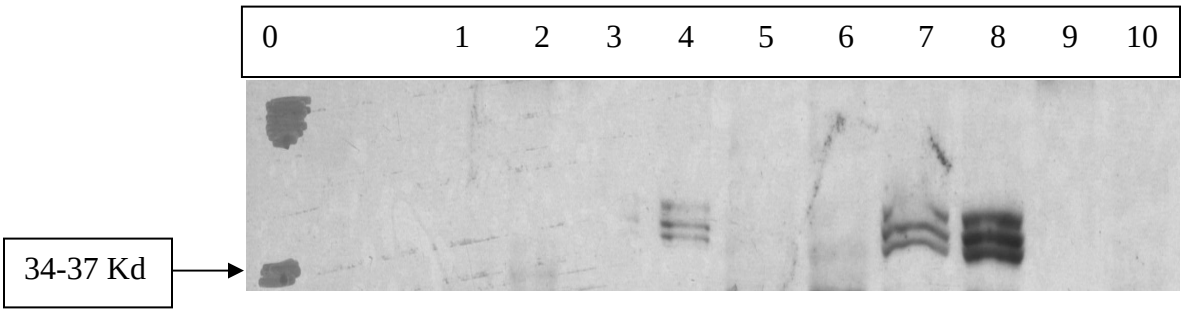

Figure 4-5. Western Blot #1 confirming the expression and secretion of hADA protein from the pSecTag2-hADA expression vector. Lane 4 demonstrates c-myc-tagged hADA protein in several isoforms at approximately 48 Kd from harvested tissue culture media at 72 hours post lipofectamine 2000-mediated transfection of 293 cells with pSecTag2-hADA (Figure 4-3). Lanes 7 and 8 contained non-secreted, c-myc-tagged hADA from 293 cell lysates at 72 hours post-lipofectamine 2000-mediated transfection with pSecTag2-hADA A negative control was utilized in Lane 9 in which the media sample demonstrated an absence of secreted hADA protein. The media in this lane was from 293 cells not transfected with any plasmid. In Lane 10 is a negative control cell lysate sample in which non-secreted hADA protein is not detected. The cell lysate used in Lane 10 was derived from 293 cells transfected only with rAAV plasmid containing the gene for green fluorescent protein (GFP), as opposed to the transgene for hADA.

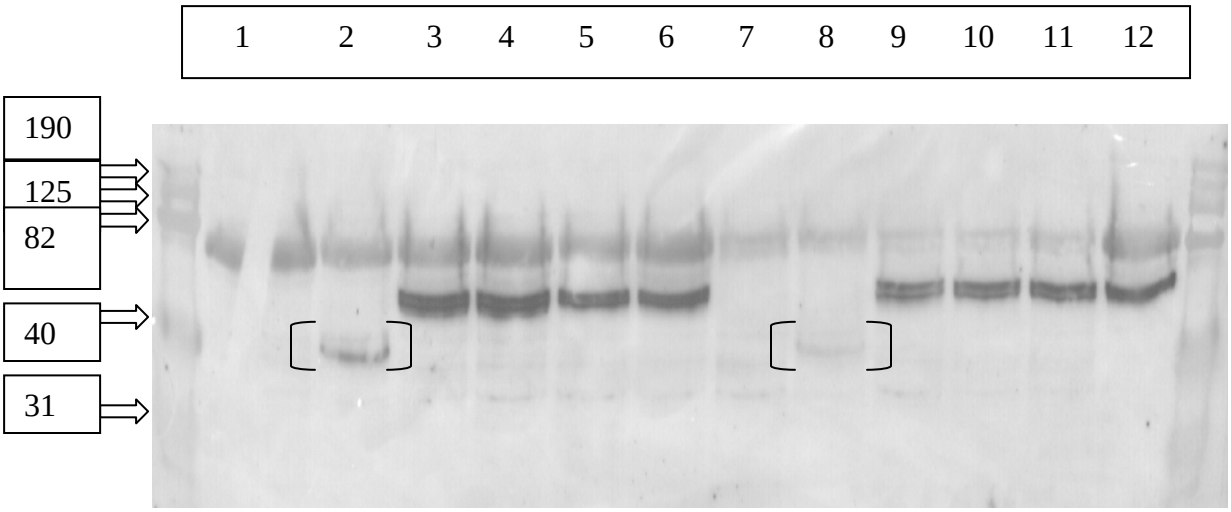

Figure 4-6. Western Blot #2 confirming both the expression and secretion of hADA protein from pSecTag2-hADA and rAAV-hADA All samples were obtained for all lanes at 72 hours post-lipofectamine 2000-mediated transfection of 293 cells: Lane 2 media contained a single band (designated by brackets) which served as a positive control, a c-myc-tagged secreted angiostatin protein. In Lane 8, the loaded cell lysate sample also contained a single band (designated by brackets) at 36Kd, which served as a positive control for non-secreted, c-myc-tagged protein. In cell media samples in Lanes 3 and 4, bands representing secretory hADA from the pSecTag2-hADA construct were found at approximately 48kD. In cell media samples in Lanes 5 and 6, bands representing secretory hADA from the rAAV-hADA vector were also observed at 48kD. Non-secreted hADA expressed from the pSecTag2-hADA plasmid and found in 293 cell lysates are seen as multiple dark bands in Lanes 9 and 10. Similarly, non-secreted hADA protein, expressed from the rAAV plasmid and harvested from 293 cell lysates, was observed as multiple dark bands in Lanes 11 and 12. The media sample in Lane 1 and the cell lysate sample in Lane 7 serve as negative control samples with an absence of secreted and non-secreted c-myc-tagged hADA, respectively.

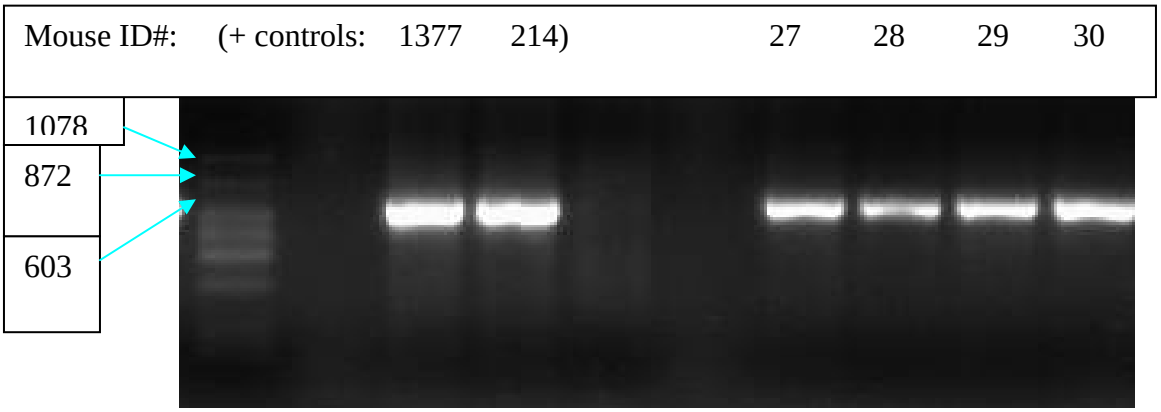

Figure 4-7. Representative image of the knockout ADA allele (700bp), on a 1.5% Agarose gel with ethidium bromide, which is characteristic of knockout ADA-SCID mice. The 700 bp knockout band was amplified from positive control genomic DNA, harvested from tail tips of mouse #1377 and mouse #214, with the aid of knockout allele-specific PCR primers. For mice identified as 27, 28, 29, and 30, the knockout allele was successfully amplified at 700bp. In the far left lane, the promega DNA molecular weight ladder phiX174 HaeIII provides molecular weight references. Though not shown, a negative control PCR reaction was run without DNA template and yielded no background DNA.

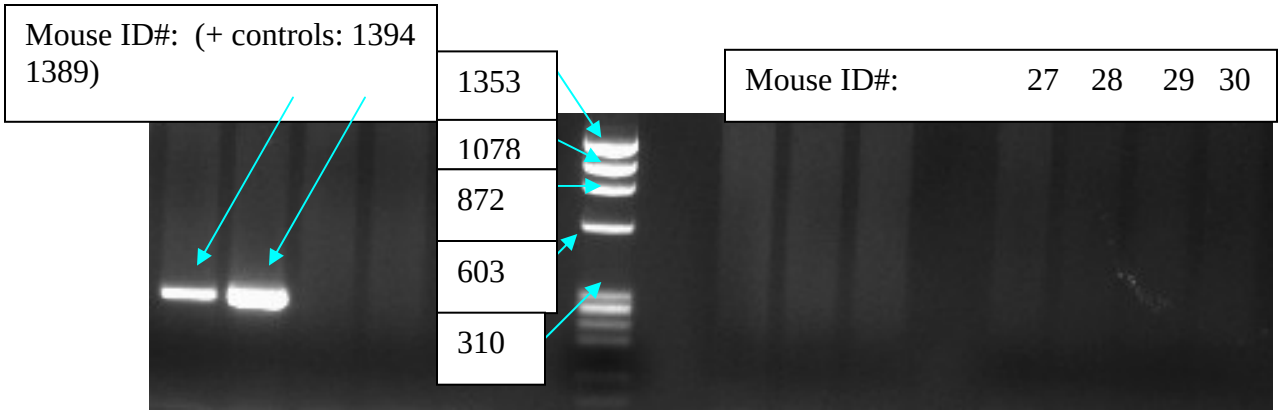

Figure 4-8. Representative image of the wildtype ADA allele (274bp), on a 1.5% Agarose gel with ethidium bromide, which is characteristic of heterozygote and/or wildtype ADA-SCID mice. The wildtype allele was PCR-amplified from positive control genomic DNA harvested from mouse #1394 and mouse #1389 using PCR primers specific for the wildtype allele. In the middle of the image is the molecular weight ladder, phiX174 HaeIII (Promega). For mice, numbered 27, 28, 29, and 30, no wildtype allele was amplified. Though not shown, negative control PCR reaction was run with no DNA template and no background DNA was detected

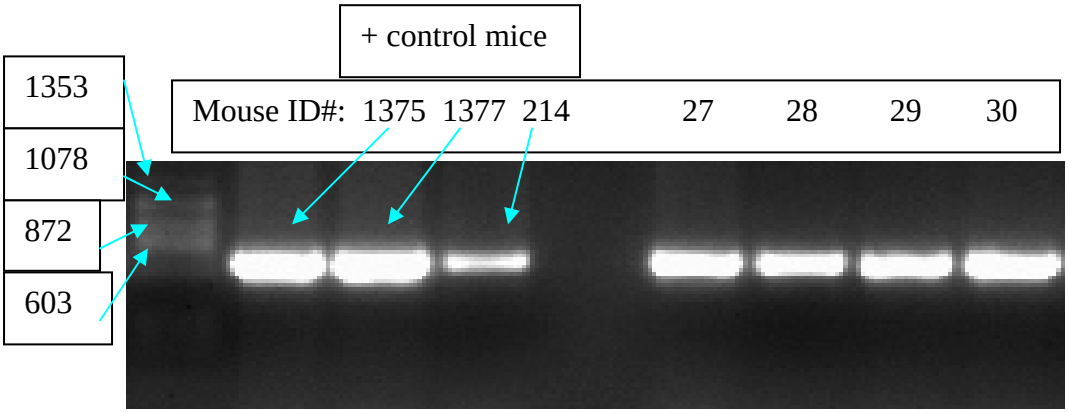

Figure 4-9. Representative image of the ADA minigene rescue (470 bp), on a 1.5% Agarose gel with ethidium bromide, which is expressed in the placenta and forestomach of knockout ADA-SCID mice, and necessary to save these knockouts from embryonic lethality and death at 3 weeks of age from pulmonary insufficiency. The phiX174 HaeIII DNA ladder was run on the far left of the gel for reference. Positive control genomic DNA from mice numbered 1375, 1377, and 214 was subjected to PCR using minigene-specific primers to produce the corresponding 470bp bands. The ADA minigene rescue was also successfully amplified from genomic DNA harvested from mice numbered 27, 28, 29, and 30. Although not on this image, a negative control PCR reaction was run without DNA template, and showed no background DNA.

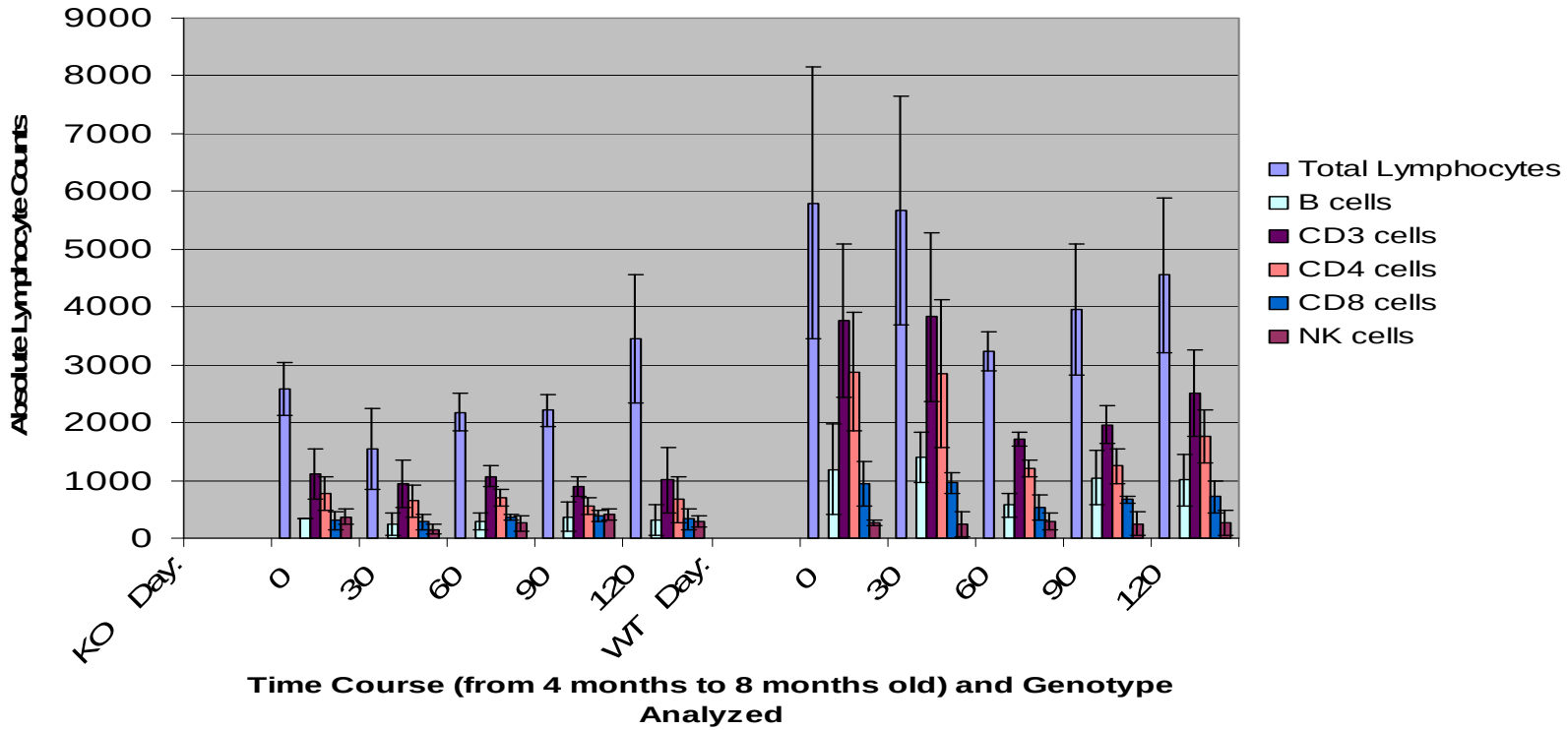

Figure 4-10. Quantification of total lymphocytes and immunological cell subsets in ADA-SCID Knockout and Wildtype Mice over time. This figure shows the relative lymphocyte populations of knockout ADA-SCID mice (KO-left) compared to their wildtype littermates (WT-right) followed over the course of 120 days. The mice were age-matched and followed from 4 months to 8 months old. The lymphocyte counts were obtained from CBC analyses and multiplied by lymphocyte subset percentages, derived from flow cytometry, to yield counts of each lymphocyte subset. Overall, even with substantial standard deviations, the data suggest that the total lymphocyte, B cell, CD3+ cell, CD4+ cell, and CD8+ cell counts of the knockout mice are substantially lower than those of the wildtype controls. Statistically, when all counts of immunological cells derived from the knockout mice, over all time points, are compared with those of the wildtype mice, over all time points, significant differences with p values less than .05 were observed for total lymphocytes and all cell subsets with the exception of natural killer (NK) cells (Total lymphocytes $p<.0001$, B cells $p<.0001$, CD3+ cells $p<.0001$, CD4+ cells $p=.0003$, CD8 $p<.0001$, NK cells $p=.8875$).

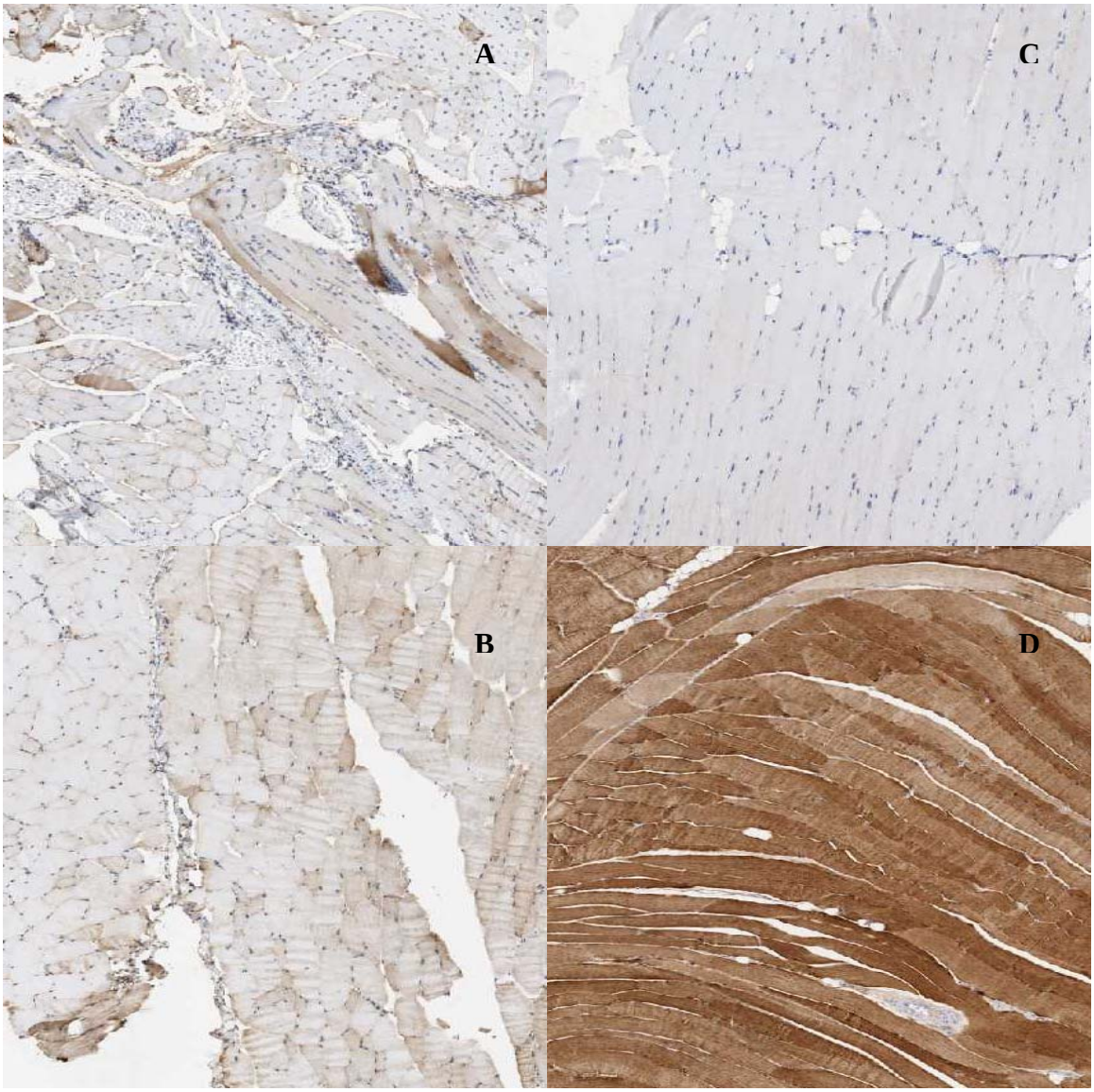

Figure 4-11. Immunohistochemical staining for hADA (human adenosine deaminase) or hAAT (human alpha-1 antitrypsin) in skeletal muscle tissue of wildtype animals of the ADA-SCID strain following intramuscular injections of rAAV1 or PBS in Experiment 1. A.) Several skeletal muscle fibers stained for hADA and derived from mouse #1354 on day 30 following rAAV1-hADA administration. B.) Alternating skeletal muscle fibers, from mouse #1356 on day 60 following rAAV1-hADA administration, show staining for hADA. C.) Control skeletal muscle, derived from mouse #1587 on day 60 following PBS injection, and stained for hADA, shows little background. D.) Skeletal muscle stained intensely for hAAT and derived from positive control mouse #1363 following administration of rAAV1-hAAT. Overall, the visible hADA staining provided an early example of limited hADA expression in the skeletal muscle target tissue for rAAV1-hADA.

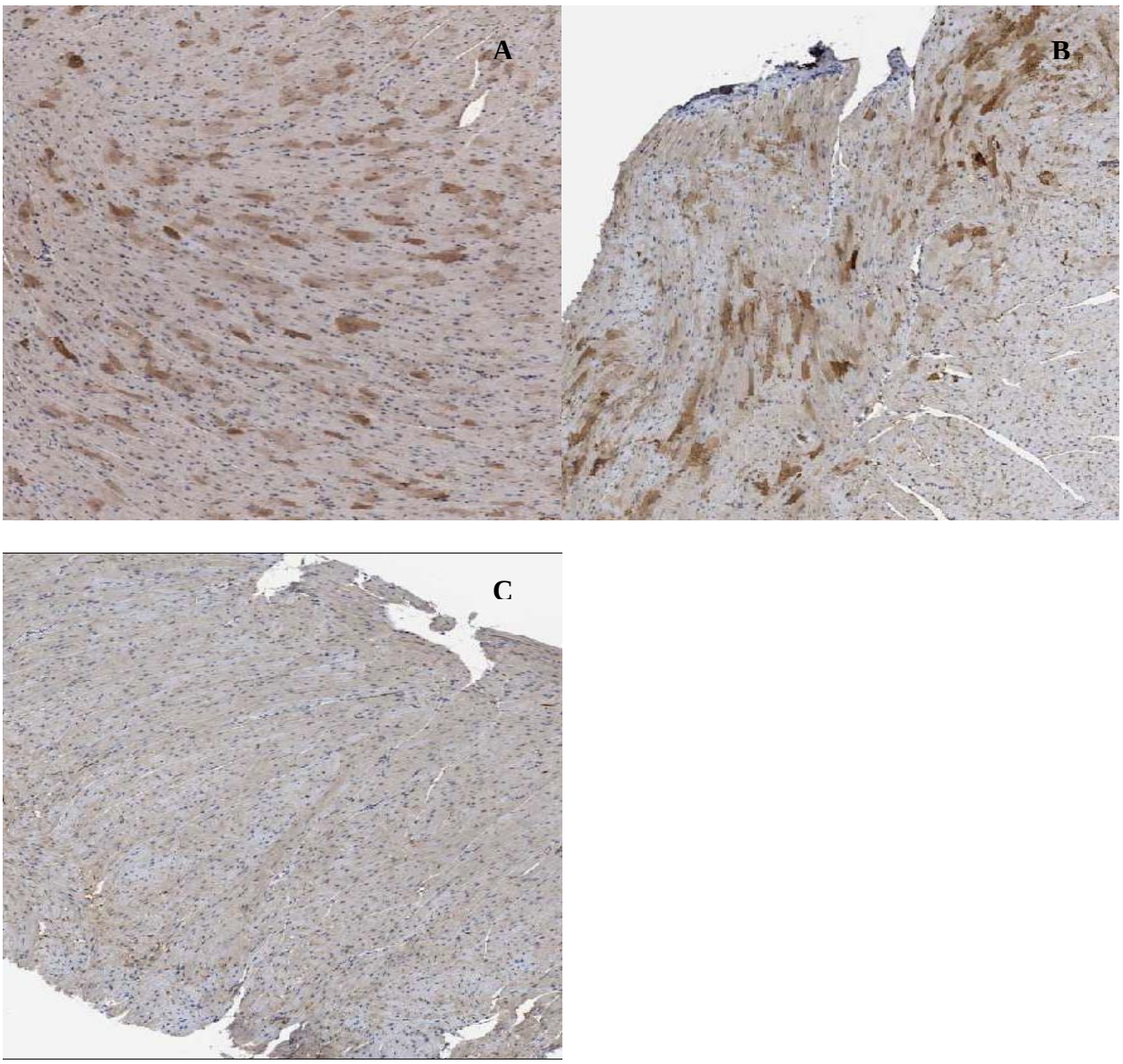

Figure 4-12. Immunohistochemical staining for hADA in cardiac muscle tissue of knockout ADA-SCID mice following intravenous injections of rAAV9-hADA or PBS for Experiment 2. A.) Cardiac muscle tissue stained for hADA and derived from mouse #1377 on day 40 following injection of rAAV9. B.) Cardiac muscle tissue stained for hADA and derived from mouse #1379 on day 60 following rAAV9 injection. C.) Cardiac muscle tissue stained for hADA from negative control mouse #1369 on day 60 following PBS injection. Overall, compared to control tissue from mouse #1369, the cardiac muscle tissues of treated mice, numbered 1377 and 1379, display an abundant number of cardiomyocytes stained darkly for hADA, suggesting a substantial amount of hADA expression in heart.

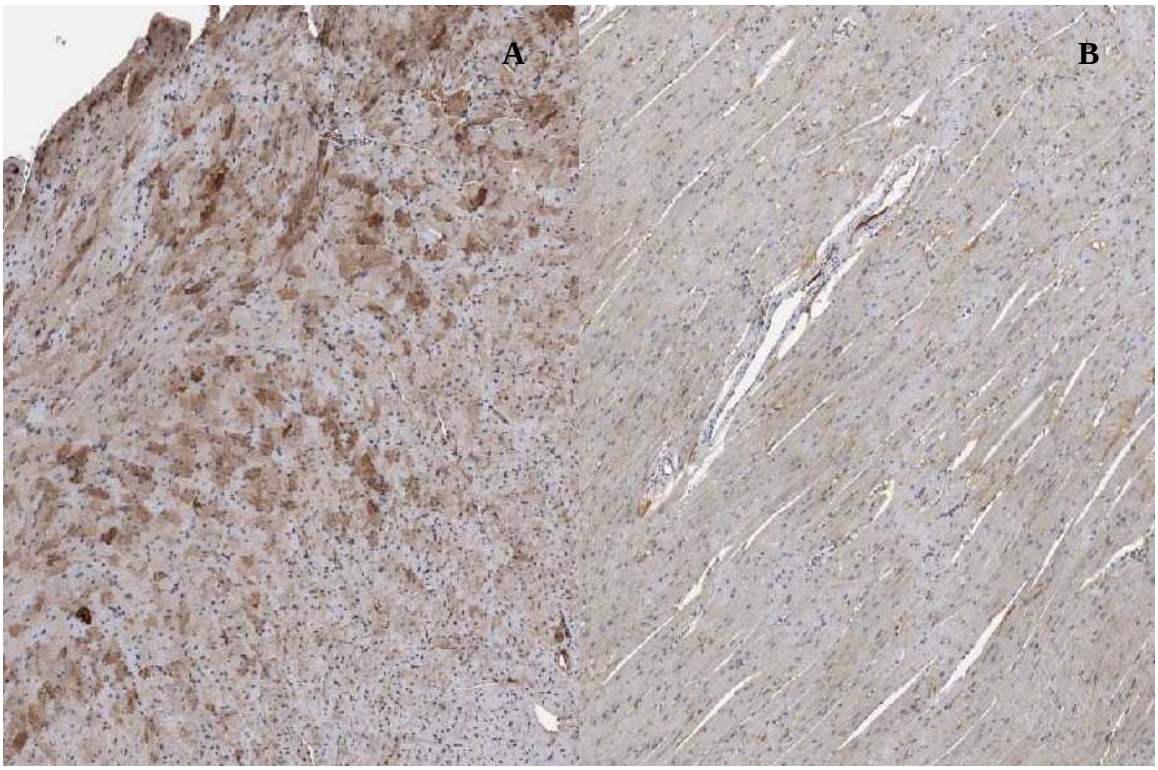

Figure 4-13. Immunohistochemical staining for human adenosine deaminase in the cardiac muscle tissue of wildtype mice of the ADA-SCID strain following intravenous administration of rAAV9-hADA or PBS in Experiment 2. A.) Cardiac muscle tissue stained for hADA and derived from mouse #206 on day 40 following rAAV9 injection. B.) Cardiac muscle tissue stained for hADA and derived from negative control mouse #1382 on day 60 following PBS injection. Overall, compared to control tissue from mouse #1382, the cardiac muscle of treated mouse #206 displays an abundant number of cardiomyocytes stained darkly for hADA, suggesting a substantial amount of hADA expression in heart.

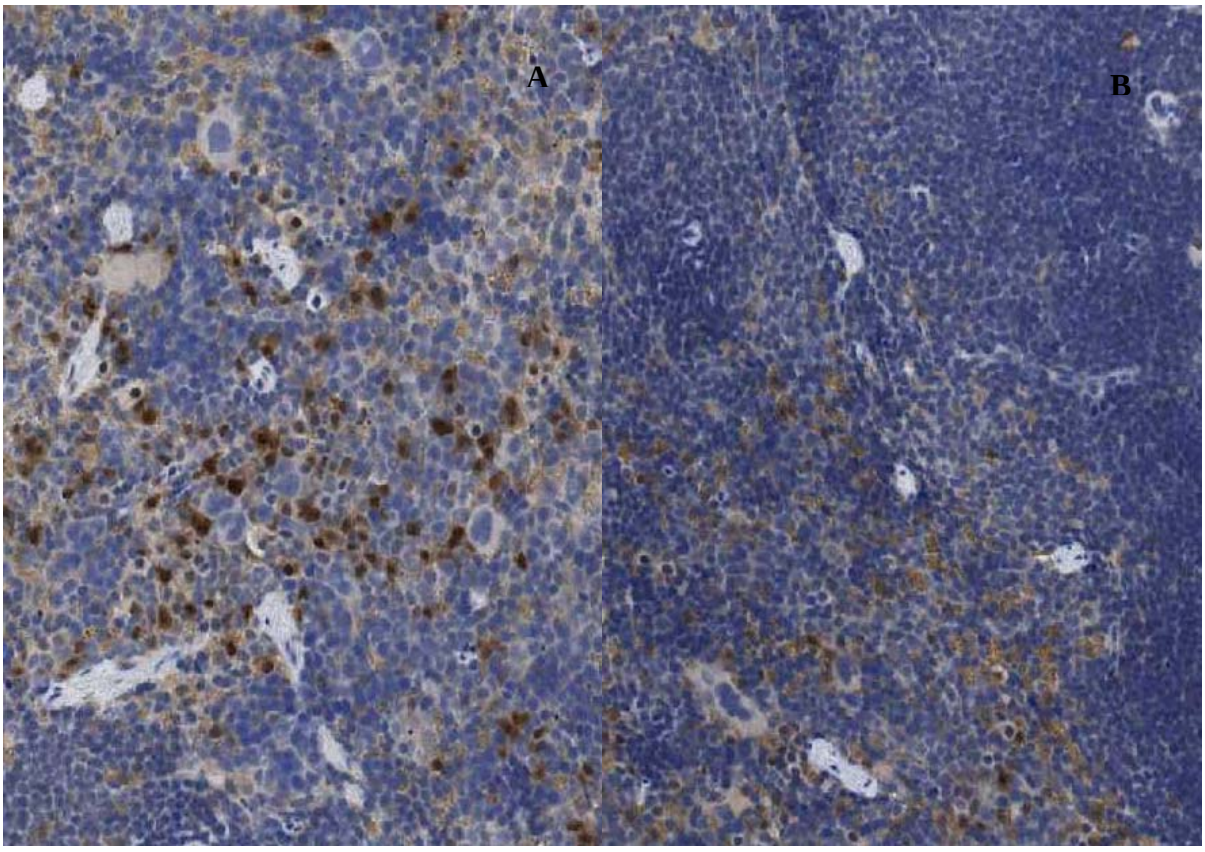

Figure 4-14. Immunohistochemical staining for hADA in the spleen of wildtype mice of the ADA-SCID strain following intravenous administration of rAAV9-hADA or PBS in Experiment 2. A.) Splenic tissue stained for hADA and derived from mouse #1383 on day 60 following administration of rAAV9-hADA. B.) Splenic tissue stained for hADA and derived from mouse #1382 on day 60 following PBS injection. Overall, though some light background staining is observed in the control tissue, a substantial number of cells stain darkly for hADA in the spleen derived from vector-injected mouse #1383. This suggests hADA expression in the murine spleen.

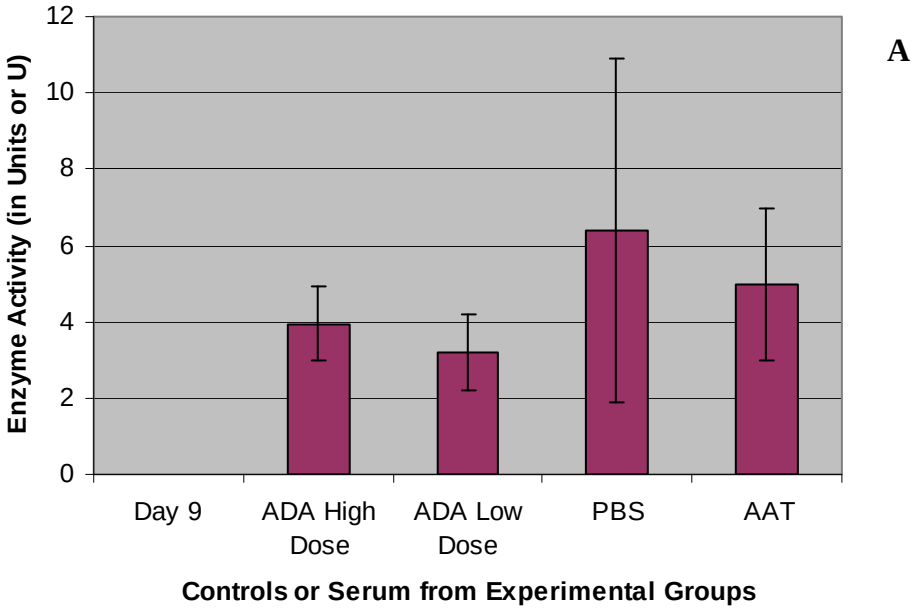

Figure 4-15. Serum enzyme activity data for Experiment 1 following intramuscular injection of rAAV1-hADA (at low or high doses of 1x10^10 vector particles or 1x10^11 vector particles, respectively), rAAV1-hAAT, or PBS. A.) Serum ADA activity (in Units, where one Unit is defined as the amount of adenosine deaminase that generates one micromole of inosine from adenosine per minute at 37 degres Celsius) measured on day 9, following intramuscular injection of rAAV1-hADA, AAT control vector, or PBS into wildtype mice of the ADA-SCID strain. At this time point, the average levels of ADA activity are higher in both control groups than the vector-injected groups. This activity pattern indicates a high degree of background ADA activity and lends little validity to the activity values observed for treated animals. B.) Map of positive control vector rAAV1-hAAT (otherwise known as pTR2-CB-AAT packaged in serotype 1 capsids)- this construct is driven by a chicken beta-actin enhance/CMV promoter (CB) and is approximately 6.7 kb in size. C.) Serum ADA activity in wildtype mice of the ADA-SCID strain on day 25 following intramuscular administration of rAAV1-hADA, AAT control vector, or PBS in Experiment 1 Although enzyme activity has increased by day 25 for the treated animals, background activity is still too high to support a conclusion of enhanced vector-driven serum ADA activity in the mice treated with rAAV1-hADA. D.) Serum Adenosine Deaminase activity measured in wildtype mice of the ADA-SCID strain on day 32 post-intramuscular administration of rAAV1-hADA, rAAV1-hAAT, or PBS in Experiment 1. At this time point, average background serum ADA activity in the control groups has dropped below that of the experimental groups for the first time. However, given the high degree of background from previous time points, the presence of increased vector-derived serum ADA activity, in the mice given rAAV1-hADA, is uncertain.

B

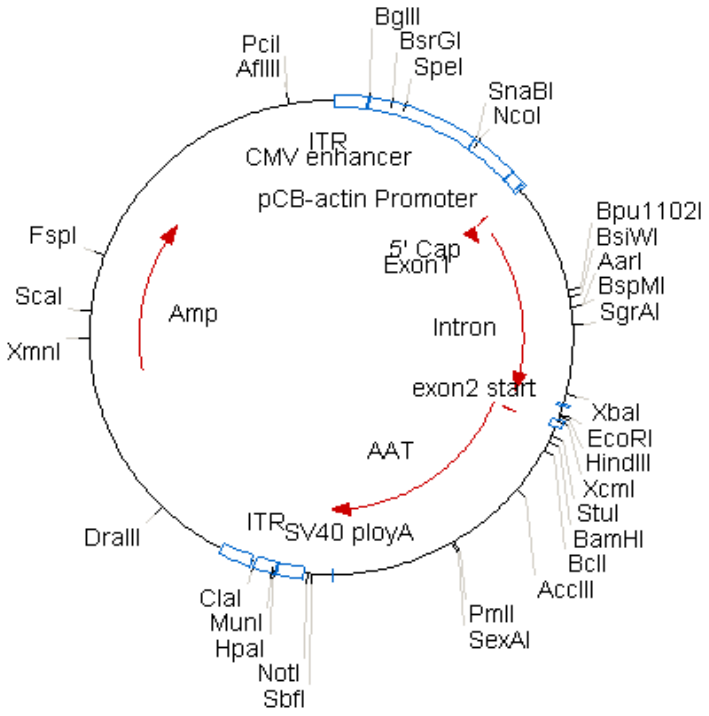

Figure 4-15. Continued

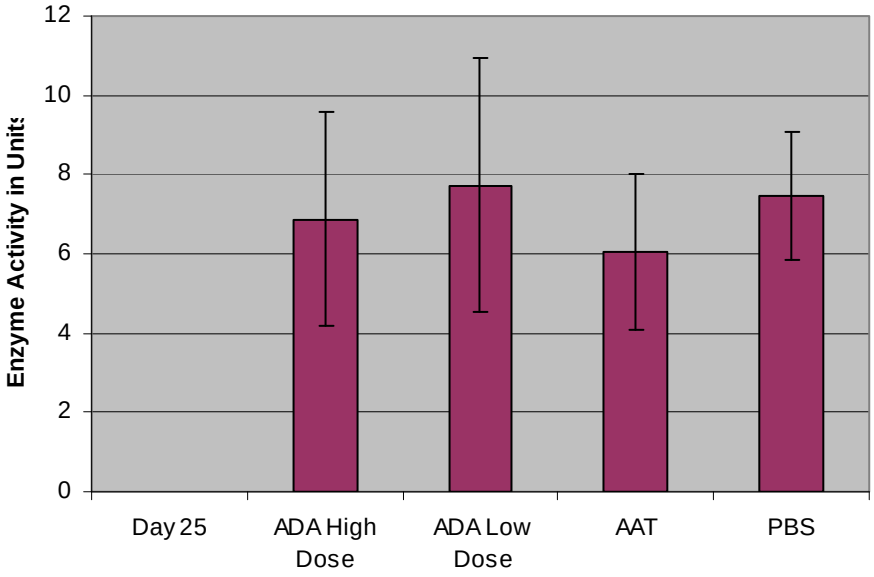

Figure 4-15. Continued

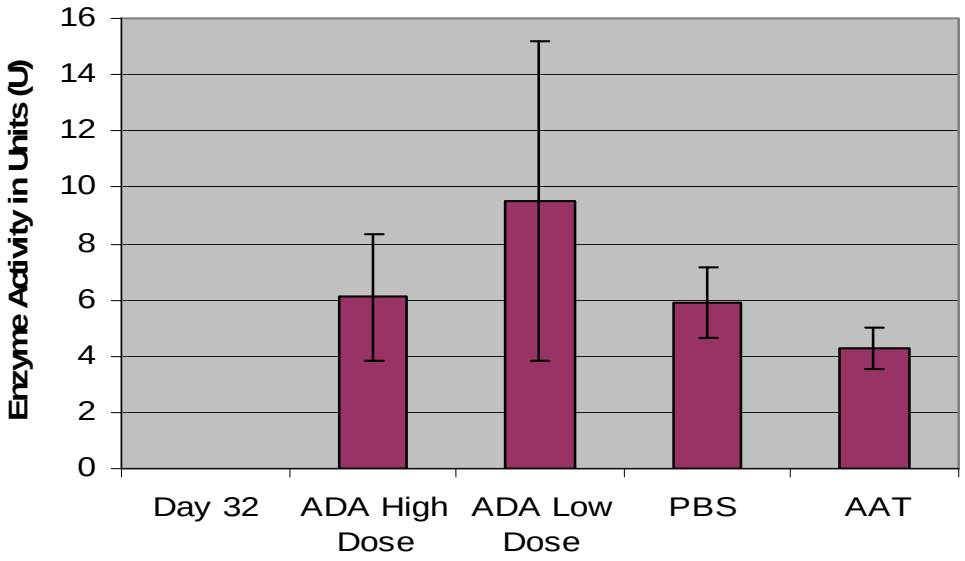

Figure 4-15. Continued

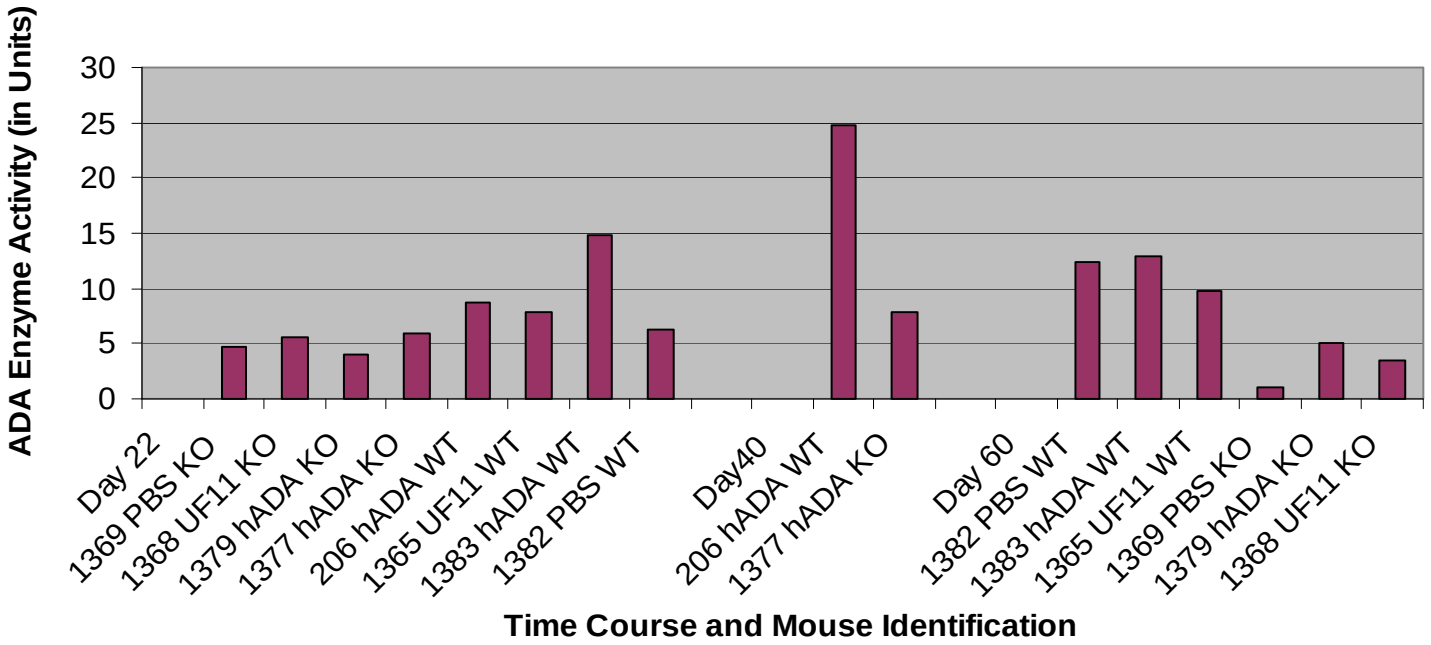

Figure 4-16. Serum ADA enzyme activity, followed over time for Experiment 2, in both knockout and wildtype mice of the ADA-SCID strain, following IV injection of rAAV9-hADA (designated by the abbreviation "hADA"), rAAV9-GFP(UF11) (designated by the abbreviation "UF11"), or lactated ringer PBS (designated by "PBS"). The serum samples for enzyme analysis were derived from the individual mice designated by the mouse identification numbers listed above. At day 22 post-vector administration, the degree of enzyme activity in knockouts given rAAV9-hADA shows no clear increase over that of controls. Interestingly, a more apparent increase in average ADA activity was observed in mice treated with rAAV9-hADA compared to controls. At day 40, two animals (#206 and #1377) were sacrificed, and average enzyme activity levels increase substantially for wildtype mouse #206 and modestly for #1377. By day 60, high background activity in the wildtype animals allow for no accurate assessment of ADA activity in the treated mouse #1383. Also, on day 60, the degree of background ADA activity remains low for control knockout animals (#1369 and #1368) and a modest increase in average ADA activity above background (and compared to day 22 values) was observed for mouse #1379 (given rAAV9-hADA). Overall, background ADA activity in wildtype animals continues to prevent an accurate evaluation of vector-driven ADA activity in treated wildtype mice. However, the degree of background ADA activity in knockout controls is relatively low and remains low throughout Experiment 2, allowing for a more accurate assessment of modest increases in serum ADA activity for mice given rAAV9-hADA.

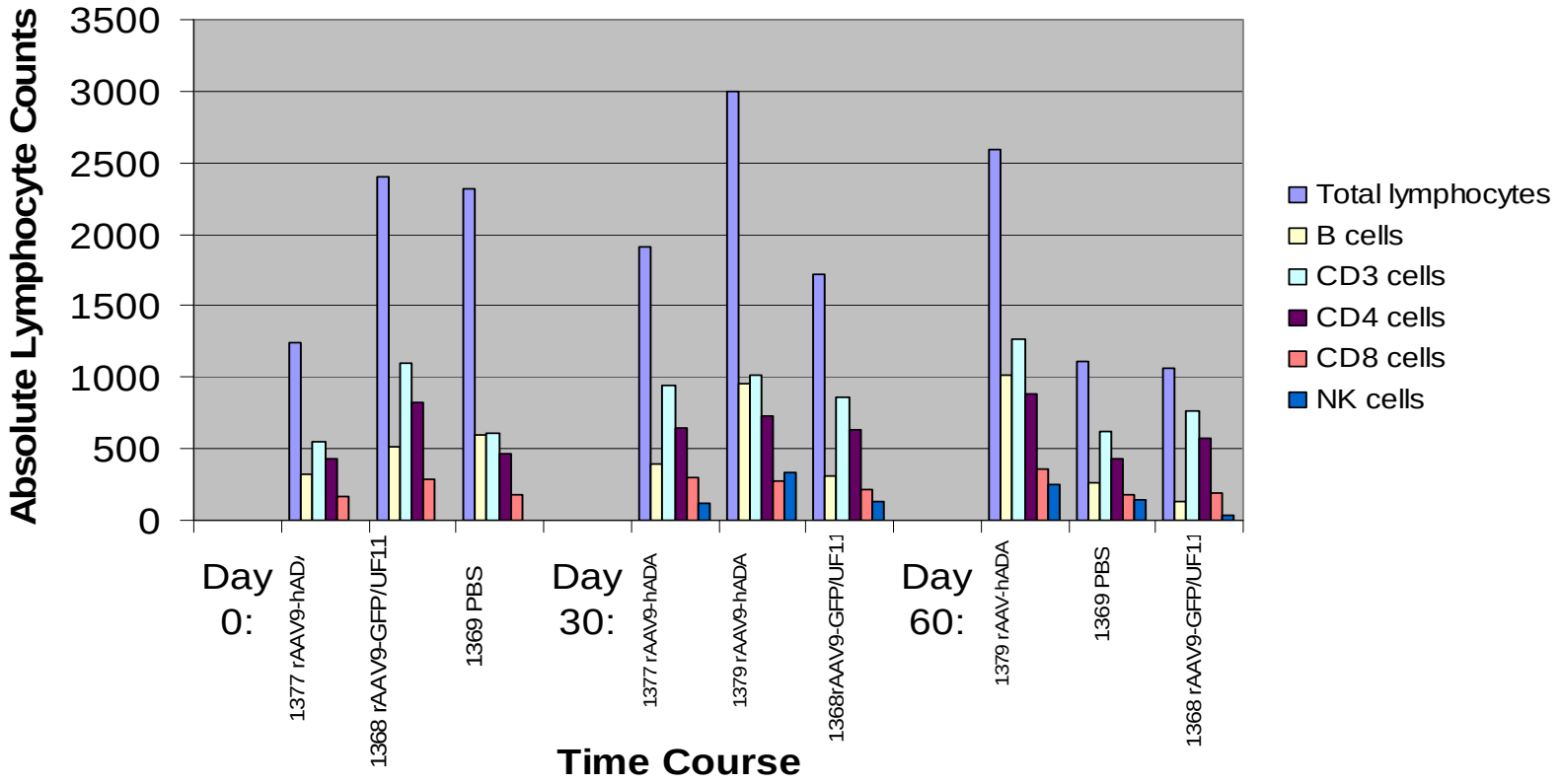

Figure 4-17. Immunological profiling over time for ADA-SCID knockout mice injected with rAAV9-hADA, rAAV9-GFP(UF11), or PBS, in Experiment 2. Similar to the immunological profiling described previously for ADA-SCID knockouts compared to their wildtype littermates, this data regarding lymphocyte populations was collected for 60 days for knockout mice administered the type 9 experimental vector, a type 9 GFP control vector, or PBS. Interestingly, just as enzyme activity increased modestly for hADA vector-treated mouse #1377, an increase in total lymphocytes as well as lymphocyte subsets by day 30 was suggested by the data. For hADA vector-treated mouse #1379, a modest increase in enzyme activity correlated with an observed modest increase in lymphocyte populations. Also, over the course of 60 days, there were observed average decreases in total lymphocyte as well as some lymphocyte subset populations for mice administered PBS or the the rAAV9-GFP control vector. Overall, although no conclusive evidence could be ascertained from this figure, the observed trends indicate a modest proliferation of lymphocytes in treated knockouts compared to controls.

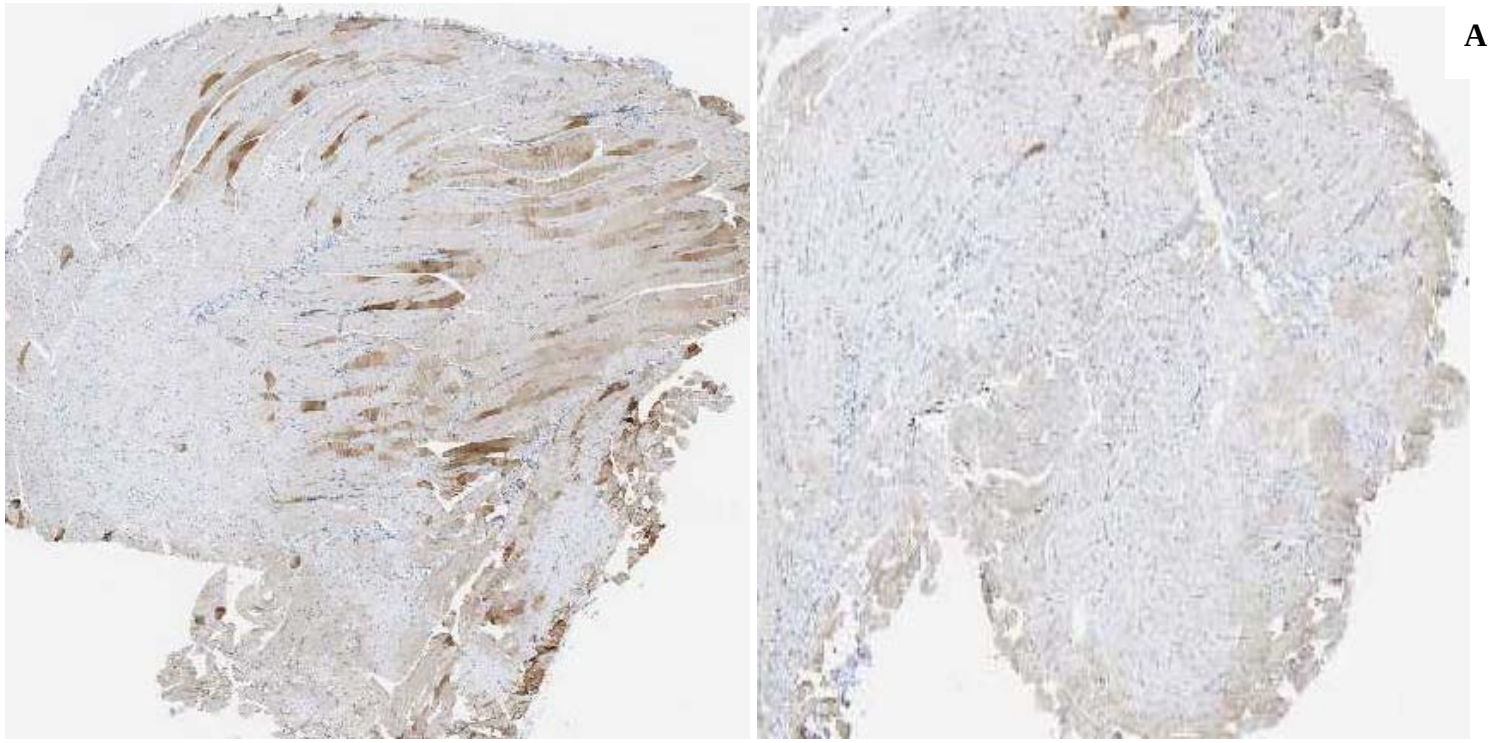

Figure 4-18. Immunohistochemical staining for hADA, and staining by hematoxylin and eosin (H&E), in murine skeletal muscle, on day 120 of Experiment 3, following intramuscular injection of rAAV1-hADA or saline. A.) Representative images of immunohistochemical staining for human adenosine deaminase (hADA) in skeletal muscle tissue of mouse#38 on day 120 following intramuscular injection of rAAV1-hADA (left1.1x) and in skeletal muscle tissue of negative control mouse #36 on day 120 following intramuscular injection of PBS (right 1.1x). B.) Representative image of H&E staining of skeletal muscle from mouse #38 on day 120 following intramuscular injection of rAAV1-hADA (1.1x). Overall, substantial hADA expression was detected in the target skeletal muscle tissue of vector-treated versus untreated mice. H&E staining revealed no visible inflammatory infiltrates in response to vector or transgene.

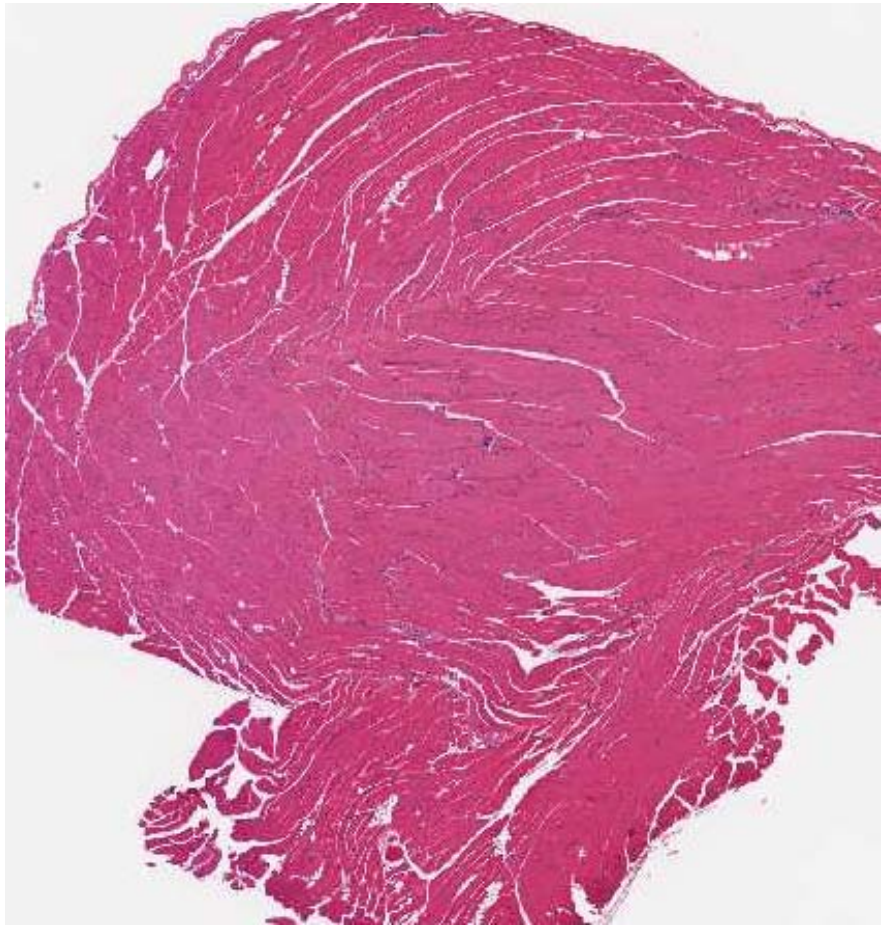

B

Figure 4-18. Continued

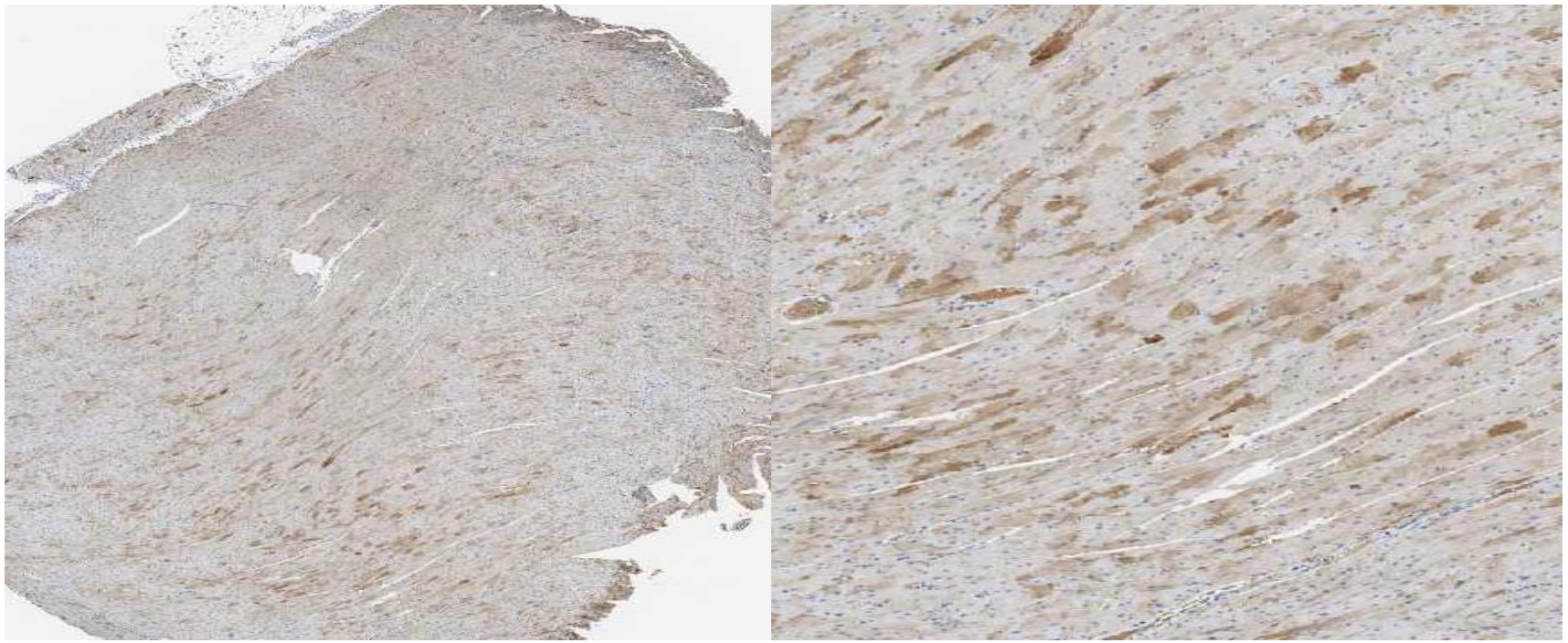

A

Figure 4-19. Immunohistochemical staining for hADA and GFP, as well as staining by H&E, of murine heart, for Experiment 3, following intravenous injection of rAAV9-hADA, rAAV9-GFP, or saline. A.) Representative images of immunohistochemical staining for human adenosine deaminase (hADA) in the cardiac muscle tissue of mouse #30 on day 120 following intravenous injection of rAAV9-hADA from Experiment 3 (1.2x(left) and 4.0x(right)). B.) Representative images of cardiac muscle harvested on day 120 post-intravenous injection of rAAV9-hADA, derived from PBS-injected negative control knockout mouse #27 from Experiment 3, and stained for hADA (1.2x (left) and 4.0x (right)). C.) Hematoxylin and Eosin staining of the cardiac muscle tissue of mouse #30 (4.0x) at day 120 post-intravenous injection of rAAV9-hADA from Experiment 3. D.) Green fluorescent protein (GFP) staining of the cardiac muscle tissue of positive control mouse #35 (4.0x) from Experiment 3 at day 120 post-intravenous injection of rAAV9-GFP. E.) Map of rAAV-GFP (green fluorescent protein) [also called rAAV-UF11], which served as a positive control vector for Experiment 3, by providing cardiac expression of GFP, driven by a chicken beta-actin enhancer and CMV promoter (abbreviated CB or CBA). Overall, a substantial degree of hADA staining was observed throughout cardiac muscle tissue in treated versus untreated knockout mice in Experiment 3. No inflammatory infiltrates were observed upon H&E staining of cardiac muscle which would indicate a host immune response to vector or transgene.

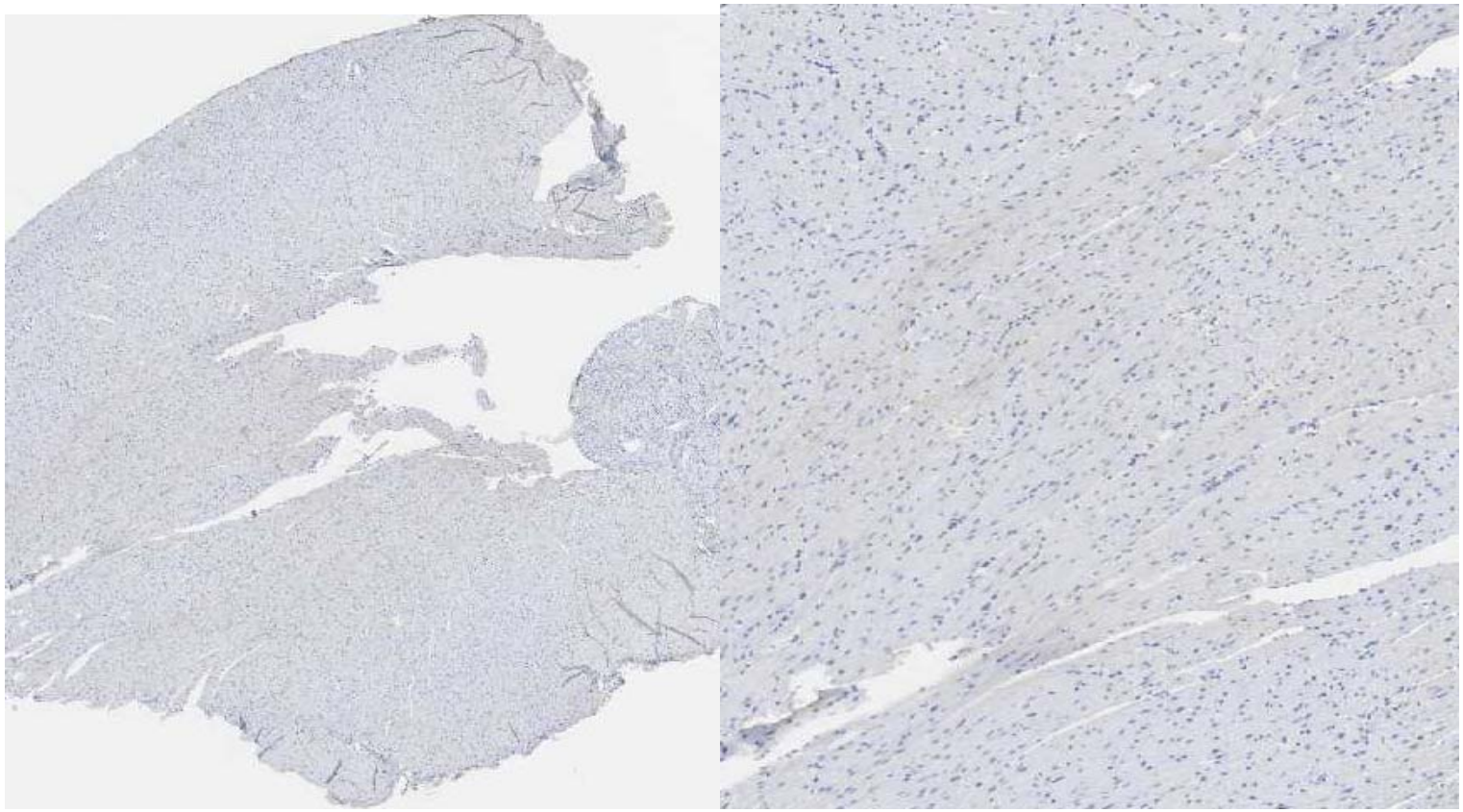

B

Figure 4-19. Continued

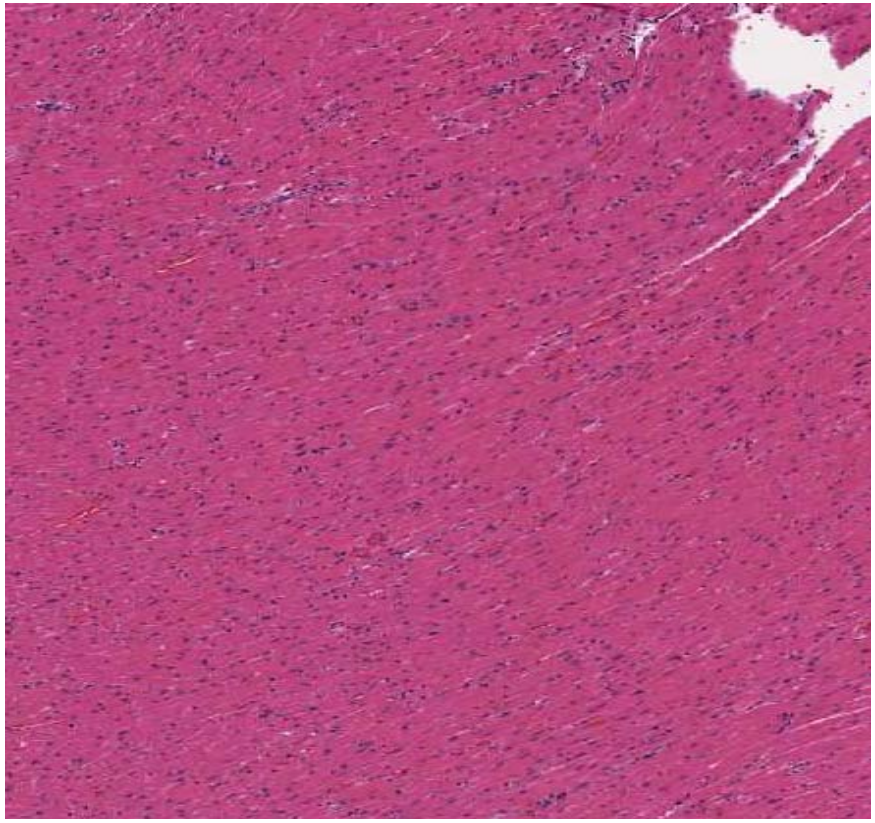

C

Figure 4-19. Continued

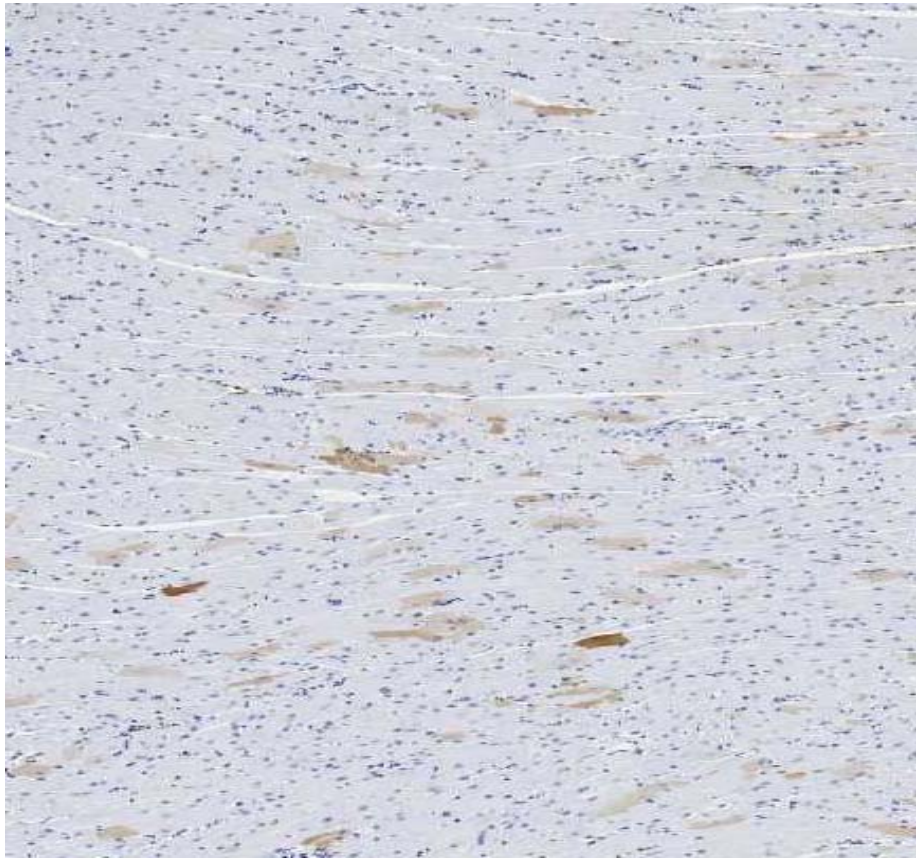

D

E

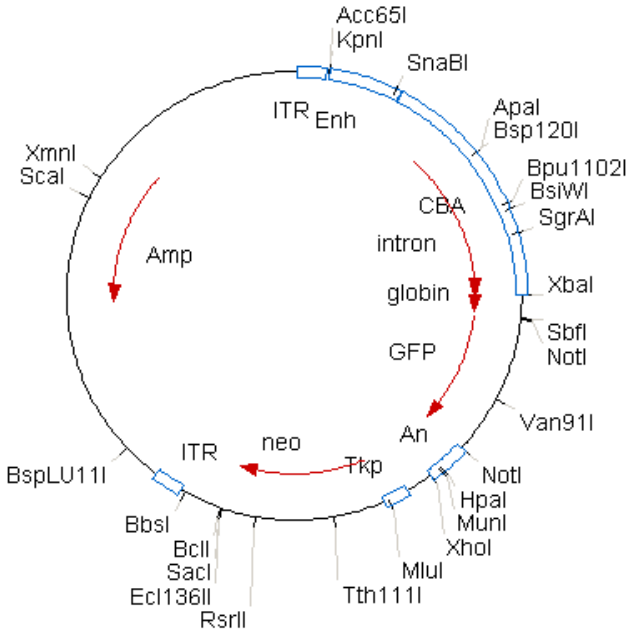

Figure 4-19. Continued

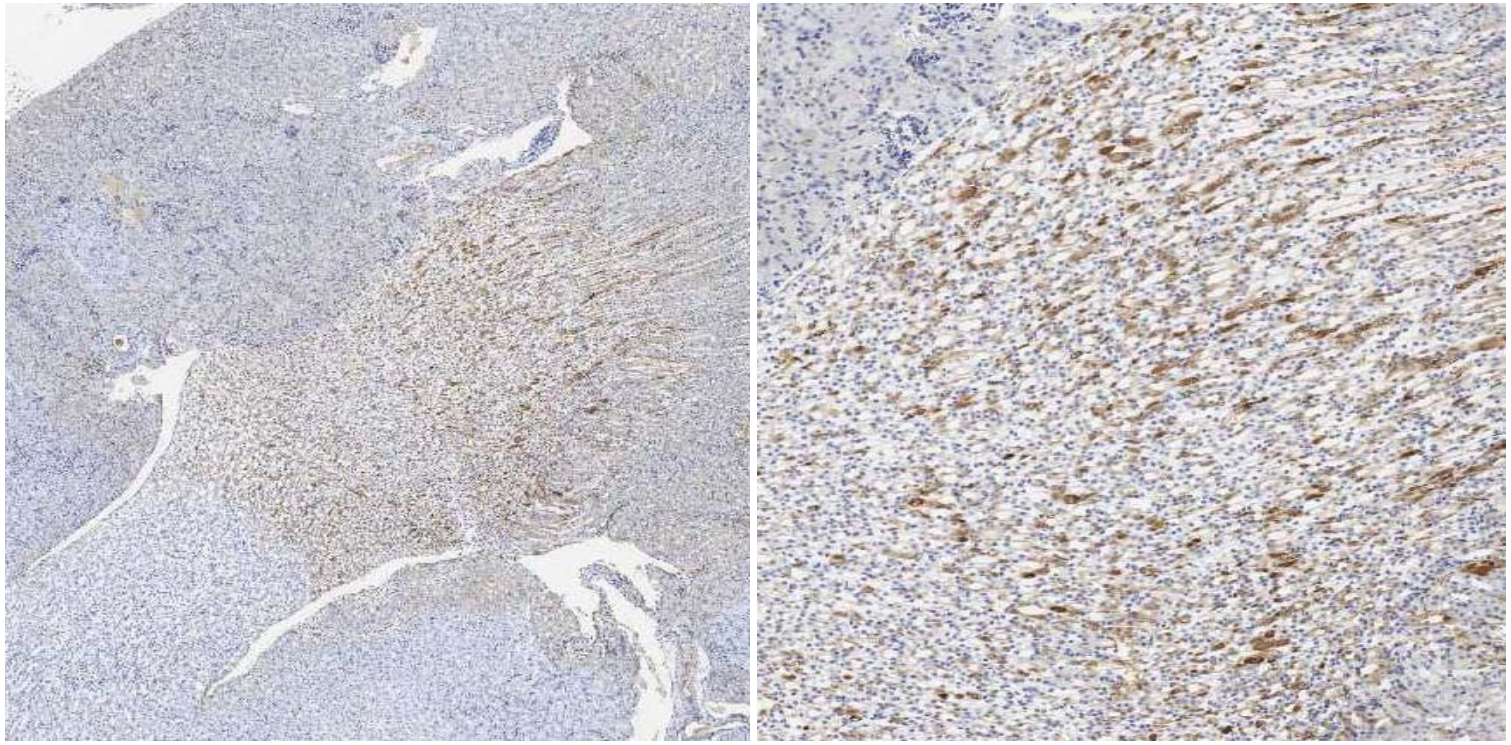

A

Figure 4-20. Immunohistochemical staining for hADA, and staining by H&E, of murine kidney tissue from ADA-SCID knockout mice of Experiment 3, following intravenous injection of rAAV9-hADA or lactated ringer. A.) Representative images of immunohistochemical staining for hADA in the kidney (renal medulla and pelvis) of mouse #40 at day 120 post-intravenous injection of rAAV9-hADA (1.8x (left) 5.4x (right)). B.) Representative images of immunohistochemical staining for hADA in the kidney (renal medulla and pelvis) of negative control mouse #27 at day 120 post-intravenous injection of PBS (1.8x (left) 5.4x (right)). C.) Representative images of Hematoxylin and Eosin staining in the kidney (renal medulla) of mouse #40 at day 120 post-intravenous injection of rAAV9-hADA (1.8x (left) 5.4x (right)). Overall, staining for hADA revealed substantial protein expression in the renal medulla of at least one vector-treated knockout compared to untreated knockouts in Experiment 3. No inflammatory infiltrate was observed upon H&E staining, indicating no inflammatory response to vector or transgene was present.

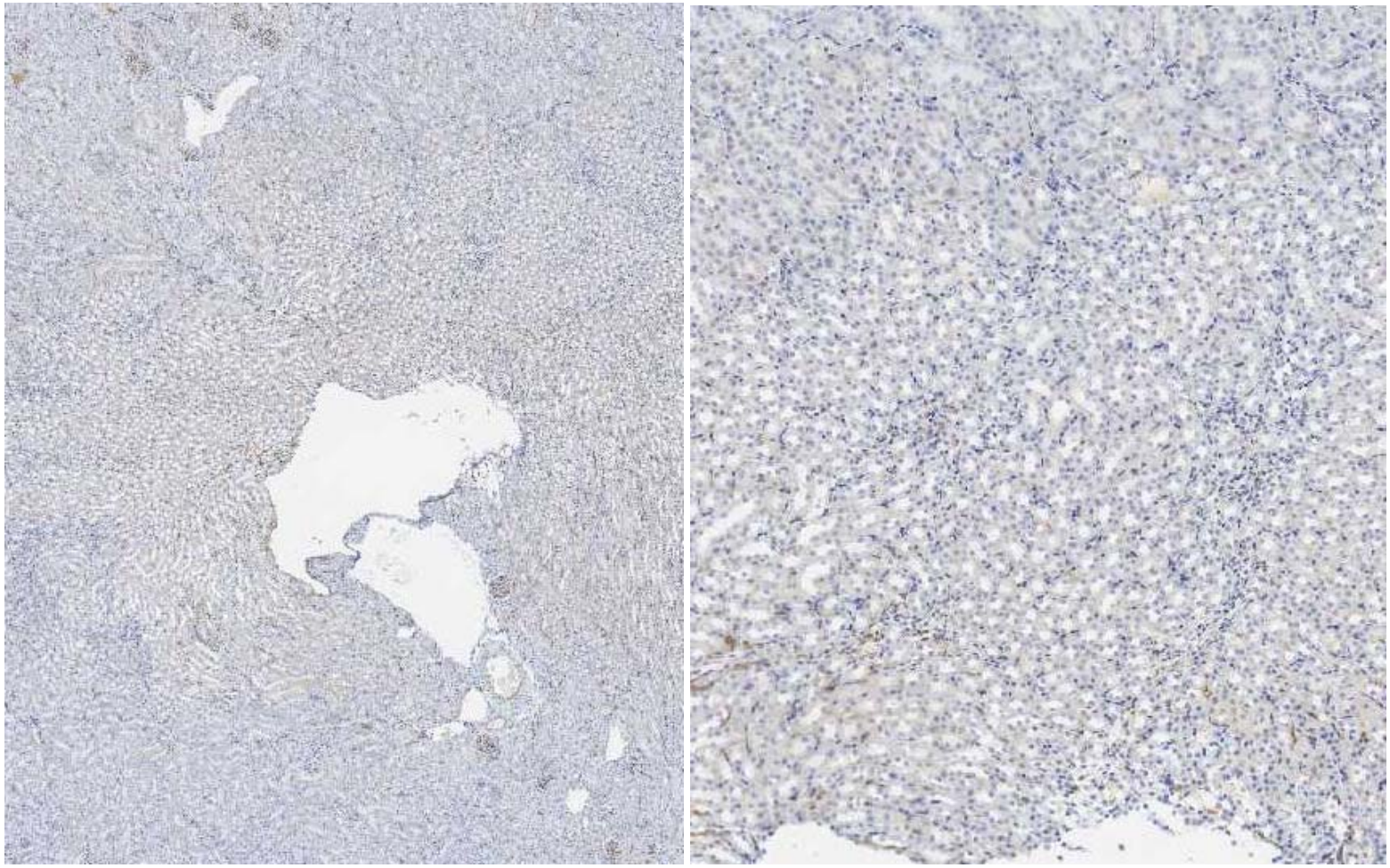

B

Figure 4-20. Continued

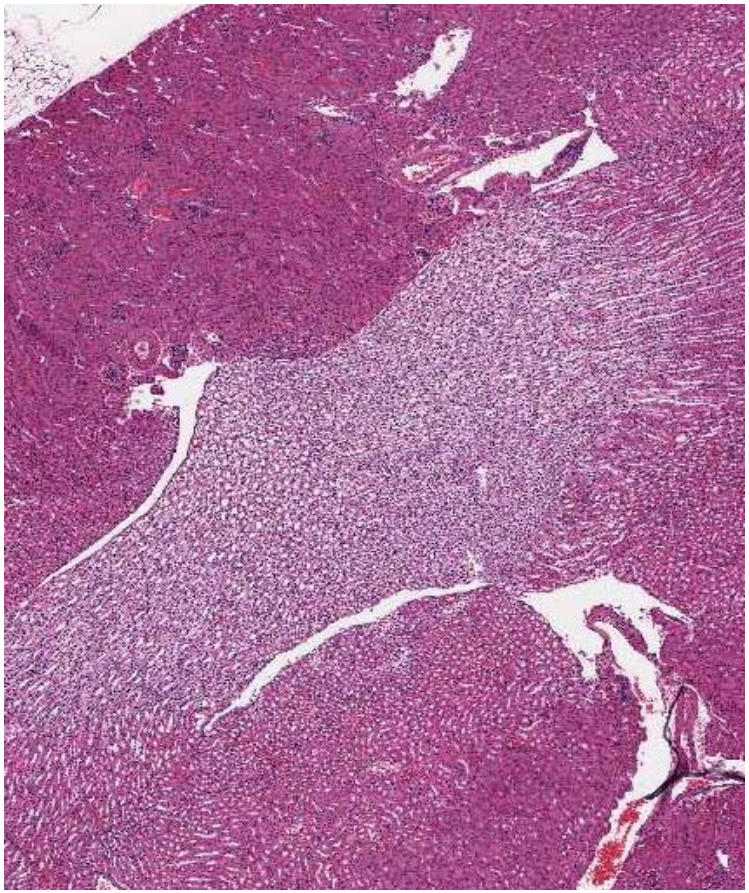

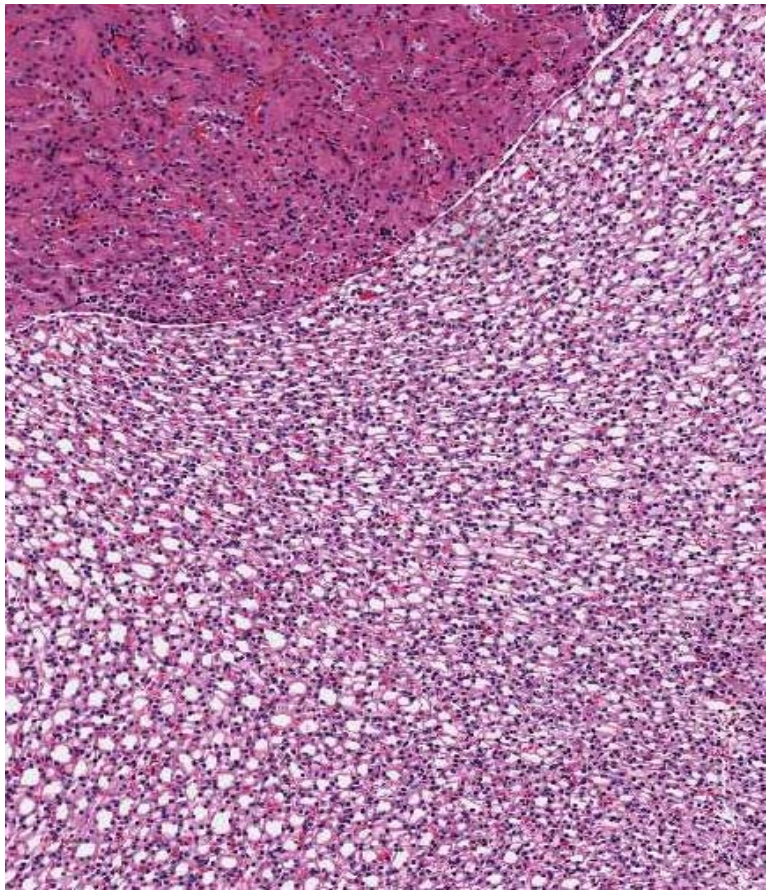

C

Figure 4-20. Continued

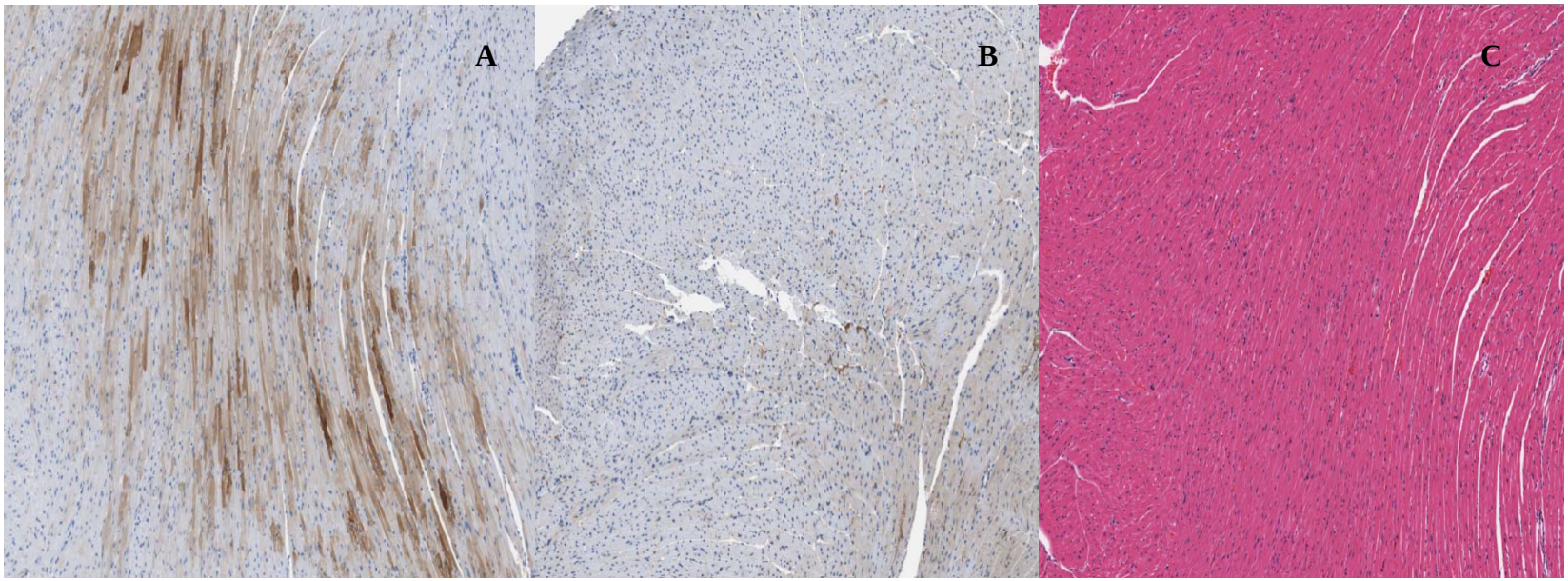

Figure 4-21. Representative images of immunohistochemical staining for hADA along with H&E staining of cardiac muscle tissue from ADA-SCID knockout mice administered rAAV9-hADA vector or lactated ringer PBS in Experiment 4. A.) Image of hADA-stained cardiac muscle obtained from mouse #186 and derived at sacrifice on day 55 post-administration of a high dose of 1x10^12 vector particles of rAAV9-hADA. B.) Image of hADA-stained cardiac muscle obtained from negative control mouse #145 and derived at sacrifice on day 55 post-administration of lactated ringer PBS. C.) Image of H&E-stained cardiac muscle obtained from mouse #186 and derived at sacrifice on day 55 post-administration of a high dose of 1x10^12 vector particles of rAAV9-hADA. Overall, consistent with observations from Experiment 3, abundant staining for hADA was detected in the cardiac muscle tissue of treated versus untreated knockout mice in Experiment 4. No inflammatory infiltrates were visible following H&E staining of cardiac muscle tissue, indicating no inflammatory response to vector or transgene was present.

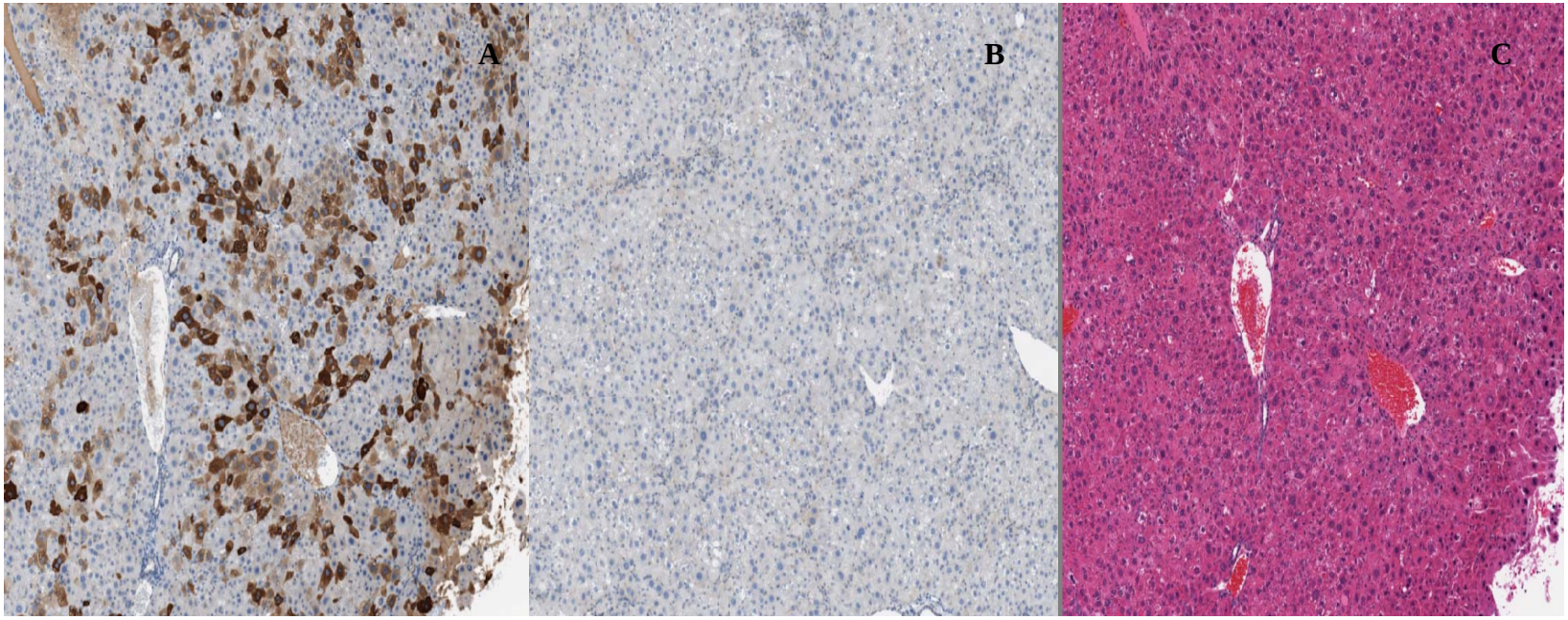

Figure 4-22. Images of immunohistochemical staining for hADA along with H&E staining of liver tissue from ADA-SCID knockout mice administered rAAV9-hADA vector or lactated ringer PBS in Experiment 4. A.) Human ADA staining of murine liver, derived from mouse #186 from Experiment 4, and harvested upon sacrifice on day 55 post-administration of a high dose of rAAV9-hADA vector (1x10^12 vector particles). B.) Human ADA staining of murine liver, derived from negative control mouse #145 from Experiment 4, and harvested upon sacrifice on day 55 post-administration of lactated ringer PBS. C.) H&E staining of murine liver, derived from mouse #186 from Experiment 4, and harvested upon sacrifice on day 55 post-administration of a high dose of rAAV9-hADA vector (1x10^12 vector particles). Overall, abundant staining for hADA was detected in the liver tissue of at least one treated knockout, compared to untreated knockouts, in Experiment 4. No inflammatory infiltrates were visible following H&E staining of liver tissue, indicating no inflammatory response to vector or transgene was present.

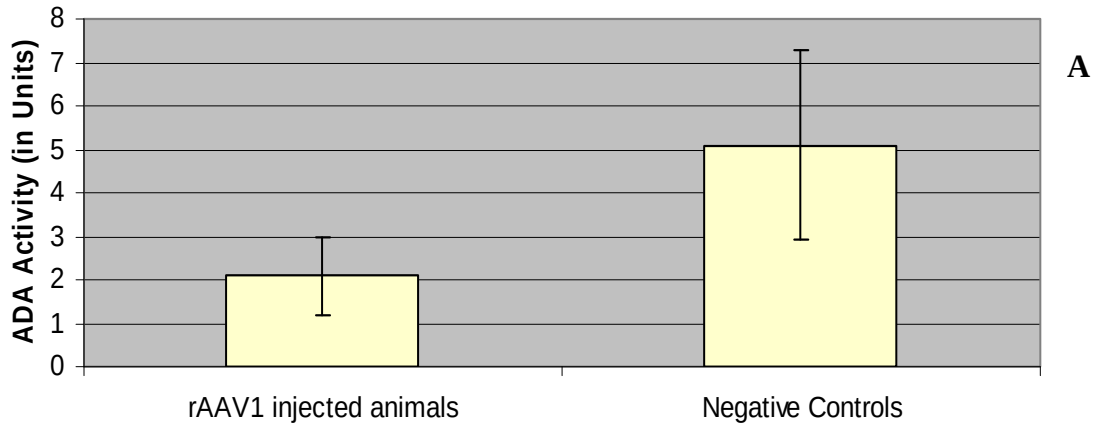

Figure 4-23. Enzyme activity in harvested mouse serum following administration of rAAV1-hADA or lactated ringer PBS to ADA-SCID knockout mice in Experiment 3. A.) Serum ADA activity on day 9 post-vector injection is low relative to that of negative control mice, indicating either a lack of vector-driven enzyme activity or a relatively high degree of background enzyme activity. B.) Observed serum enzyme activity on day 30 following rAAV1-hADA or PBS administration to ADA-SCID knockout mice. At this time point, the average level of serum enzyme activity increases approximately 3-fold, while background ADA activity from untreated mice remains relatively stable, decreasing by 1 Unit. C.) Adenosine deaminase activity found in mouse serum on day 45 following rAAV1-hADA or PBS administration to ADA-SCID knockout mice. At this final time point, enzyme activity in the mouse serum of treated animals decreases, while enzyme activity for the untreated animals remains stable at approximately 4 Units. Overall, this time-couse study suggests a trend of increasing and decreasing levels serum ADA activity in treated versus untreated knockout mice, which may parallel cycles of enzyme synthesis and degradation in the treated mice. However, given the large standard deviations, the observed trend is not statistically significant.

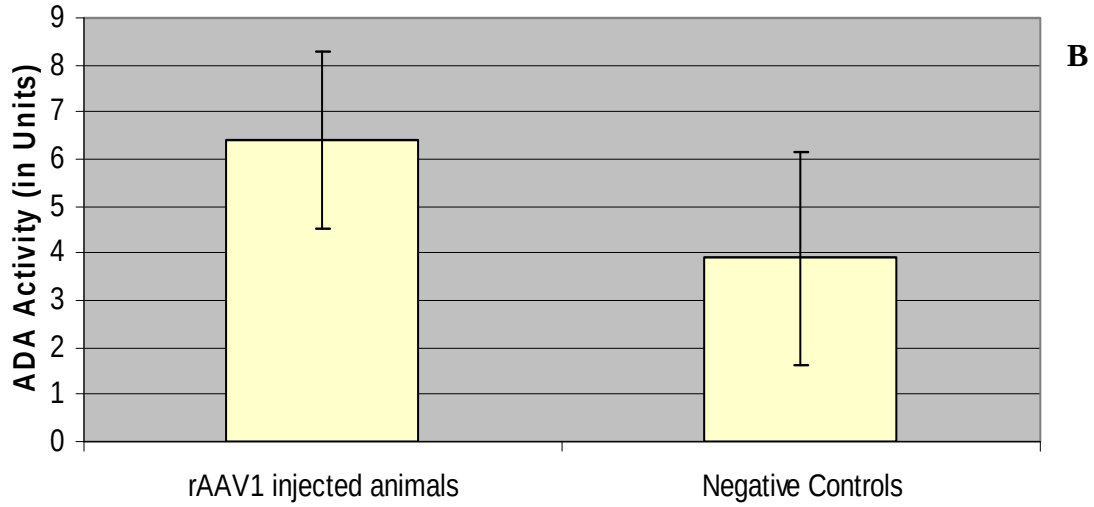

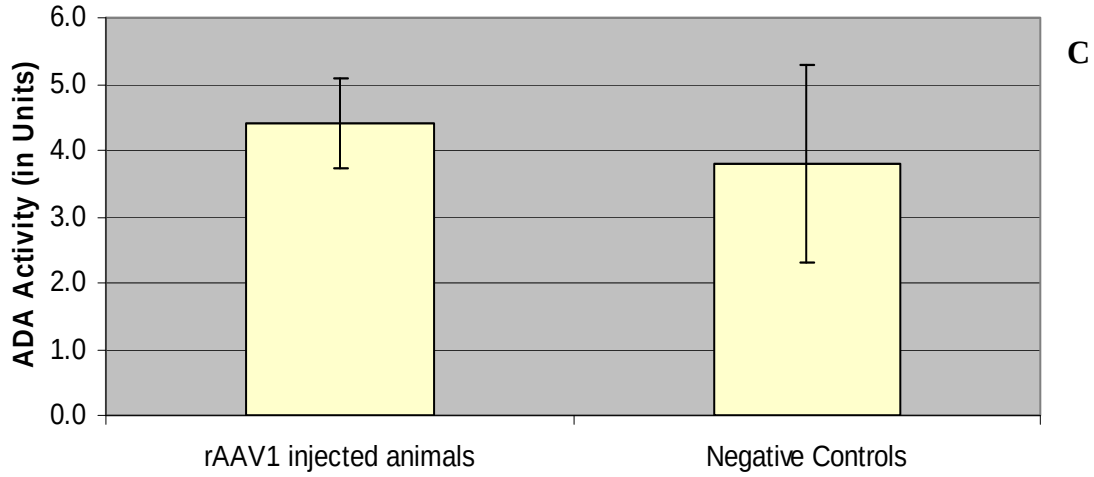

Figure 4-23. Continued

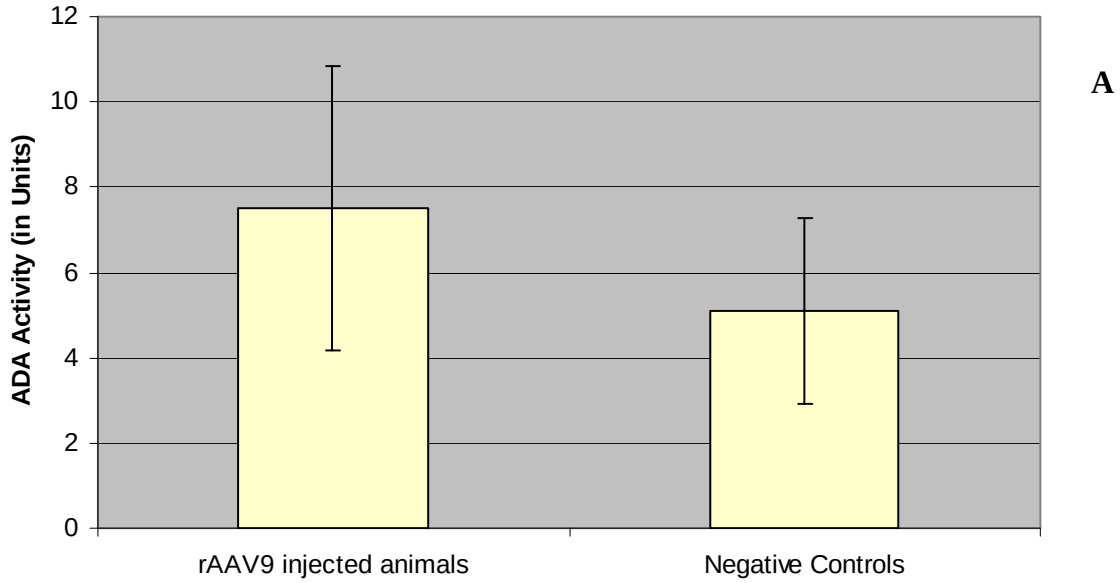

Figure 4-24. Serum enzyme activity following rAAV9-hADA or lactated ringer PBS administration to ADA-SCID knockout mice in Experiment 3. A.) Human adenosine deaminase activity in mouse serum on day 9 following vector or PBS injection. At this time point, the average level of enzyme activity is 2-3 Units higher in treated versus untreated knockout mice. B.) Adenosine deaminase activity on day 30 following rAAV9-hADA or PBS administration to ADA-SCID knockout mice. At this time point, the average level of ADA activity decreases in the treated mice, though enzyme activity remains relatively stable in the untreated mice. C.) Observed serum enzyme activity on day 45 following administration of rAAV9-hADA vector to ADA-SCID knockout mice. On day 45, though the average level of ADA activity continues to remain stable at approximately 4 Units for untreated mice, average enzyme activity increases to about 8 Units in treated mice. Overall, this time-couse study suggests a trend of increasing and decreasing levels serum ADA activity in treated versus untreated knockout mice, which may parallel cycles of enzyme synthesis and degradation in the treated mice. However, given the large standard deviations, the observed trend is not statistically significant.

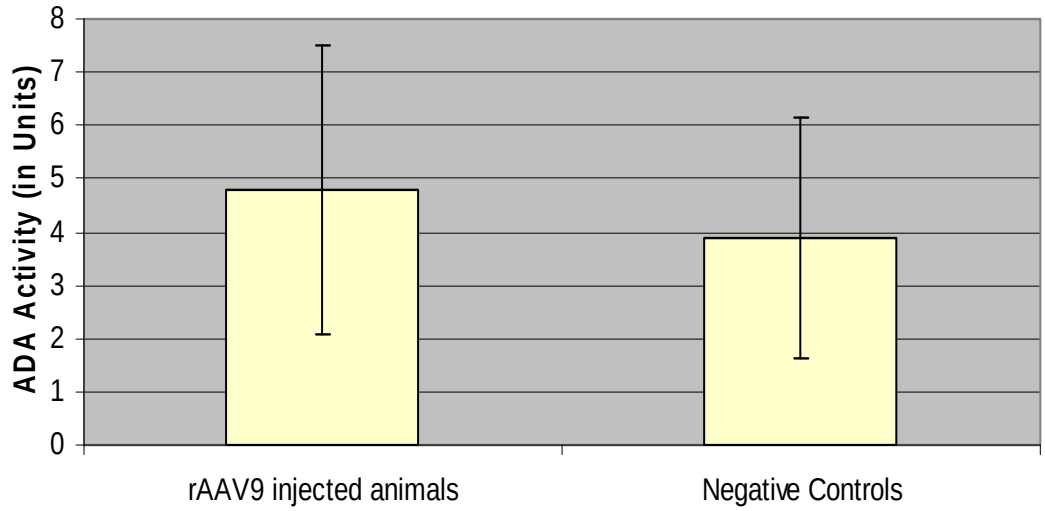

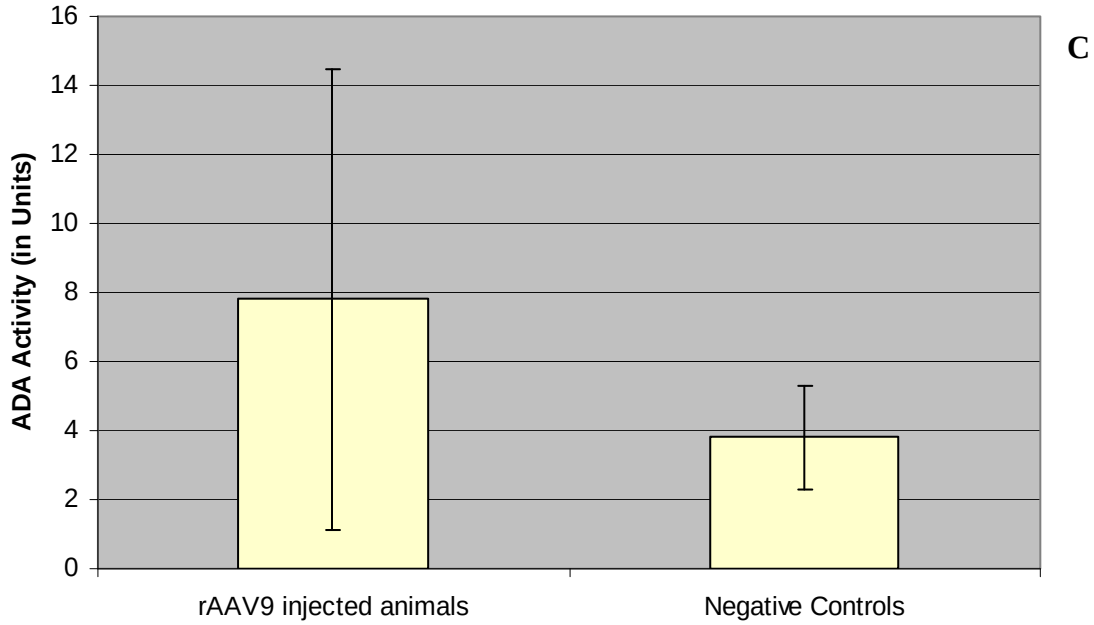

Figure 4-24. Continued

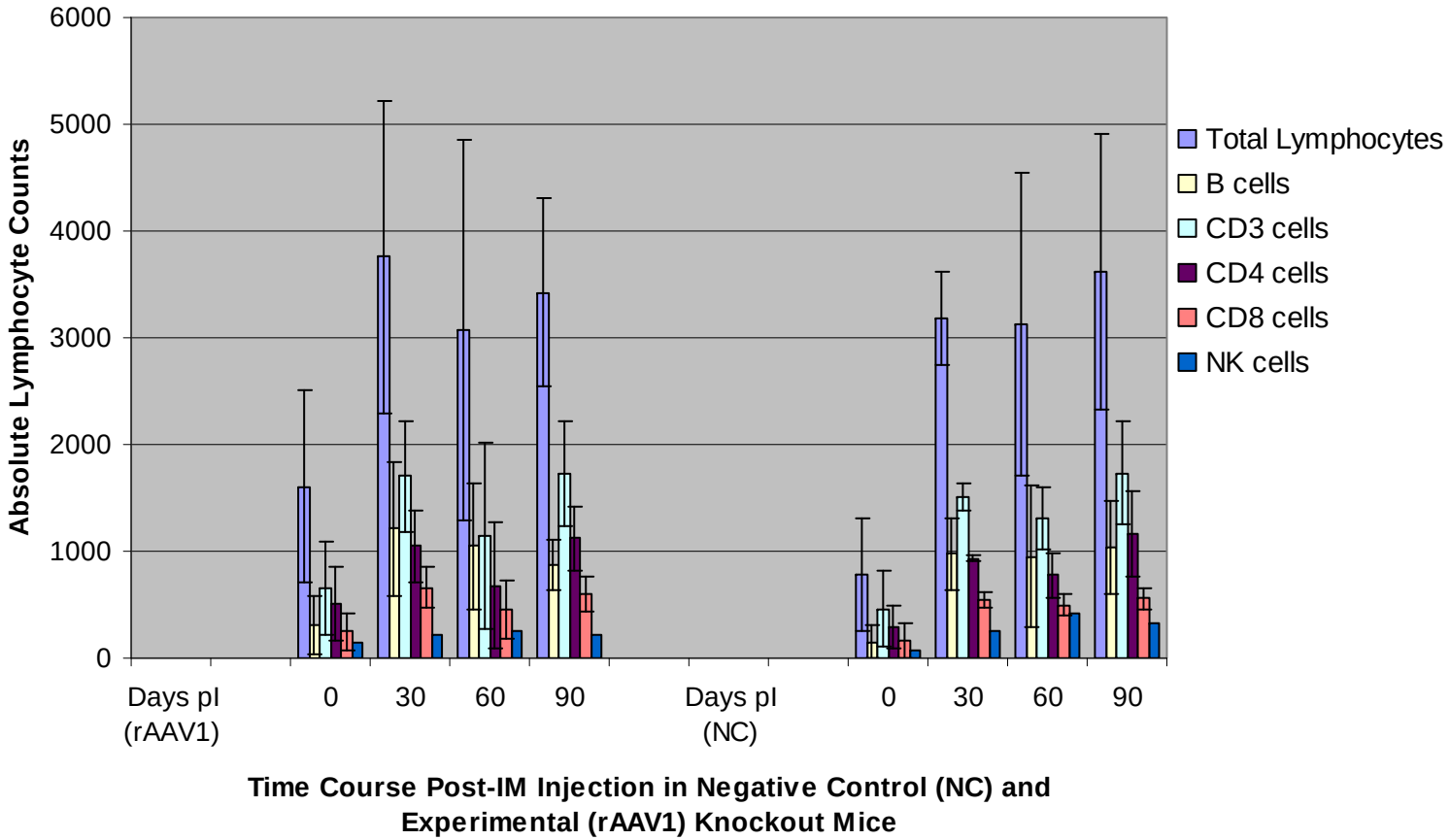

Figure 4-25. Lymphocyte populations followed over a 90-Day Time Course Following IM Injections of rAAV1-hADA or lactated ringer PBS in ADA-SCID Knockout Mice. The left half of the above figure follows total lymphocyte and lymphocyte subset populations at monthly time points post-injection of rAAV1-hADA into knockout mice. The right half of the above figure follows the same lymphocyte populations for untreated knockout mice administered PBS. Overall, a comparison of lymphocyte populations in the treated versus the untreated knockout mice reveals no positive trend toward lymphocyte proliferation in the treated group.

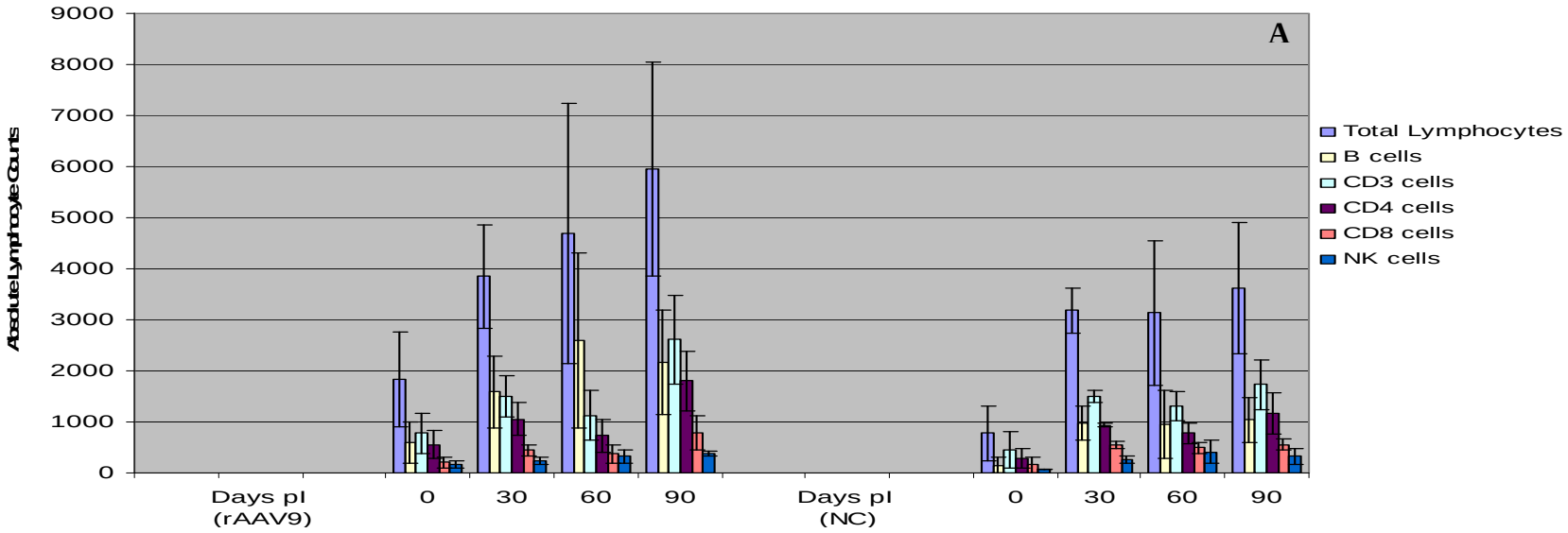

Figure 4-26. Lymphocyte proliferation following IV injections of rAAV9-hADA vector or lactated ringer PBS in ADA-SCID knockout mice from Experiment 3. A.) Total lymphocyte and lymphocyte subset counts, followed over 90 days, at 30 day intervals, in knockout mice administered rAAV9-hADA by intravenous injection (labeled "rAAV9"), are shown on the left half of the diagram. Equivalent lymphocyte populations, at equivalent time points, in negative control knockout mice administered PBS (labeled "NC), are shown on the right half of the figure. Interestingly, a positive, progressive trend in total lymphocytes as well as lymphocyte subset populations was observed in the treated versus the untreated knockout mice. B.) Total lymphocyte counts, followed over time, and following injection of vector or PBS, show a positive, progressive, increasing trend for the treated animals relative to the untreated animals. C.) B cell counts, followed over time, and following injection of vector or PBS, show a positive trend at most time points, for the treated animals relative to the untreated animals. Though the average B cell counts decrease by day 90 for treated animals, they are still substantially higher than the B cell counts of untreated mice. D.) CD3+ cell counts, followed over time, and following injection of vector or PBS, show a positive trend over the 90-day experiment, for the treated animals relative to the untreated animals. E.) CD4+ cell counts, followed over time, and following injection of vector or PBS, show a positive trend over the 90-day experiment, for the treated animals relative to the untreated animals. F.) CD8+ cell counts, followed over time, and following injection of vector or PBS, show a positive trend over the 90-day experiment, for the treated animals relative to the untreated animals. G.) NK cell counts, followed over time, and following injection of vector or PBS, show a steady, but weaker, positive trend over the 90-day experiment for the treated relative to the untreated animals.

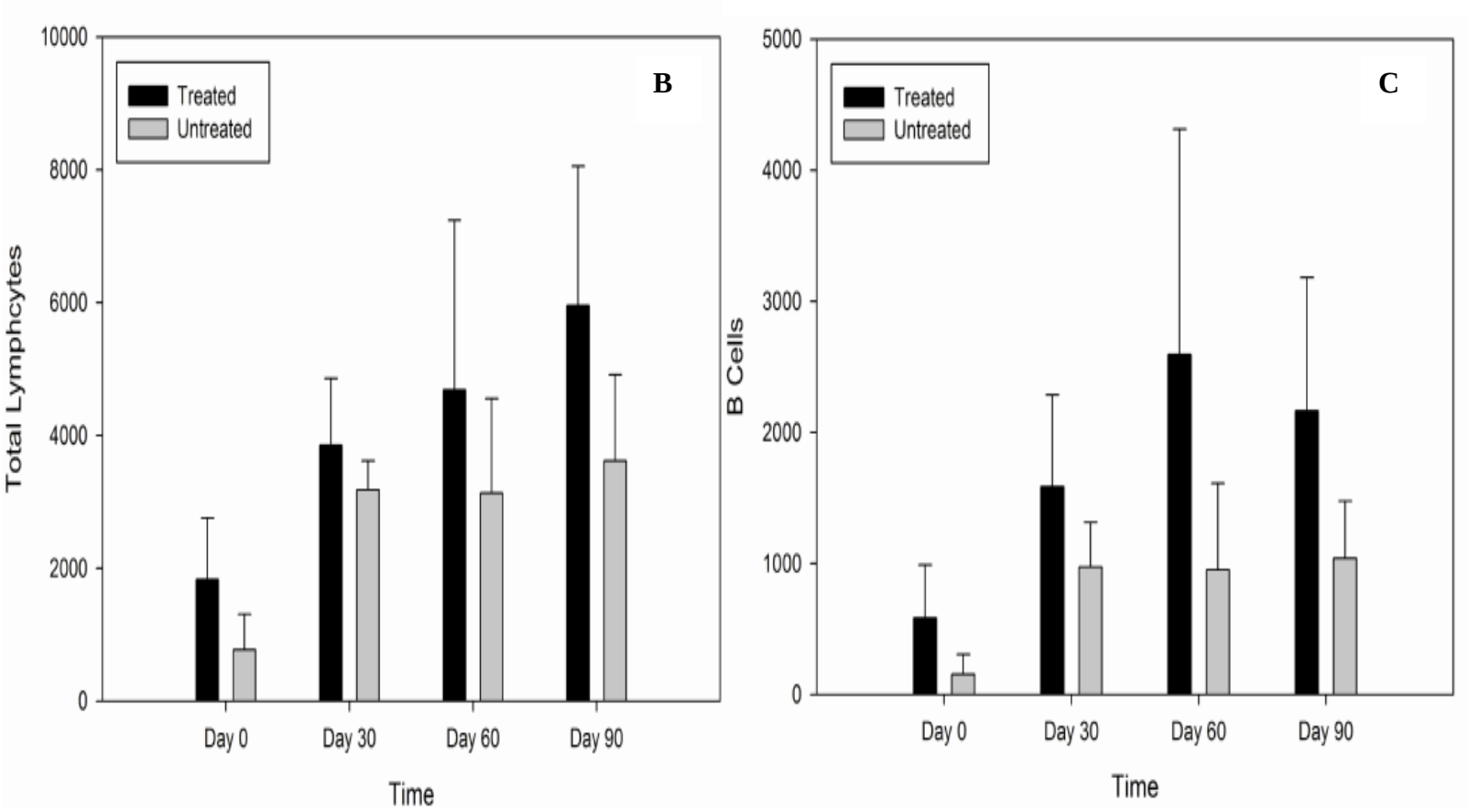

Figure 4-26. Continued

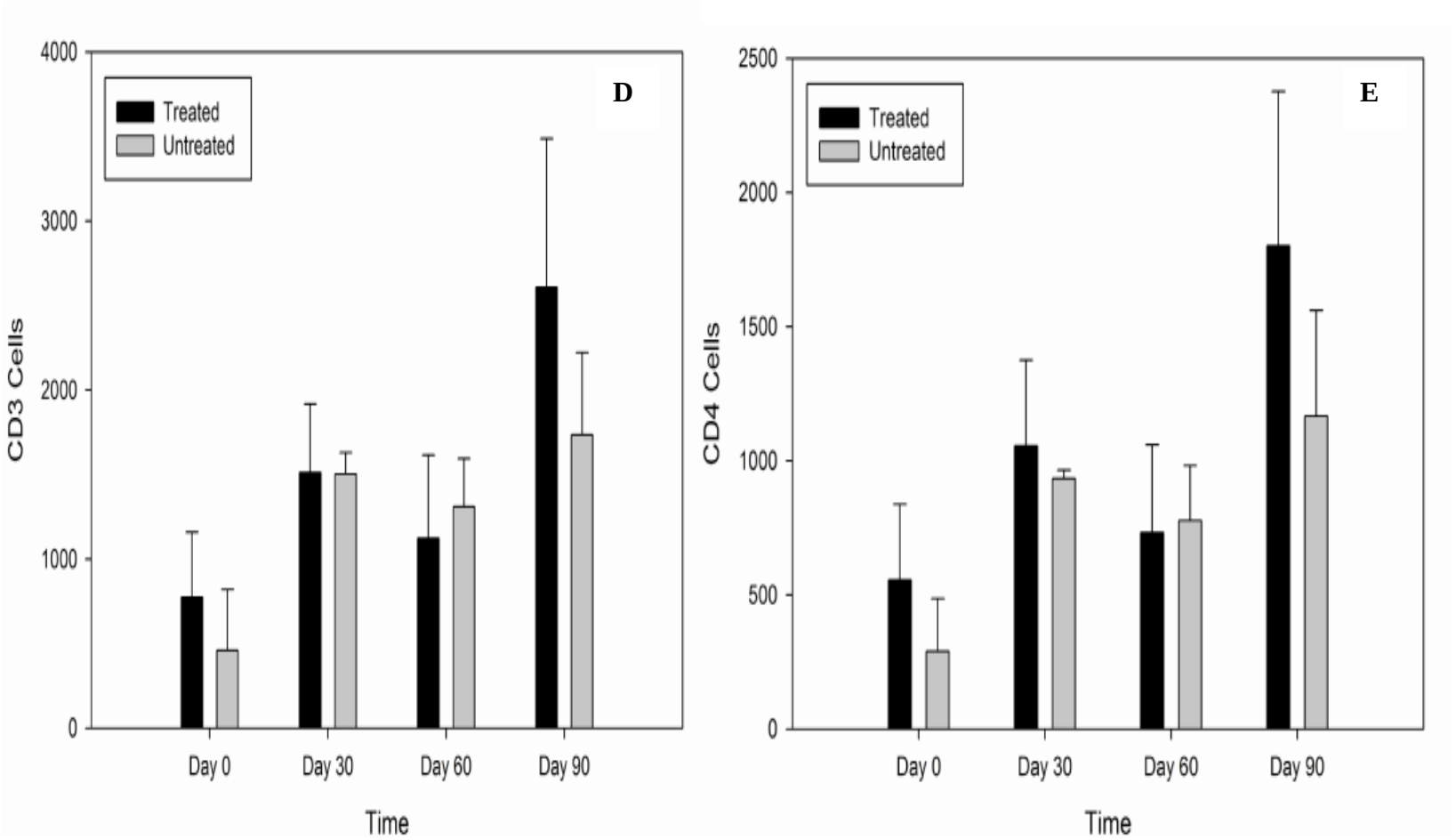

Figure 4-26. Continued

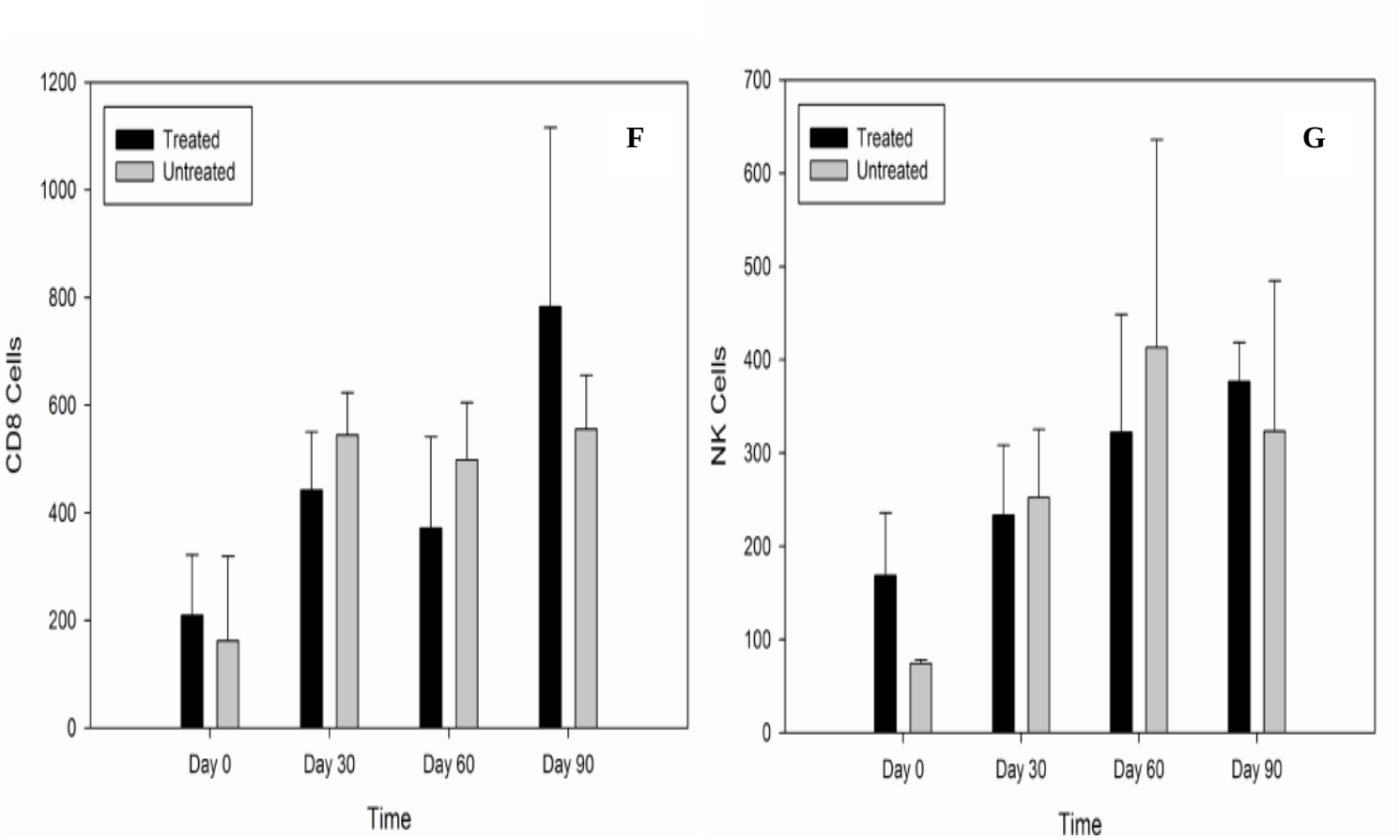

Figure 4-26. Continued

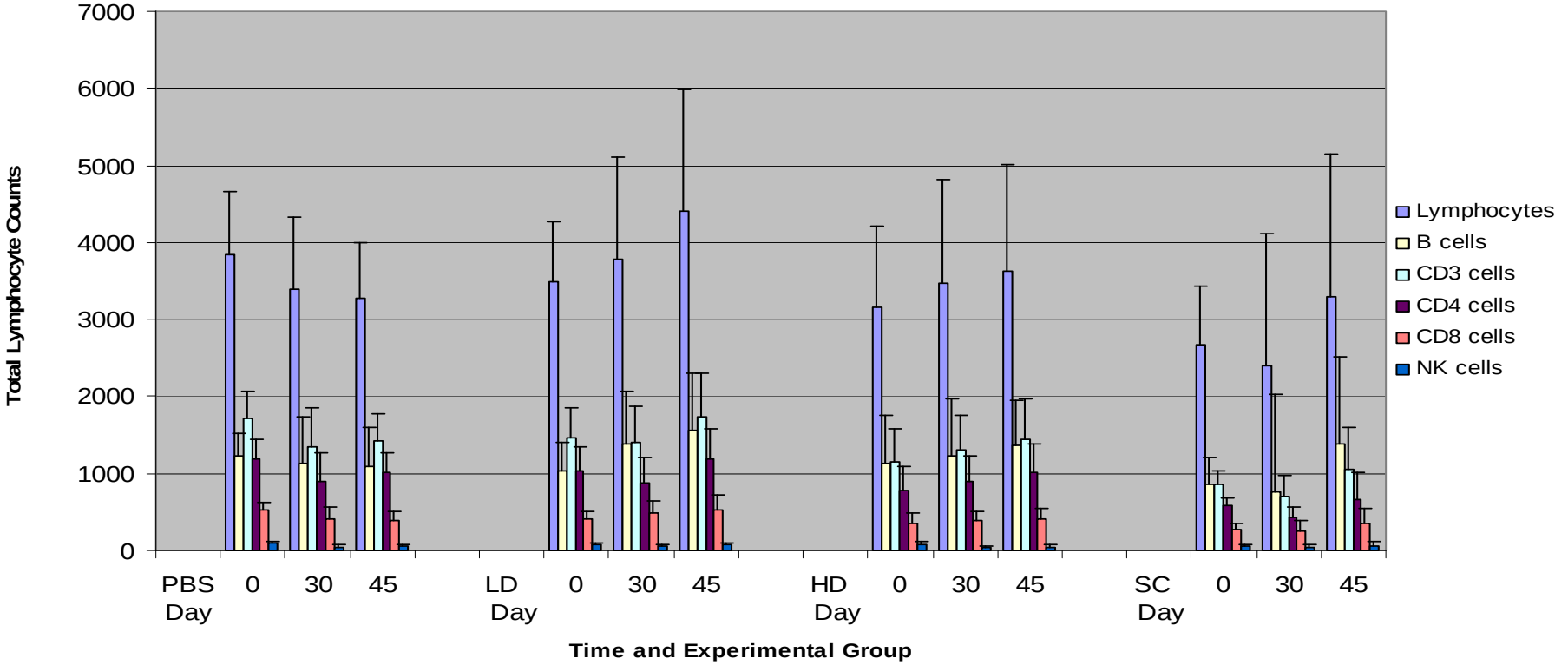

Figure 4-27. Total lymphocyte and lymphocyte subset counts followed for 45 days post-vector injection, during Experiment 4, in knockout mice administered by intravenous injection either PBS, single-stranded rAAV9-hADA vector by low dose ("LD"- 3x10^11 vector particles), single-stranded rAAV9-hADA vector by high dose ("HD"-1x10^12 vector particles) , or self-complementary rAAV9-hADA vector (3x10^11 vector particles). Interestingly, the PBS-injected, untreated knockout mice demonstrated modest decreases or stability in lymphocyte populations over time. All other groups of treated knockout mice, administered either single-stranded or self-complementary rAAV9-hADA vector, showed modest, steady increases in average lymphocyte counts over time. Though not statistically significant, the data shown in the above figure was gathered relatively early in Experiment 4. Flow cytometry and CBC analyses at later time points (approximately day 100 and day 150 post-vector or PBS injection) will determine if the observed trends hold and become statistically significant.

Table 4-1. Gene delivery data following rAAV1-hADA vector administration to wildtype, non-immune deficient mice of the ADA-SCID strain of interest for Experiment 1. The background vector copy numbers, or, in effect, negative control values, for negative control tissues, derived from PBS-injected wildtype mice of the ADA-SCID strain are on average relatively low. By contrast, vector copy number in the skeletal muscle of positive control wildtype mice of the ADA-SCID strain administered rAAV1-hAAT, which may be called positive control values, are on average relatively high. These values indicate substantial gene delivery is possible for type 1 vector in this particular mouse model. Lastly, while the vector copy number values are low in the skeletal muscle tissues of wildtype mice administered the low dose of rAAV1-hADA, some substantial gene delivery was detected in skeletal muscle for wildtype mice administered the high dose of rAAV1-hADA, compared to the average degree of background in the negative control, PBS-injected mice.

	Vector/				#Vector Genomes per microgram DNA per tissue:		
Mouse ID	PBS	Dose (#vector particles)	Day of Sacrifice	Genotype	Spleen	Liver	Skeletal Muscle: Quadriceps
1352	rAAV1-hADA	High	60	WT	32	229	1067
1353	rAAV1-hADA	High	60	WT	4	53	89
1356	rAAV1-hADA	High	60	WT	2	636	1205
1358	rAAV1-hADA	Low	60	WT	1	18	470
1359	rAAV1-hADA	Low	60	WT	6	12	
1363	rAAV1-AAT	1x10^11	60	WT	1	12	5737
1583	PBS	100 microliters	60	WT	0	11	6
1587	PBS	100 microliters	60	WT	0	3	273
1592	rAAV1-hADA	Low	60	WT	0	41	202
1598	rAAV1-hAAT	1x10^11	60	WT	1	13	403294
1599	rAAV1-hAAT	1x10^11	60	WT	0	9	801
	High dose is 1x10^11 vector particles						
	Low dose is 1x10^10 vector particles						

Table 4-2. Gene delivery data following rAAV9-hADA vector administration to both ADA-SCID knockout mice and their wildtype littermates in Experiment 2. The background vector copy numbers, or, in effect, negative control values, for negative control tissues, derived from PBS-injected wildtype mice of the ADA-SCID strain, are zero. By contrast, vector copy numbers in the kidney, spleen, pancreas, liver, heart, and skeletal muscle of positive control wildtype and knockout mice of the ADA-SCID strain, administered rAAV9-GFP(UF11), which also may be called positive control values, are high. These values indicate abundant gene delivery is possible for type 9 vector in this particular mouse model. Lastly, abundant gene delivery was detected for all types of tissue in both knockout and wildtype mice administered rAAV9-hADA, compared to background in the negative control, PBS-injected mice.

	Vector			#Vector Genomes per microgram DNA per tissue:						
Mouse ID	PBS	Day of Sacrifice	Genotype	Kidney	Spleen	Pancreas	Liver	Heart	Thymus	Skeletal Muscle: Quadriceps
1368	rAAV9-GFP (UF11)	60	knockout	9655	28270	6122	91619	13263		38942
1369	PBS	60	knockout	0	0	0	0	0	0	0
1379	rAAV9-hADA	60	knockout	11275	12974	3254	19752	14596	32203	55222
1365	rAAV9-GFP (UF11)	60	wildtype	43578	216825	12820	1568907			2505
1382	PBS	60	wildtype	0	0	0	0	0	0	0
1383	rAAV9-hADA	60	wildtype	7878	75835	243	129805	42191		174
1377	rAAV9-hADA	40	knockout	6665	49232	1842	2739	15234	43770	4041
206	rAAV9-hADA	40	wildtype	3084	199563	3991	14091	34344	1970	2535

Table 4-3. Supplement to Figure 4-16, providing the enzyme activity values in response to administration of rAAV9-hADA, rAAV9-GFP(UF11), or PBS for Experiment 2. The trends observed in the table below are described in the text as well as in the Figure 4-16 legend.

Time Point/Mouse ID	ADA Activity (in Units)
Day 22	
1369 – KO	4.73
1368 UF11 KO	5.64
1379 hADA KO	3.93
1377 hADA KO	5.92
206 hADA WT	8.65
1365 UF11 WT	7.86
1383 hADA WT	14.86
1382 PBS WT	6.32
Day40	
206 hADA WT	24.8
1377 hADA KO	7.8
Day 60	
1382 PBS WT	12.3
1383 hADA WT	12.87
1365 UF11 WT	9.85
1369 – KO	1.08
1379 hADA KO	5.12
1368 UF11 KO	3.53

Table 4-4. Gene delivery data for Experiment 3 is shown in the table below, describing vector copy numbers in various murine tissues, collected at sacrifice, on day 120 post-injection of 3x10^11 particles of rAAV1-hADA, rAAV9-hADA, or PBS, in ADA-SCID knockout mice. Overall, with one exception being background rAAV in one sample of pancreas, consistent negative control values are found through low to absent vector copy numbers (or background) in negative control tissues from PBS-injected mice. By contrast, substantial vector copy numbers were found in heart, lung, kidney, liver, pancreas, and skeletal muscle for knockouts administered type 9 vector, while abundant vector copy numbers were found in the skeletal muscle of knockouts given type 1 vector. This data indicates substantial gene delivery and transduction efficiency in multiple tissues for knockouts treated with rAAV9-hADA, and in skeletal muscle for knockouts given rAAV1-hADA, compared to knockouts administered PBS.

Mouse ID	Vector or PBS	rAAV serotype	Day of Sacrifice	Vector	Heart	Kidney	Liver	Lung
36	PBS		120	Copy	3	0	0	0
27	PBS		120	Number	0	1	0	0
41	N/A		120	/ Tissue	6	0	0	26
				/ug DNA:				
				Average	*3*	*0.333333*	*0*	*8.666667*
				Standard Deviation	*3*	*0.57735*	*0*	*15.01111*
29	Vector	9	120		7178	1303	1921	8484
30	Vector	9	120		3864	588	251	1273
40	Vector	9	120		1631	752	944	1253
28	Vector	9	120		3011	1328	1545	1112
31	Vector	9	120		N/A	10672	312	N/A
				Average	*3921*	*2928.6*	*994.6*	*3030.5*
				Standard Deviation	*2358.212*	*4341.104*	*738.6815*	*3636.373*
34	Vector	1	120		118	92	1638	297
39	Vector	1	120		292	98	592	2801
38	Vector	1	120		17	33	369	37
33	Vector	1	120		N/A	42	292	N/A
				Average	*142.3333*	*66.25*	*722.75*	*1045*
				Standard Deviation	*139.1055*	*33.49005*	*623.2877*	*1526.287*
35	Vector (+ Control, rAAV1-GFP)	1	120		2042	1716	13551	36000

Table 4-4. Continued

Mouse ID	Vector or PBS	Vector	Pancreas	Skeletal Muscle	Spleen	Stomach	Thymus
36	PBS	Copy	4	28	0	1	0
27	PBS	Number	26	34	0	9	0
41	N/A	/ Tissue /ug DNA:	583	66	2	1	5
		Average	*204.3333*	*42.66667*	*0.666667*	*3.666667*	*1.666667*
		Standard Deviation	328.1194	20.42874	1.154701	4.618802	2.886751
29	Vector		2340	5922	667	92	12073
30	Vector		2643	11268	2244	116	15
40	Vector		64	703	100	23	88
28	Vector		533	724	188	46	213
31	Vector		N/A	2227	N/A	N/A	N/A
		Average	*1395*	*4168.8*	*799.75*	*69.25*	*3097.25*
		Standard Deviation	1286.485	4503.37	994.5466	42.35859	5984.392
34	Vector		44	117056	122	1	0
39	Vector		3581	31523	150	33	147
38	Vector		16	6198	15	8	152
33	Vector		37	159927	34	N/A	24
		Average	*919.5*	*78676*	*80.25*	*14*	*80.75*
		Standard Deviation	1774.373	71998.18	65.84008	16.8226	80.01406
35	Vector		4116	43981	1460	647	2804

Table 4-5. Gene delivery data for Experiment 4 describing vector copy numbers/ug DNA in various murine tissues, collected at sacrifice, on day 55 post-injection of PBS, single-stranded type 9 vector at a low dose (LD) of 3x10^11 vector particles, single-stranded type 9 vector at a high dose (HD) of 1x10^12 vector particles, or self-complementary type 9 vector at 3x10^11 vector particles. While negative control values, or vector copy numbers of PBS-injected mice, reflect typically no detectable background AAV vector in the negative control murine tissues, low dose rAAV9-hADA injections yielded substantial gene delivery to murine heart, liver, pancreas, kidney, thymus, and skeletal muscle tissues of the ADA-SCID knockout mice by day 55 post-vector injection. Knockout mice injected with the high dose of rAAV9-hADA vector, over 3 times as much as the low dose (LD) group, manifested increased vector copy numbers in numerous tissues, which reflected a dose-response relationship. The response, or increased vector copy number, ranged from approximately a 2-fold increase in copy number (ie HD pancreas) to as much as a 23-fold increase in copy number (ie HD skeletal muscle sample #2) in HD tissues compared to the vector copy numbers of LD tissues.

Mouse ID	vector	Heart	Liver	Pancreas	Kidney	Thymus	Skeletal Muscle 1	Skeletal Muscle 2
145	PBS	0	0	0	0	0	0	0
156	PBS	3	0	0	0	0	0	0
	avg	1.5	0	0	0	0	0	0
	std. dev.	2.12132						
18	LD	3215	9412	2202	7653	4863	1639	656
19	LD	6147	9073	687	15930	11748	22242	16194
139	LD	1895	1078	313	2863	199	1245	552
142	LD	5733	685	329	5791	0	1636	887
	avg	4247.5	5062	882.75	8059.25	4202.5	6690.5	4572.25
	std. dev.	2034.299	4831.874	896.2873	5605.346	5509.381	10369.32	7749.098
20	HD	23661	16668	3604	36246	139568	79715	93814
21	HD	5874	6909	175	13405	1462	1341	1523
147	HD	10527	8384	371	24494	3369	6558	31563
186	HD	24315	27795	3637	21810	17161	2455	334502
	avg	16094.25	14939	1946.75	23988.75	40390	22517.25	115350.5
	std. dev.	9314.58	9586.711	1934.383	9438.541	66487.61	38197.76	151072

Table 4-6. Supplement to Figure 4-25, which shows no observed proliferation of lymphocytes, and thus, no detected vector-driven immunological response, in ADA-SCID knockout mice, administered rAAV1-hADA injections. The following table displays this data numerically, rather than the graphical representation in Figure 4-25. Also included are the standard deviations for each of the values below at each time point. Further descriptive information can be found in the Figure 4-25 Legend.

	Total lymphocytes	B cells	CD3 cells	CD4 cells	CD8 cells	NK cells
Days pI (rAAV1)						
0	1609	300.35	655.95	500.46	245.58	150.95
30	3757	1214.14	1702.35	1045.7	663.37	220.32
60	3065	1050.41	1149.64	681.46	451.6	259.47
90	3423	876.9	1727.8	1123.4	594	212.1
Days pI (NC)						
0	777	153.9	460.6	290.3	162	74.4
30	3180	973.2	1503.2	933.3	544.2	252.3
60	3133	952.8	1310.5	776.9	498.5	413
90	3618	1038.6	1734.6	1166.5	555.3	323.4

Table 4-6. Continued

Standard Deviations:						
	Total lymphocytes	B cells	CD3 cells	CD4 cells	CD8 cells	NK cells
	Day 0 900	272.4	436.4	345	165.3	152.9
	30 1466	623.6	515.5	344.2	184.1	79.2
(rAAV1)	60 1783	590	871.3	583.5	276.6	98.3
	90 886	232.7	492.7	299.3	166.2	11.6
	Day 0 530	151	360	196	157	4
	30 438	341	127	32	79	73
(NC)	60 1417	660	284	205	106	223
	90 1294	436	487	394	100	161

Table 4-7: Supplement to Figure 4-26, which describes the observed proliferation of lymphocytes, or vector-driven immunological response, in ADA-SCID knockout mice, administered rAAV9-hADA injections. The following table displays this data numerically, rather than the graphical representation of Figure 4-26. Also included are the standard deviations for each of the values below at each time point. Further descriptive information can be found in the Figure 4-26 Legend.

	Total lymphocytes	B cells	CD3 cells	CD4 cells	CD8 cells	NK cells
Days pI (rAAV9)						
0	1834	584.6	774.39	556.17	209.38	168.53
30	3852	1585.91	1510.97	1054.73	442.33	233.34
60	4688	2593.91	1124.21	732.4	371.35	322.43
90	5960	2166.6	2608.7	1800.9	783.4	376.3
Days pI (NC)						
0	777	153.9	460.6	290.3	162	74.4
30	3180	973.2	1503.2	933.3	544.2	252.3
60	3133	952.8	1310.5	776.9	498.5	413
90	3618	1038.6	1734.6	1166.5	555.3	323.4

Table 4-7. Continued

Standard Deviations						
		Total lymphocytes	B cells	CD3 cells	CD4 cells	CD8 cells	NK cells
	Day 0	925	405	386	281	112	67
(rAAV9)	30	1008	701	405	320	108	75
	60	2553	1720	491	327	170	126
	90	2094	1016	879	576	332	42
	Day 0	530	151	360	196	157	4
(NC)	30	438	341	127	32	79	73
	60	1417	660	284	205	106	223
	90	1294	436	487	394	100	161

CHAPTER 5
DISCUSSION

Testing of a potential rAAV-based gene therapy for ADA-SCID *in vivo* necessitated two prerequisite studies, assessment of the genotype of the mice to be administered vector and confirmation and general characterization of the immunological phenotype of the ADA-SCID knockout mice. Genotyping according to the Blackburn protocol (Chapter 3 Materials and Methods) provided clear knockout allele and/or wildtype allele PCR products for the mice of interest. Also, amplification of the ADA minigene helped confirm the presence of the transgene rescue in the mice. The immunological profile of the ADA-SCID knockout mice compared to wildtype littermates of the same age reveals, on average, a substantial lymphocyte deficiency with specific deficiencies in B, CD3+, CD4+, and CD8+ cell subsets at most time points (Figure 4-10). For NK cell populations, no substantial deficiency in the knockout mice was observed (Figure 4-10).

In vivo analyses of ADA-SCID knockout mice administered rAAV1-hADA and rAAV9-hADA vectors, began with evaluation of rAAV transduction efficiency. For mice injected with rAAV9 vector in Experiment 3, gene delivery (Table 4-4) was most efficient in heart and lung tissues with substantial numbers of vector genomes in all injected animals. Substantial numbers of vector genomes also were found in kidney, liver, pancreas, and skeletal muscle tissues, although levels were not as consistent as those observed for heart and lung. Spleen, stomach, and thymus tissues showed no consistent indication of substantial gene delivery. Alternatively, for mice injected with rAAV1 vector in Experiment 3 (Table 4-4), the picture of gene delivery was expected and starkly different from that of the rAAV9-hADA vector. While heart, kidney, liver, lung, spleen, stomach, and thymus for rAAV1-hADA-injected mice did not demonstrate consistent substantial levels of gene delivery, an abundance of vector was found consistently and

long-term in the primary target tissue, quadriceps skeletal muscle. The qPCR data from Experiments 2, 3, and 4 (Tables 4-2, 4-4, and 4-5 respectively) demonstrated that moderate to abundant levels of rAAV9-mediated gene delivery was achieved and persisted over a prolonged period of time in a variety of murine tissues, especially heart, lung, liver, kidney, and skeletal muscle. The qPCR data from Experiments 1 and 3 also showed modest to high levels of rAAV1-mediated gene delivery and long-term persistence in skeletal muscle tissues (Tables 4-1, and 4-4 respectively).

A qualitative analysis of murine tissues by immunohistochemical staining revealed abundant hADA expression in several tissues (as shown in Figure 4-11 for Experiment 1, Figures 4-12, 13, and 14 for Experiment 2, Figures 4-18, 19, and 20 for Experiment 3, and Figures 4-21 and 4-22 for Experiment 4). For knockout mice administered rAAV1-hADA, the tropism of this serotype for skeletal muscle was also observed in this study as in numerous previous studies by Lu et al., Toromanoff et al., and Yan et al. In Experiments 1 and 3, intramuscular injection successfully delivered type1 vector to the quadriceps muscle of experimental animals and resulted in substantial hADA staining of skeletal myofibers in Experiment 3, as shown in Figure 4-18A (left image). By contrast, skeletal muscle derived from PBS-injected knockout animals showed no substantial background staining for hADA in Experiment 3, as shown in Figure 4-18A (right image). Finally, an H&E stain of the skeletal muscle utilized in Figure 4-18A was performed. The resulting image, Figure 4-18B, showed no signs of an inflammatory infiltrate in response to vector or transgene. (Lu, *et al.* 2006, Toromanoff, *et al.* 2008, Yan, *et al.* 2005)

For knockout mice administered rAAV9-hADA, abundant protein expression was observed consistently in murine cardiac muscle tissue, as shown in Figures 4-12 A and B along with Figures 4-19A and 4-21A, in Experiments 2, 3, and 4. By contrast, the cardiac muscle

tissue derived from knockout mice administered saline instead of vector showed little background staining for hADA (as shown Figure 4-12 C for Experiment 2, Figure 4-19B for Experiment 3, and Figure 4-21B for Experiment 4). Also, when the identical cardiac muscle tissue harvested from vector-injected mice and shown in Figures 4-19A and 4-21A, was stained with hematoxylin and eosin (H&E), no apparent inflammatory infiltrate in response to vector or transgene was observed in Figure 4-19C (Experiment 3) and Figure 4-21C (Experiment 4). Moreover, GFP staining of cardiac muscle tissue derived from positive control knockout mouse administered the rAAV9-GFP control vector showed a number of cardiomyocytes stained positively for GFP (Figure 4-19D for Experiment 3). Given intravenous delivery of rAAV9 vector, the innate ability of this serotype to cross endothelial barriers, and in a number of previous studies, target heart, significant hADA expression in murine cardiac tissue was anticipated and indicated by the observed results. (Inagaki 2006, Miyagi, *et al.* 2008, Vandendriessche 2007)

Also observed by immunohistochemical staining was substantial hADA expression in renal medulla/pelvis and liver of rAAV9-injected mice in Experiment 3 (Figure 4-20A) and Experiment 4 (Figure 4-22A), respectively. Murine kidney and liver tissues, like cardiac muscle, are also heavily vascularized and exposed to a constant high degree of blood flow. Consequently, with such blood flow, exposure of renal tissue or liver to vector may explain the abundance of hADA expression in these tissues observed in some treated animals. Moreover, Figures 4-20B and 4-22B show minimal background hADA staining in kidney (renal medulla/pelvis) and liver tissues, respectively, harvested from negative control knockout mice administered PBS instead of vector. While some pockets of light background staining were observed, the renal medulla/pelvis and liver of the negative control PBS-injected knockouts, are

relatively clear of background. Figures 4-20C and 4-22C show H&E staining of the identical renal and hepatic tissues, respectively, shown in Figures 4-20A and 4-22A. No inflammatory infiltrates were observed, providing at least one indicator that an adverse immune response to vector or trangene was not produced.

Interestingly, the distribution of rAAV9-hADA and expression of hADA in tissues such as heart, kidney, and liver may one day provide therapeutic benefits unseen previously for retroviral gene therapies. First, recombinant AAV-mediated gene delivery and hADA protein expression in various murine target tissues offer the potential for enzyme secretion into the circulation and thus, the potential benefit of direct systemic detoxification. Second, the expression of hADA in various target tissues throughout the mouse body may offer sites that can serve as metabolic depots or metabolic "sinks," as Carbonaro et al. and Donald Kohn, a pioneer in the field of ADA-SCID gene therapy research, recently described in a lentiviral study directed at amelioration of ADA-SCID through the overexpression of ADA in liver and lung in a more severely immune deficient mouse model of this disease. In other words, similar to the Kohn lentiviral study, regional sites of rAAV-mediated, intracellular, over-expression of hADA could serve to provide not only local benefit to a variety of tissues throughout the body, but also handle detoxification of circulating body metabolites, which may ultimately produce a more indirect systemic benefit including restoration of lymphocyte populations and function. The potential for single-stranded, self-complementary, or mutant rAAV vectors to provide both local and systemic benefits, offers a more global approach to the amelioration of this potentially fatal disease which adversely affects not only the immune system but also numerous non-immunological tissues of the body. (Carbonaro, *et al* 2006)

The next endpoint of interest, enzyme activity analysis, proved to be a challenging process. Although no statistically significant data was gathered, the trend observed for average serum ADA activity values, in the context of rAAV1-hADA and rAAV9-hADA administration (Experiment 3), was one of enhanced serum enzyme activity above background levels, especially for the serotype 9 vector. While enzyme activity levels varied from time point to time point perhaps reflecting cycles of enzyme degradation and synthesis over time, this data [especially with parallel assessments of the general immunological profile of the mice following vector administration] suggested vector-derived, serum-based enzyme activity, which may be on the order of double the background levels (as described in Chapter 4, and shown in Figures 4-23 A, B, and C for rAAV1-injected mice, and in Figures 4-24 A, B, and C for rAAV9-injected mice from Experiment 3). While no conclusive evidence has yet been obtained, further serum analyses of ADA activity, as well as the development of an ADA-ELISA for quantification of serum ADA protein, may further corroborate the observed trends.

Yet, what may account for the background ADA activity observed in Experiments 1, 2, and 3, in serum of both wildtype and knockout control mice? Since hADA and murine ADA are not typically secreted in the mouse, one likely explanation for the presence of any ADA activity in negative control mouse serum is the tendency for some red blood cell lysis during the serum separation process from peripheral blood, especially for Experiment 1 and 2 when wildtype mice were used for *in vivo* testing of rAAV vectors. The most likely explanation for the level of background enzyme activity in negative control knockout mice may be related to the natural cycles of cellular growth, proliferation, death, and degeneration inherent to all murine tissues, especially those tissues which are rescued in this ADA-SCID mouse model, including the forestomach and intestine. Over time, degradation of foregut-derived tissues, stomach,

duodenum, and intestine may release proteins such as ADA into the extracellular space and ultimately, the blood. Subsequently, when blood is harvested for serum analysis, a certain level of background ADA protein and enzyme activity may consistently be present. This possible explanation is supported by the observation that background enzyme activity levels in negative control mouse sera remain relatively steady at approximately 4-5 Units from time point to time point, reflecting perhaps a steady level of cell death and cellular degeneration in the mouse model, and thus, a steady release of ADA protein into the murine circulation. (Blackburn, *et al* 1996)

The large standard deviations in enzyme activity observed for the experimental groups relate directly to the number of animals used in Experiment 3 as well as the variability of serum-based enzyme activity levels among the different knockout animals at any given time point. Two possible explanations for the variability in observed enzyme activity for each vector-injected animal are that some animals of a particular experimental group may have expressed and secreted ADA more efficiently than others, or that synthesis/secretion of hADA may have occurred in some animals at a given time point while greater enzyme degradation [following a period of secretion] may have occurred in other animals of the same experimental group at the same time point.

Yet, why would some vector-injected mice express and secrete hADA more efficiently than others? Particularly in the case of rAAV9-injected mice, the overall vector transduction efficiency may have varied from mouse to mouse if, for example, delivery of vector by tail vein injection also varied in efficiency. Using ADA-SCID mice, which are agouti in color, the tail vein, especially in young mice, can be difficult to visualize and inject. Thus, not all tail vein injections may have been as efficient. Consequently, the number of transduced cells, the amount

of expressed and secreted hADA, and thus, the level of serum ADA activity may have varied from mouse to mouse. If this sequence of events occurred in some treated animals, a large standard deviation and no statistical significance for the measured levels of enzyme activity would have resulted for the entire group of treated mice.

Also, once the serotype 9 vector was administered, migration of the vector through the bloodstream to a variety of organs and tissues may have varied, and led to substantial standard deviations and lack of statistical significance observed for collected enzyme activity data. In some experimental mice, the vector may have migrated more efficiently to some tissues than to others. Table 4-2, 4-4, and 4-5 illustrate this variability through variation in vector copy number observed for heart, liver, pancreas, skeletal muscle, and kidney tissues between mice in the same experimental group. In several mice of the rAAV9-hADA experimental group, vector transduction may have been superior in heart and kidney tissues and less substantial in liver and skeletal muscle. In other mice of the same experimental group, the pattern of vector transduction may have been the opposite of that previously described. In this case, protein expression may very well have occurred in variety of tissues. However, the ability of different cell types to secrete protein may vary substantially. In the mice in which substantial vector copy numbers could be found in tissues with high capacity for secretion, substantial protein expression coupled with secretion may have occurred. In mice in which substantial vector copy numbers could be found in tissues with lower capacity for secretion, protein may have been expressed, but not secreted. Therefore, in the former group of mice, serum ADA activity may have been substantially higher than in the latter group of mice. A large standard deviation and no statistical significance for the calculated levels of ADA activity may have resulted.

In addition, the immunological profiling of ADA-SCID knockout mice in Experiment 3 presented a positive trend toward lymphocyte reconstitution over time following administration of rAAV9-hADA vector. As shown in Figure 4-26, total lymphocyte and lymphocyte subset numbers increased over time in the vector-injected animals while stabilizing over time in control animals. A similar trend was beginning to manifest in Figure 4-27 for Experiment 4, though confirmation of this trend will be subject to data collected in the near future for Experiment 4. By contrast, no similar pattern was observed in mice which received rAAV1-hADA vector (Figure 4-25), indicating that perhaps transduced cells and tissue of the heart, or the combination of multiple transduced cell/tissue types, such as heart, liver, and kidney, serve as a superior site or sites, respectively, of ectopic hADA expression and/or secretion than skeletal muscle alone. Interestingly, if confirmed by ongoing experiments, B cells appeared to be the first lymphocyte subset to proliferate following rAAV9-hADA injection in treated knockout mice compared to untreated knockout mice (please refer to the Day 60 data in Table 4-7 and Figure 4-26). Coincidentally, B cells are also the lymphocyte type in ADA-SCID, which typically develop first in patients with ADA-SCID treated with PEG-ADA. Thus, any serum-based detoxification would be predicted to facilitate B cell proliferation ahead of T cell proliferation, which requires more time due to T cell ontogeny. Consistent with this prediction was the reconstitution of additional lymphocyte subsets, including CD3+ and CD4+ cells, only after B cell proliferation (please refer to the Day 90 data in Table 4-7 and Figure 4-26).

Lastly, the safety of these rAAV vectors was observed for all *in vivo* experiments. While two knockout mice during Experiment 3 died at the end of the experimental period, both had experienced recent, heavy blood loss during bleeds that were conducted under substantial anesthesia. The bleeds were meant to facilitate enzyme activity, flow cytometry and CBC

analyses. But, the degree of fluid loss from the bleeds in two mice for which blood clotting proved difficult likely resulted in the two mouse deaths. Of the remaining mice utilized to date for testing of the rAAV vectors, all remained alive and well until their respective dates of sacrifice. This low toxicity for rAAV vectors is consistent with numerous preclinical and clinical rAAV studies.

Overall, rAAV-based gene therapy for ADA-SCID shows promise in preclinical studies conducted using a partially immune deficient mouse model. A transgene cassette, composed chiefly of a cmyc/polyHis-tagged secretory version of the hADA gene, was cloned into single-stranded recombinant AAV serotype 2 cloning vector, to generate the plasmid, rAAV-hADA. This plasmid was tested in tissue culture and shown to express and secrete hADA protein. The cloning and tissue culture data collectively achieved Aims 1 and 2 of this research. Then, a partially immune deficient mouse model of ADA-SCID was successfully characterized by PCR-based genotyping and flow cytometry/CBC analysis-based phenotyping. Such characterization of the partial immune deficiency accomplished Aim 3 of this research. The rAAV-hADA plasmid was then packaged into serotype 1 and 9 capsids, and administered by intramuscular or intravenous injection, respectively, to ADA-SCID knockout mice or their wildtype littermates, in a series of *in vivo* experiments. A number of endpoints were analyzed over time periods which extended up to 120 days. These endpoints included confirmation of long-term, moderate gene delivery and transduction efficiency, as well as qualitative observation of vector-mediated hADA expression in skeletal muscle, cardiac muscle, kidney, and liver tissues. This gene delivery and protein expression data achieved Aim 4 of this research. Subsequent serum-based analysis of enzyme activity revealed a trend towards increased levels of ADA activity in experimental vector-injected knockout animals compared to control knockout mice over time. This observed

trend (for Experiment 3) was not statistically significant, but was corroborated by the final endpoint for this study, an analysis of lymphocyte development following rAAV injection. Though the data (for Experiment 3) revealed no trend or immune reconstitution for knockout mice which received the rAAV1-hADA vector, a partial, progressive, prolonged, reconstitution of lymphocytes was indicated for knockout mice which received the rAAV9-hADA vector. Expanded statistical analysis of this immunological data is pending, though Experiment 4 data may ultimately corroborate the immunological data from Experiment 3. The observed, but not statistically significant trend in serum enzyme activity and analyzed immunological data helped accomplish Aim 5 of this research, though further substantiation is needed.

While further studies are needed which vary the dose of injected vector, alter the vector with different secretory sequences, or vary the type of vector to include, for example, various mutant and self-complementary rAAV vectors (see Chapter 6 Future Directions), the data presented here support the feasibility of a rAAV-based gene therapy for ADA-SCID and for primary immune deficiencies as a whole.

CHAPTER 6
FUTURE DIRECTIONS

This thesis was a preclinical exploration of possible rAAV treatment modalities for the amelioration of ADA-SCID. Along the way, a number of alternative avenues for a rAAV-based gene therapy of ADA-SCID have arisen, a description of which may prove beneficial for the continuity of the described research, and ultimately, for the development of a viable, effective, safe, clinical rAAV gene therapy for ADA-SCID. While not attempted in the aforementioned research, rAAV packaged in serotype 7 capsids may offer a valuable tool to deliver a non-secretory version of the hADA transgene to hematopoietic progenitor cells. A single-stranded rAAV plasmid containing a non-secretory form of the hADA transgene has already been cloned for later analysis. Additional information regarding a rAAV7-based approach in the treatment of ADA-SCID may be found in Chapter 2 Introduction.

Secondly, a number of rAAV vectors containing type 2 capsid mutations at various tyrosine residues may also provide a valuable tool for the amelioration of ADA-SCID. These vectors with mutant capsids have been shown by Srivastava group to dramatically enhance transduction efficiency in liver tissue. The eventual targeting of liver, with the secretory rAAV-hADA vector containing capsid mutations, may facilitate highly efficient gene delivery to hepatocytes, and lead to an overexpression of hADA with several possible effects. First, transduced liver tissue could serve as a metabolic sink to detoxify circulating metabolites. Second, overexpression in liver could lead to a localized correction of the ADA deficiency. Third, rAAV-mediated transfer of a secretory version of the hADA gene may lead to expression of hADA with subsequent exploitation of the hepatocyte secretory apparatus. Ultimately, this process may release hADA into the blood for direct systemic detoxification. Given the greater efficiency with which these capsid mutant vectors may transduce liver tissue, when compared to

their single-stranded (or even self-complementary) vector counterparts, a gene therapy approach based on the application of these mutant vectors (ie mutant rAAV serotype 2 or 8) to the targeting of liver tissue, as the primary site of ectopic hADA expression and secretion, may provide an alternative and enhanced approach to the amelioration of ADA-SCID.

Another approach to enhancing a rAAV-mediated treatment of ADA-SCID would be the utilization of alternative secretory sequences, such as that of interleukin-2 (ie IL2ss), as opposed to the current immunoglobulin Kappa chain signal sequence (IgKss). An alternative secretory sequence, such as IL-2ss, engineered upstream and in-frame with the hADA transgene [and c-myc/polyHis tags] within a rAAV vector backbone, may be utilized to produce a transgene cassette capable of enhanced secretion of hADA protein *in vitro* and/or *in vivo* over that of its 5' IgKss-hADA-c-myc/polyHis 3' transgene cassette counterpart. A rAAV construct containing a 5' IL-2ss-hADA-cmyc/polyHis 3' transgene cassette has already been engineered and awaits preliminary analysis in tissue culture.

An additional suggestion for future directions of rAAV-mediated ADA-SCID gene therapy should include studies in the alternative mouse model for ADA-SCID. This model, while provided embryologically an ADA minigene rescue which is expressed in the placenta, lacks the ADA minigene rescue expressed in the forestomach and intestine of the mouse model used for these studies. Consequently, this alternative model suffers from a more severe form of ADA-SCID than the currently studied model. At 3 weeks of age, this particular model suffers from a pronounced pulmonary eosinophilia, with subsequent pulmonary insufficiency, and ultimately death. Given the relatively early age of death of this mouse model, there may not be sufficient time even for early post-natal administration of single-stranded rAAV vectors to transduce target cells, foster protein expression/secretion, and facilitate a beneficial immune

response to rescue the alternative model from death. High doses of single stranded vector on the order of 1x10^12 to 5x10^12 may be sufficient to rescue this alternative mouse model if administered either at birth or perhaps at 1 week of age. Intra-uterine injections may also be an option. High doses of single-stranded vector will still require 1-2 weeks at a minimum for protein expression, yet a greater number of transduced cells due to a greater dose of vector may provide a greater initial production of secreted hADA protein to foster a more potent systemic detoxification earlier in the mouse life cycle than lower doses of the same single-stranded vector. On the other hand, a double-stranded vector, such as a self-complementary form of rAAV-hADA (sc-AAV-hADA), may provide a substantial level of protein expression/secretion along with an immunological benefit earlier than its single-stranded counterpart. Self-complementary vectors bypass the need for double-stranded DNA synthesis and, therefore, are capable of earlier protein expression than single-stranded vectors. Moreover, a double-stranded sc-AAV-hADA vector may provide added genomic stability for longer-term protein expression when compared to its single-stranded rAAV-hADA counterpart. Both earlier protein expression and enhanced genomic stability may improve a gene therapy designed for testing in the more severe ADA-SCID mouse model with only a placental ADA minigene rescue.

LIST OF REFERENCES

Aiuti, A. (2004) Gene therapy for adenosine-deaminase-deficient severe combine immunodeficiency. *Best Practice & Research Clinical Haematology,* **17,** 505-516.

Aiuti, A., Cassani, B., Andolfi, G., Mirolo, M., Biasco, L., Recchia, A., Urbinati, F., Valacca, C., Scaramuzza, S., Aker, M., Slavin, S., Cazzola, M., Sartori, D., Ambrosi, A., Di Serio, C., Roncarolo, M. G., Mavilio, F., and Bordignon, C (2007) Multilineage hematopoetic reconstitution without clonal selection in ADA-SCID patients treated with stem cell gene therapy. *The Journal of Clinical Investigation,* **8,** 2233-2240.

Aiuti, A., Ficara, F., Cattaneo, F., Bordignon, C., and Roncarolo, M.G. (2003) Gene therapy for adenosine deaminase deficiency. *Current Opinion in Allergy and Clinical Immunology,* **3,** 461-466.

Aiuti, A., Slavin, S., Aker, M., Ficara, F., Deola, S., Mortellaro, A., Morecki, S., Andolfi, G., Tabucchi, A., Carlucci, F., Marinello, E., Cattaneo, F., Vai, S., Servida, P., Miniero, R., Roncarolo, M.G., Bordignon, C. (2002a) Correction of ADA-SCID by Stem Cell Gene Therapy Combined with Nonmyeloablative Conditioning. *Science,* **296,** 2410-2413.

Aiuti, A., Vai, S., Mortellaro, A., Casorati, G., Ficara, F., Andolfi, G., Ferrari, G., Tabucchu, A., Carlucci, F., Ochs, H.D., Notarangelo, L.D., Roncarolo, M.G., and Bordignon, C. (2002b) Immune reconstitution in ADA-SCID after PBL gene therapy and discontinuation of enzyme replacement. *Nature Medicine,* **8,** 423-425.

Anderson, W.F., Blaese, R.M. & Culver, K. (1990) The ADA human gene therapy clinical protocol: Points to Consider response with clinical protocol, July 6, 1990. *Hum Gene Ther,* **1,** 331-362.

Banerjee, S.K., Young, H.W., Barczak, A., Erle, D.J. & Blackburn, M.R. (2004) Abnormal alveolar development associated with elevated adenine nucleosides. *Am J Respir Cell Mol Biol,* **30,** 38-50.

Baum, C. (2007) Insertional mutagenesis in gene therapy and stem cell biology. *Current Opinion in Hematology,* **14,** 337-342.

Baum, C., von Kalle, C., Stalle, F.J., Li, Z., Fehse, B., Schmidt, M., Weerkamp, F., Karlsson, S., Wagemaker, D., Williams, D.A. (2004) Chance or necessity? Insertional mutagenesis in gene therapy and its consequences. *Molecular Therapy,* **9,** 5-13.

Blackburn, M.R., Datta, S.K. & Kellems, R.E. (1998) Adenosine deaminase-deficient mice generated using a two-stage genetic engineering strategy exhibit a combined immunodeficiency. *J Biol Chem,* **273,** 5093-5100.

Blackburn, M.R., Datta, S.K., Wakamiya, M., Vartabedian, B.S. & Kellems, R.E. (1996) Metabolic and immunologic consequences of limited adenosine deaminase expression in mice. *J Biol Chem,* **271,** 15203-15210.

Blaese, R.M., Culver, K.W., Miller, A.D., Carter, C.S., Fleisher, T., Clerici, M., Shearer, G., Chang, L., Chiang, Y., Tolstoshev, P., Greenblatt, J.J., Rosenberg, S.A., Klein, H., Berger, M., Mullen, C.A., Ramsey, W.J., Muul, L., Morgan, R.A., Anderson, W.F. (1995) T lymphocyte-directed gene therapy for ADA- SCID: initial trial results after 4 years. *Science,* **270,** 475-480.

Board of the European Society of Gene and Cell Therapy (2008) Case of leukaemia associated with X-linked severe combined immunodeficiency gene therapy trial in London. *Human Gene Therapy,* **19,** 3-4.

Booth, C.H., M., Notarangelo, L., Buckley, R., Hoenig, M., Mahlaoui, N., Cavazzana-Calvo, M., Aiuti, A., and Gaspar, H. B. (2007) Management options for adenosine deaminase deficiency; proceeding of the EBMT satellite workshop (Hamburg, March 2006). *Clinical Immunology,* **123,** 139-147.

Bordignon, C., Notarangelo, L.D., Nobili, N., Ferrari, G., Casorati, G., Panina, P., Mazzolari, E., Maggioni, D., Rossi, C., Servida, P., Ugazio, A.G., and Mavilio, F. (1995) Gene therapy in peripheral blood lymphocytes and bone marrow for ADA-immunodeficient patients. (adenosine deaminase deficiency). *Science,* **270,** 470-476.

Buckley, R.H. (2002) Primary cellular immunodeficiencies. *Journal of Allergy and Clinical Immunology,* **109,** 747-757.

Bushman, F.D. (2007) Retroviral integration and human gene therapy. *Journal of Clinical Investigation,* **117,** 2083-2086.

Carbonaro, D.A., Jin, X., Petersen, D., Wang, X., Dorey, F., Kil, K.S., Aldrich, M., Blackburn, M.R., Kellems, R.E. & Kohn, D.B. (2006) *In vivo* transduction by intravenous injection of a lentiviral vector expressing human ADA into neonatal ADA gene knockout mice: a novel form of enzyme replacement therapy for ADA deficiency. *Mol Ther,* **13,** 1110-1120.

Cavazzana-Calvo, M. & Fischer, A. (2007) Gene therapy for severe combined immunodeficiency: are we there yet? *J Clin Invest,* **117,** 1456-1465.

Cavazzana-Calvo, M.a.F., A. (2007) Gene therapy for severe combined immunodeficiency: are we there yet? *Journal of Clinical Investigation,* **117,** 1456-1465.

Chan, B., Wara, D., Bastian, J., Hershfield, M.S., Bohnsack, J., Azen, C.G., Parkman, R., Weinberg, K., Kohn, D.B. (2005) Long-term efficacy of enzyme replacement therapy for adenosine deaminase (ADA)-deficient severe combined immunodeficiency (SCID). *Clinical Immunology,* **117,** 133-143.

Coloma, M.J., Hastings, A., Wims, L.A., Morrison, S.L. (1992) Novel vectors for the expression of antibody molecules using variable regions generated by polymerase chain reaction. *Journal of Immunological Methods,* **152,** 89-104.

Dave, U.P., Jenkins, N.A., Copeland, N.G. (2004) Gene therapy insertional mutagenesis insights. *Science,* **303,** 333.

Deichmann A, H.-B.-A.S., Schmidt M, et al. (2007) Vector integration is nonrandom and clustered and influences the fate of lymphopoiesis in SCID-X1 gene therapy. *Journal of Clinical Investigation,* **117,** 2225-2232.

Di Nunzio, F., Piovani, B., Cosset, F.L., Mavilio, F., Stornaiuolo, A. (2007) Transduction of Human Hematopoietic Stem Cells by Lentiviral Vectors Pseudotyped with RD114-TR Chimeric Envelope Glycoprotein. *Human Gene Therapy,* **18,** 811-820.

Donsante, A., Miller, D. G., Li, Yi., Vogler, C., Brunt, E. M., Russell, D. W., and Sands, M. S (2007) AAV Vector Integration Sites in Mouse Hepatocellular Carcinoma. *Science,* **317,** 477.

Engel, B.C., Podsakoff, G.M., Ireland, J.L., Smogorzewska, E.M., Carbonaro, D. A., Wilson, K., Shah, A., Kapoor, N., Sweeney, M., Borchert, M., Crooks, G. M., Weinberg, K.I., Parkman, R., Rosenblatt, H.M., Wu, S.Q., Hershfield, M.S., Candotti, F., and Kohn, D. B. (2007) Prolonged pancytopenia in a gene therapy patient with ADA-deficient SCID and trisomy 8 mosaicism: a case report. *Blood*, **109,** 503-506.

Flotte, T.R. (2002) Recombinant Adeno-Associated Virus Gene Therapy for Cystic Fibrosis and alpha1-Antitrypsin Deficiency. *Chest,* **121,** 98S-102S.

Flotte, T.R. (2004) Gene Therapy Progress and Prospects: Recombinant adeno-associated virus (rAAV) vectors. *Gene Therapy,* **11,** 805-810.

Flotte, T.R. (2005) Adeno-Associated Virus-Based Gene Therapy for Inherited Disorders. *Pediatric Research,* **58,** 1143-1147.

Flotte, T.R. (2007) Gene Therapy: The first two decades and the current state-of-the-art. *The Journal of Cell Physiology,* **213,** 301-305.

Fozard, J.R. (2003) The case for a role of adenosine in asthma: almost convincing? *Current Opinion in Pharmacology,* **3,** 264-269.

Gao, G.P., Alvira, M.R., Wang, L., Calcedo, R., Johnston, J., Wilson, J.M. (2002) Novel adeno-associated viruses from rhesus monkeys as vectors for human gene therapy. *Proceedings of the National Academy of Sciences of the United States of America,* **99,** 11854-11859.

Gaspar, H.B., Bjorkegren, E., Parsley, K., Gilmour, K.C., King, D., Sinclair, J., Zhang, F., Giannakopoulous, A., Adams, S., Fairbanks L.D., Gaspar, J., Henderson, L., Xu-Bayford, J. H., Davies, E.G., Veys, P. A., Kinnon, C., and Thrasher, A. J. (2006) Successful Reconstitution of Immunity in ADA-SCID by Stem Cell Gene Therapy Following Cessation of PEG-ADA and Use of Mild Preconditioning. *Molecular Therapy,* **14,** 505-513.

GEHealthcare/Lumigen Inc. (2006) Amersham ECL Advance Western Blotting Detection Kit Product Booklet Code RPN2135 http://www1.gelifesciences.com/aptrix/upp00919.nsf/Content/5E2EC600736AC010C12572C0008120D6/$file/RPN2135_Rev_E_2006_web.pdf (August 2008)

Hacein-Bey-Abina S, V.K.C., Schmidt M, et al (2003) LMO2-associated clonal T cell proliferation in two patients after gene therapy for SCID-X1. *Science,* **302,** 415-419.

Han, Z., Zhong, L., Maina, N., Hu, Z., Li, X., Chouthai, N.S., Bischof, D., Weigel-Van Aken, K.A., Slayton, W.B., Yoder, M.C. & Srivastava, A. (2008) Stable integration of recombinant adeno-associated virus vector genomes after transduction of murine hematopoietic stem cells. *Hum Gene Ther,* **19,** 267-278.

Hauck, B., Xiao, W. (2003) Characterization of Tissue Tropism Determinants of Adeno-Associated Virus Type 1. *Journal of Virology,* **77,** 2768-2774.

Hershfield, M. (2003) Genotype is an important determinant of phenotype in Adenosine Deaminase Deficiency. *Current Opinion in Immunology,* **15,** 571-577.

High, K.A. (2007) Update on progress and hurdles in novel genetic therapies for hemophilia. *Hematology Am Soc Hematol Educ Program,* **2007,** 466-472.

Honig, M., Albert, M.H., Schulz, A., Sparber-Sauer, M., Schutz, C., Belohradsky, B., Gungor, T., Rojewski, M.T., Bode, H., Pannicke, U., Lippold, D., Schwarz, K., Debatin, K.M., Hershfield, M.S. & Friedrich, W. (2007) Patients with adenosine deaminase deficiency surviving after hematopoietic stem cell transplantation are at high risk of CNS complications. *Blood,* **109,** 3595-3602.

Honig, M., Albert, M.H., Schulz, A., Sparber-Sauer, M., Schutz, C., Belohradsky, B, Gungor, T., Rojewski, M.T., Bode, H., Pannicke, U., Lippold, D., Schwarz, K., Debatin, K.M., Hershfield, M.S., and Friedrich, W. (2007) Patients with adenosine deaminase deficiency surviving hematopoetic stem cell transplantation are at high risk of CNS complication. *Blood,* **109,** 3595-3602.

Huang, H. & Manton, K.G. (2005) Newborn Screening For Severe Combined Immunodeficiency (SCID): A Review. *Frontiers in Bioscience,* **10,** 1024-1039.

Inagaki, K., Fuess, S., Storm, T. A., Gibson, G.A., Mctiernan, C. F., Kay, M.A., and Nakai, H. (2006) Robust Systemic Transduction with AAV9 Vectors in Mice: Efficient Global Cardiac Gene Transfer Superior to That of AAV8. *Molecular Therapy,* **14,** 45-53.

Jaroszeski, M.J. & Radcliff, G. (1999) Fundamentals of flow cytometry. *Mol Biotechnol,* **11,** 37-53.

Kapturczak, M.H., Chen, S., Agarwal, A. (2005) Adeno-associated virus vector-mediated gene delivery to the vasculature and kidney. *Acta Biochimica Polonica,* **52,** 293-299.

Kaufman, D.A., Hershfield, M.S., Bocchini, J.A., Moissidis, I.J., Jeroudi, M., and Bahna S.L. (2005) Cerebral Lymphoma in an Adenosine Deaminase-Deficient Patient With Severe Combined Immunodeficiency Receiving Polyethylene Glycol-Conjugated Adenosine Deaminase. *Pediatrics,* **116,** e876-e879.

Kawamura, N., Ariga, T., Ohtsu, M., Kobayashi, I., Yamada, M., Tame, A., Furuta, H., Okano, M., Egashira, M., Niikawa, N., Kobayashi, K, and Sakiyama, Y. (1999) *In vivo* Kinetics of Transduced Cells in Peripheral T Cell-Directed Gene Therapy: Role of CD8+ Cells in Improved Immunological Function in an Adenosine Deaminase (ADA)- SCID Patient. *The Journal of Immunology,* **163,** 2256-2261.

Kohn, D.B., Sadelain, M., Dunbar, C., et al. (2003a) American Society of Gene Therapy (ASGT) ad hoc subcommittee on retroviral-mediated gene transfer to hematopoietic stem cells. *Molecular Therapy,* **8,** 180-187.

Kohn, D.B., Sadelain, M., Glorioso, J.C. (2003b) Occurrence of leukaemia following gene therapy of X-linked SCID. *Nature Reviews/Cancer,* **3,** 477-488.

Lainka, E.H., M. S., Santisteban, I., Bali, P., Seibt, A., Neubert, J., Friedrich, W., and Niehues, T. (2005) Polyethylene Glycol-Conjugated Adenosine Deaminase (ADA) Therapy Provides Temporary Immune Reconstitution to a Child with Delayed-Onset ADA Deficiency. *Clinical and Diagnostic Laboratory Immunology,* **12,** 861-866.

Lu, Y., Choi, Y.K., Campbell-Thompson, M., Li, C., Tang, Q., Crawford, J.M., Flotte, T.R. & Song, S. (2006) Therapeutic level of functional human alpha 1 antitrypsin (hAAT) secreted from murine muscle transduced by adeno-associated virus (rAAV1) vector. *J Gene Med,* **8,** 730-735.

Malacarne, F., Benicchi, T., Notarangelo, L.D., Mori, L., Parolini, S., Caimi, L., Hershfield, M., Notarangelo, L.D., Imberti, L. (2005) Reduced thymic output, increased spontaneous apoptosis and oligoclonal B cells in polyethylene glycol-adenosine deaminase-treated patients. *European Journal of Immunology,* **35,** 3376-3386.

Manno, C.S., Pierce, G.F., Arruda, V.R., Glader, B., Ragni, M., Rasko, J.J., Ozelo, M.C., Hoots, K., Blatt, P., Konkle, B., Dake, M., Kaye, R., Razavi, M., Zajko, A., Zehnder, J., Rustagi, P.K., Nakai, H., Chew, A., Leonard, D., Wright, J.F., Lessard, R.R., Sommer, J.M., Tigges, M., Sabatino, D., Luk, A., Jiang, H., Mingozzi, F., Couto, L., Ertl, H.C., High, K.A., Kay, M.A. (2006) Successful transduction of liver in hemophilia by AAV-Factor IX and limitations imposed by the host immune response. *Nature Medicine,* **12,** 342-347.

Manton, K.G.a.H., H (2005) Newborn Screening For Severe Combined Immunodeficiency (SCID): A Review. *Frontiers in Bioscience,* **10,** 1024-1039.

Miyagi, N., Rao, V.P., Ricci, D., Du, Z., Byrne, G.W., Bailey, K.R., Nakai, H., Russell, S.J. & McGregor, C.G. (2008) Efficient and durable gene transfer to transplanted heart using adeno-associated virus 9 vector. *J Heart Lung Transplant,* **27,** 554-560.

Muul, L.M., Tuschong, L.M., Soenen, S.L., Jagadeesh, G.J., Ramsey, W.J., Long, Z., Carter, C.S., Garabedian, E.K., Alleyne, M., Brown, M., Bernstein, W., Schuman, S.H., Fleisher, T. A., Leitman, S.F., Dunbar, C.E., Blaese, R.M., and Candotti, F. (2003) Persistence and expression of the adenosine deaminase gene for 12 years and immune reaction to gene transfer components: long-term results of the first clinical gene therapy trial. *Blood,* **101,** 2563-2569.

National Cancer Institute flow cytometry http://www.cancer.gov/Templates/db_alpha.aspx?CdrID=335066 (August 2008)

Parkmam, R., Weinberg, K., Crooks, G., Nolta, J., Kapoor, N., and Kohn, D. (2000) Gene Therapy for Adenosine Deaminase Deficiency. *Annual Review of Medicine,* **51,** 33-47.

Pierce, G.F., Lillicrap, D., Pipe, S.W., and Vandendriessche, T. (2007) Gene therapy, bioengineered clotting factors and novel technologies for hemophilia treatment. *Journal of Thrombosis and Haemostasis,* **5,** 901-906.

Pike-Overzet, K., van der Burg, M., Wagemaker, G., van Dongen, J.J., Staal, F.J. (2007) New insights and unresolved issues regarding insertional mutagenesis in X-linked SCID gene therapy. *Molecular Therapy,* **15,** 1910-1916.

Poirier, A., Campbell-Thompson, M., Tang, Q., Scott-Jorgensen, M., Combee, L., Loiler, S., Crawford, J., Song, S. & Flotte, T.R. (2004) Toxicology and biodistribution studies of a recombinant adeno-associated virus 2-alpha-1 antitrypsin vector. *Preclinica,* **2,** 43-51.

Protocol Online, Your lab's reference book (1998-2008) http://www.protocol-online.org/prot/Molecular_Biology/Protein/Western_Blotting/ (August 2008)

Qasim, W., Gaspar H. B., and Thrasher, A. J. (2004) Gene therapy for severe combined immune deficiency. *Expert Reviews in Molecular Medicine,* **6,** 1-12.

Ren, C., Kumar, S., Shaw, D.R., and Ponnazhagan, S (2005) Genomic Stability of Self-Complementary Adeno-Associated Virus 2 During Early Stages of Transduction in Mouse Muscle *In vivo*. *Human Gene Therapy,* **16,** 1047-1057.

Rogers, M.H., Lwin, R., Fairbanks, L., Gerritsen, B. & Gaspar, H.B. (2001) Cognitive and behavioral abnormalities in adenosine deaminase deficient severe combined immunodeficiency. *J Pediatr,* **139,** 44-50.

Schmidt, M., Carbonaro, D.A., Speckmann, C., Wissler, M., Bohnsack, J., Elder, M., Aronow, B.J., Nolta, J.A., Kohn, D.B., von Kalle, C. (2003) Clonality analysis after retroviral-mediated gene transfer to CD34+ cells from the cord blood of ADA-deficient SCID neonates. *Nature Medicine,* **9,** 463-468.

Sharoyan, S., Antonyan, A., Mardanyan, S., Lupidi, G. & Cristalli, G. (2006) Influence of dipeptidyl peptidase IV on enzymatic properties of adenosine deaminase. *Acta Biochimica Polonica,* **53,** 539-546.

Song, S., Scott-Jorgensen, M., Wang, J., Poirier, A., Crawford, J., Campbell-Thompson, M. & Flotte, T.R. (2002) Intramuscular administration of recombinant adeno-associated virus 2 alpha-1 antitrypsin (rAAV-SERPINA1) vectors in a nonhuman primate model: safety and immunologic aspects. *Mol Ther,* **6,** 329-335.

Tenenbaum, L., Lehtonen, E., Monahan, P.E. (2003) Evaluation of risks related to the use of adeno-associated virus-based vectors. *Current Gene Therapy,* **3,** 545-565.

Toromanoff, A., Cherel, Y., Guilbaud, M., Penaud-Budloo, M., Snyder, R.O., Haskins, M.E., Deschamps, J.Y., Guigand, L., Podevin, G., Arruda, V.R., High, K.A., Stedman, H.H., Rolling, F., Anegon, I., Moullier, P. & Le Guiner, C. (2008) Safety and efficacy of regional intravenous (r.i.) versus intramuscular (i.m.) delivery of rAAV1 and rAAV8 to nonhuman primate skeletal muscle. *Mol Ther,* **16,** 1291-1299.

Trobridge, G.D., Beard, B. C., Gooch, C., Wohlfahrt. M., Olsen, P., Fletcher, J., Malik, P., Kiem, H.P. (2008) Efficient transduction of pigtailed macaque hematopoietic repopulating cells with HIV-based lentiviral vectors. *Blood***,** 1-33.

Vandendriessche, T., Thorrez, L., Acosta-Sanchez, A., Petrus, I., Wang, L., Ma, L., De Waele, L., Iwasaki, Y., Gillijns, V., Wilson, J.M., Collen, D., and Chuah, M.K.L. (2007) Efficacy and safety of adeno-associated viral vectors based on serotype 8 and 9 vs. lentiviral vectors for hemophilia B gene therapy. *Journal of Thrombosis and Haemostasis,* **5,** 16-24.

Wang, Z., Allen, J.M., Riddell, S.R., Gregorevic, P., Storb, R., Tapscott, S.J., Chamberlain, J.S., Kuhr, C.S. (2007) Immunity to adeno-associated virus-mediated gene transfer in a random-bred canine model of Duchenne muscular dystrophy. *Human Gene Therapy,* **18,** 18-26.

Wingard, J.R., Vogelsang, G.B., Deeg, H.J. (2002) Stem Cell Transplantation: Supportive Care and Long-Term Complications. *Hematology Am Soc Hematol Educ Program***,** 422-444.

Yan, H., Guo, Y., Zhang, P., Zu, L., Dong, X., Chen, L., Tian, J., Fan, X., Wang, N., Wu, X. & Gao, W. (2005) Superior neovascularization and muscle regeneration in ischemic skeletal muscles following VEGF gene transfer by rAAV1 pseudotyped vectors. *Biochem Biophys Res Commun,* **336,** 287-298.

BIOGRAPHICAL SKETCH

Jared N. Silver was born in 1979, in Raleigh, North Carolina. His father, Frank M. Silver, was a chemist and consultant, while his mother; Dale R. Silver, was an artist and art teacher. Along with two older sisters, Mandie and Erika, Jared was raised in a number of locations on the east coast including Raleigh, North Carolina; Akron, Ohio; and Longmeadow, Massachusetts. In these locations, Jared attended elementary and middle schools with a special interest in art and science, thanks largely to the influence of an artist mother and a scientist father. Later, after a family relocation to Pensacola, Florida in 1994, Jared attended high school where his primary interests included science and history. High school chemistry class and his chemistry teacher, Ms. Marshman, as well as ancient history class and its instructor, Ms. Thomas, helped shaped Jared's interests in secondary education.

Upon graduation in 1997, Jared returned to the state of his birth, North Carolina, to attend college at the University of North Carolina in Chapel Hill (UNC-CH). Jared majored and minored in two distinct programs, which, at the time, were relatively new at UNC-CH. The major was chemistry along a biological track and the minor was medical anthropology. Jared also worked in the laboratory of Dr. Michael Goy in the Department of Cell and Molecular Physiology, where his research was directed at understanding and identifying novel genes involved in blood pressure regulation. This combined background in both science and the humanities was meant to prepare Jared for what he viewed as his burgeoning interest, passion, and dream, a dual career in both clinical medicine and translational research. Subsequently, after graduating college in 2001, Jared moved back to Florida, this time to the University of Florida in Gainesville, to join the MD/PhD program in the College of Medicine, and to earn both medical and doctoral degrees in pursuit of his dream.